STUDY OF COMPLEXITY DYNAMICS AND STATISTICAL ANALYSIS DURING YOGA EXERCISE, BUCKET LIFTING AND HAND GRIP STRENGTH: ECG, HRV AND EMG BASED APPROACH

A thesis submitted towards the partial fulfilment for the degree of

Masters of Engineering

In

Biomedical Engineering

Submitted by

ANADI BISWAS

EXAMINATION ROLL NUMBER: M4BMD19002

CLASS ROLL NUMBER: 001730201004

REGISTRATION NUMBER: 104265 of 2008-2009

Under the supervision of

Dr. Monisha Chakraborty

Associate professor,

School of Bioscience and Engineering

Jadavpur University

Kolkata- 700032

School of Bioscience and Engineering

Jadavpur University

Kolkata- 700032

India

2019

M.E. (Biomedical Engineering) course affiliated to
Faculty of Engineering and Technology
Jadavpur University
Kolkata -700032

CERTIFICATE OF RECOMMENDATION

This is to certify that the thesis entitled "**Study of Complexity Dynamics and Statistical Analysis During Yoga exercise, Bucket Lifting and Hand Grip Strength: ECG, HRV and EMG Based Approach"** that is being submitted by **Anadi Biswas,** in partial fulfillment for the award of degree of Master in Biomedical Engineering of Jadavpur University (Session 2017-2019) is a record of bona fide work carried out by him under my guidance and supervision. The project, in our opinion, is worthy for its acceptance.

Monisha Chakraborty 27/05/2019.

(THESIS ADVISOR)
Dr. Monisha Chakraborty
Associate Professor
School of Bioscience and Engineering
Jadavpur University
Kolkata-700032

Dr. MONISHA CHAKRABORTY
Associate Professor
School of Bio-Science & Engineering
Jadavpur University
Kolkata-700 032

Piyali Basak

Dr. Piyali Basak
Director
School of Bioscience and Engineering
Jadavpur University
Kolkata-700032

Dr. Piyali Basak
Director
School of Bioscience & Engineering
Jadavpur University
Kolkata-700 032

Dean
Faculty Council of Interdisciplinary Studies, Law and Management
Jadavpur University
Kolkata – 700032

M.E. (Biomedical Engineering) course affiliated to

Faculty of Engineering and Technology
Jadavpur University
Kolkata, India

CERTIFICATE OF APPROVAL**

The forgoing thesis is hereby approved as a creditable study of an engineering subject carried out and presented in a manner satisfactory to warrant its acceptance as a prerequisite to the degree for which it has been submitted. It is understood that by this approval the undersigned do not necessarily endorse or approve any statement made, opinion expressed or conclusion drawn therein but approve the thesis only for the purpose for which it is submitted.

Dr. Monisha Chakraborty
(Thesis Advisor)
Associate Professor
School of Bioscience and Engineering
Jadavpur University
Kolkata-700032

Signature of the Examiner

**Only in case the thesis is approved

DECLARATION

I hereby declare that this submission is my own work and that, to the best of my knowledge and belief, it contains no material previously published or written by another person nor material which has been accepted for the award of any other degree or diploma of the university or other institute of higher learning, except where due acknowledgment has been made in the text. All information in this document has been obtained and presented in accordance with academic rules and ethical conduct.

Place:

……..……..

Date: **ANADI BISWAS**

Registration number: 104265

ACKNOWLEDGEMENT

I express my heartiest gratitude to my respected thesis advisors Dr. Monisha Chakraborty, Associate Professor, School of Bioscience & Engineering, Jadavpur University for her esteemed guidance, constant encouragement and supportduring the entire period of my project work.

I am grateful to Dr. PiyaliBasak, director, School of Bioscience and Engineering for her constant support throughout the tenure of my master degree program at School of Bioscience and Engineering, Jadavpur University.

I am very thankful to Mr. Debanjan Parbat (PhD scholar) and Mr. Nilotpal Das (PhD scholar) for their invaluable suggestion, guidance and encouragement. They always helped me to keep my spirit high.

I express my gratitude love to all my batch mates, seniors, nonteaching stuffs and all my juniors for their kind co-operation.

I would also like to thank all the member of New Boys' Hostel, Jadavpur University for their kind co-operation and all kind of support.

Last, but not the least, I want to express my profound gratitude and my love for my family who have been the constant support and strength for me to go on with my higher education.

Date: **Anadi Biswas**

Dedicated to Jadavpur University

Preface

The muscular systems are complex and compact in normal state. When a force or load is applied on the systems they change their phenomena. The Vrms value give us a clear picture about degree of activation of muscles . In the first study , establishment of EMG-force obtained during simultaneous contraction of two different muscle groups with hand grip strength exercise our goal to find direct relation between the percent of maximum voluntary contraction(MVC) with Vrms or Vpp. This approach provides wide scope to the Physiotherapy field.

Now a days the joint pain or back pain is very common problem to us. During heavy weight lifting (Bucket lifting) with various posture and weight different muscle group produced different force . The force produced by muscle is directly proportional to the Vrms. During our study we also very keen to know the changes of complexity phenomena .This process just a beginning to give a proper guidance to those , who are involved with Water bucket lifting regularly .

The study process effect of yoga on cardiovascular system our main objective to find nonlinear as well as the frequency domain parameter. We try to find whether the subject relaxes more or less after the yoga exercise.

CONTENTS

LIST OF FIGURES

Page No.

INTRODUCTION

DEFINATION OF BIOSIGNAL:

A signal can be defined as any physical quantity, carries some information that varies with time, space or any other independent variable[1]. We are all immersed in a sea of signals. All of us from the smallest living unit, a cell, to the most complex living organism (Humans) are all-time receiving signals and are processing the signals appropriately.

Bio-signals refers to all the signals generated in the human body or any living organs which carries some information of organs system. Bio-signals are used primarily for extracting information on a biological system under investigation. The basic source of Bio-signal is the cell membrane potential under certain conditions may be excited to generate an action potential

Living organisms are made up of many functional components. For example, the nervous system, the cardiovascular system, the musculoskeletal system, Respiratory system. Each system has several subsystems that carry on many physiological processes. This physiological phenomenon can be monitored as bio-signal. Typically, the changes in potential difference across an in body's certain tissue are measured in case of bio-electric signals[2].

Physiological processes are very complex phenomena, including nervous or hormonal stimulation; outputs and inputs that could be in the form of physical material, neurotransmitters, or information; and action that could be mechanical, electrical, or biochemical. Most physiological processes are accompanied by themselves as signals that reflect their nature and activities. Such signals can be of different types, including biochemical in the form of hormones and neurotransmitters and physical in the form of pressure or temperature.

Diseases in a biological system cause alterations in its normal physiological processes, leading to pathological processes that affect the performance and health of the system. If we possess a good understanding of a system of interest, it becomes possible to observe the corresponding signals. The task is very easy when the signal is simple and appears at the outer surface of the body. For example, most infections cause a rise in the temperature of the body, which may be sensed very easily, albeit in a relative and qualitative manner, via the

palm of one's hand. Objective or quantitative measurement of temperature requires an instrument, such as a simple thermometer.

The action potential (AP) is the electrical signal that causes of mechanical contraction of a single cell when stimulated by an electrical current (neural or external). It is caused by the flow of sodium (Na+), chloride (Cl-), potassium (K+), and other ions across the cell membrane.

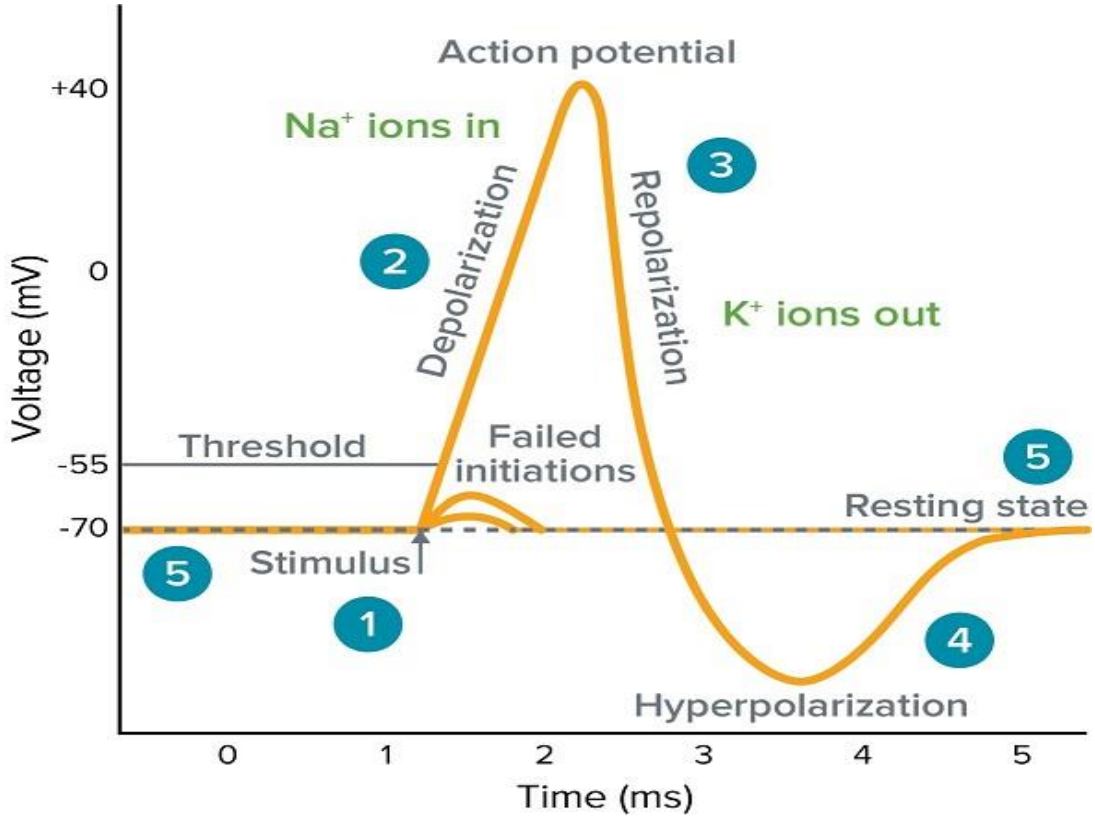

Fig 1.1 Action potential generation

The action potential is the basic component of bioelectrical signals. It provides information about the nature of physiological activity at the single-cell level. Recording an action potential requires the isolation of a single cell and microelectrodes with tips of the order of a few micrometres to activate the cell and record the response. Resting potential: Nerve and muscle cells are encased in a semi-permeable membrane that permits selected substances to pass through while others are kept out. Body fluids surrounding cells are conductive solutions containing charged atoms known as ions. In their resting state, membranes of excitable cells readily permit the entry of Cl-and K+ ions, but effectively block the entry of Nu+ ions (the permeability for K+ is 50-100 times that for Na+). Various ions seek to establish a balance between the inside and the outside of a cell according to charge and concentration. The

inability of Na+ to penetrate a cell membrane results in the following Na+ concentration inside the cell is far less than that outside. 0 The outside of the cell is more positive than the inside of the cell. 0 To balance the charge, additional K+ ions enter the cell, causing higher K+ Charge balance cannot be reached due to differences in membrane permeability concentration inside the cell than outside. For the various ions. A state of equilibrium is established with a potential difference, with the inside of the cell being negative with respect to the outside. A cell in its resting state is called polarized. Most cells maintain a resting potential of the order of -60 to - 100 mV until disturbance or stimulus upsets the equilibrium.

Depolarization: When a cell is excited by ionic currents or an external stimulus, the membrane changes its characteristics and begins to allow Na+ ions to enter the cell. This movement of Na+ ions constitutes an ionic current, which further reduces the membrane barrier to Na+ ions. This leads to an avalanche effect. K+ ions try to leave the cell as they were in higher concentration inside the cell in the preceding resting state but move slow compare to the Na+ ions. The net result is that the inside of the cell becomes more positive with respect to the outside due to an imbalance of K+ ions. A new state of equilibrium is reached after the rush of Na+ ions stops. This change represents the beginning of the action potential, with a peak value of about +20 mV for most cells. An excited cell displaying an action potential is said to be depolarized; the process is called depolarization.

Repolarization: After a certain period of being in the depolarized state the cell becomes polarized again and returns to its resting potential via a process known as repolarization. Repolarization occurs by processes that are analogous to those of depolarization, except that instead of Nu+ ions, the principal ions involved in repolarization are K+ ions. Membrane depolarization, while increasing the permeability for Na+ ions, also increases the permeability of the membrane for K+ ions via a specific class of ion channels known as voltage-dependent K+ channels. Although this may appear to be paradoxical at first glance, the key to the mechanism for repolarization lies in the time-dependence and voltage-dependence of the membrane permeability changes for K+ ions compared with that for Na+ ions. The permeability changes for K+ during depolarization occur considerably more slowly than those for Na+ ions, hence the initial depolarization is caused by an inrush of Na+ ions. However, the membrane permeability changes for Na+ spontaneously decrease near the peak of the depolarization, whereas those for K+ ions are beginning to increase. Hence, during repolarization, the predominant membrane permeability is for K+ ions. Because K+ concentration is much higher inside the cell than outside, there is a net efflux of K+ from the

cell, which makes the inside more negative, thereby effecting repolarization back to the resting potential. It should be noted that the voltage-dependent K+ permeability change is due to a distinctly different class of ion channels than those that are responsible for setting the resting potential. A mechanism known as the Na+ - K+ pump extrudes Na+ ions in exchange for transporting K+ ions back into the cell. However, this transport mechanism carries very little current in comparison with ion channels, and therefore makes a minor contribution to the repolarization process. The Na+ - K+ pump is essential for resetting the Nu+ - K+ balance of the cell, but the process occurs on a longer time scale than the duration of an action potential. Nerve and muscle cells repolarize rapidly, with an action potential duration of about 1ms. Heart muscle cells repolarize slowly, with an action potential duration of 150-300ms.

The action potential is always the same for a given cell, regardless of the method of excitation or the intensity of the stimulus beyond a threshold: this is known as the all-or-none or all-or-nothing phenomenon. After an action potential, there is a period during which a cell cannot respond to any new stimulus, known as the absolute refractory period (about 1 me in nerve cells)[7,9].

EXAMPLES OF BIO-SIGNAL:

Most of the physiological processes are accompanied by or manifest themselves as signals that reflect their nature and activity. Any signal transduced from a biological or medical source could be called a Bio-signal.

Clinically the Bio-signals are primarily acquired for monitoring specific pathological or physiological states for diagnosis purposes and evaluating therapy. In research case, bio-signals are also used for decoding and modelling of specific biological systems.[1,6,8]

There can be various types of Bio-signals. They are classified depending upon their nature and also the origin of generation. Regardless of their simplicity, we can appreciate their importance in the assessment of the person. Some of the important bio-signals as follows:

- Electrocardiogram (ECG): The ECG deals with the electrical signal, which generates the contractile activity of the heart.
- Magnetocardiogram (MCG): The MCG is the measurement procedure of magnetic fields produced by electrical activity in the heart.

- Vectorcardiogram (VGC): The VGC is the recording system of magnitude and direction of the electrical forces of the heart.
- Phonocardiogram (PCG): The vibration or sound signal related to the activity of cardio hemic system (heart and blood together) is detecting by PCG.
- Electromyogram (EMG): This measurement of motor unit action potential generated in muscle fibres known as Electromyogram. When stimulated by a neural signal, each motor unit contracts and causes an electrical signal that is the summation of action potentials of all its constituent cells.
- Nerve Conduction Study (NCS): The electrical signal measurement of motor and sensory nerves by giving some stimulus is called Nerve Conduction study.
- Electroencephalogram (EEG): The electrical activity of the brain detects by EEG.
- Magnetoencephalogram (MEG): This is the recording procedure of magnetic fields produced by electrical signal occurring in the brain[2,5].

All bio-signals are very important in the field of medical, sports, physiotherapy as well as daily work in our life. But the spontaneous electrical activity recording as ECG, EMG and EMG are most widely used. The cardiovascular system, neuromuscular system, nerves system is basically carried all electrical activity.

During project work in a master's degree course, my main focus is on EMG and ECG.

EMG: The electromyography (EMG) signal is an electrical indication of the neuromuscular actuation connected with a contracting muscle. It is an exceedingly complicated sign which is influenced by the anatomical and physiological properties of muscles, the control plan of the fringe sensory system, and also the attributes of the instrumentation that is utilized to identify and watch it. Most of the connections between the EMG signal and the properties of a contracting muscle which will be quickly utilized have developed serendipitously. The absence of a fitting portrayal of the EMG signal is likely the most noteworthy single variable which has hampered the improvement of EMG into an exact discipline.

During muscular contractions, electrical signals generate which detected by EMG. So basically electromyography (EMG) is the study process the function of the neuromuscular system. The muscular condition can be monitored by setting proper protocol and analysis of the signal. Muscle contraction can be voluntary or involuntary. The tension of the muscular system is the main cause behind voluntary contraction. This muscle fibre contracts when the

action potentials (impulse) of the motor nerve supplies it. The functional unit of muscle fibres is the motor unit (MU), which is basically a single alpha motor neuron. EMG signal is the summation of motor unit action potential (MUAP) within the signal motor unit.

Fig 1.2 EMG machine

Electromyography (EMG) signals are usable in order to applications of biomedical, clinical, modern human-computer interaction and Evolvable Hardware Chip (EHW) improvement. Advanced methods are needed for perception, disassembly and classification and processing of EMG signals acquired from the muscles. The objective of this article is to show various methods and algorithms in order to analyse an electromyogram signal to ensure effective and efficient ways of understanding signal and its nature. Early diagnosis was indispensable and very important in medical health practice. For this reason, it is important to design accurate diagnostic methods. Today, diagnostic methods include evaluating the patient's story, blood tests, and muscle biopsies. In this article, analysis and Electromyogram signals classification and electromyography are mostly used. The system has been successfully implemented utilizing MATLAB software that can distinguish EMG signals from different patients. This article also provides the researcher with a well understanding of electromyogram signalling and analysis processes. This information will auxiliary to improve stronger, more resilient and effective implementations [12,16,78]

EMG signals can be recorded using invasive and non-invasive methods, with the latter referred to as SEMG [2]. Invasive techniques utilize needle electrodes to monitor EMG signals directly from the muscles. By contrast, SEMG collects data using surface electrodes placed on the skin . SEMG technique has considerable advantages over the invasive method, including the easier detection of SEMG signal over the skin and more comfort for subjects . Thus, recognizing muscle behaviour through SEMG detection is more feasible. A raw SEMG signal has peak-to-peak amplitudes of 0-2 mV with a band frequency ranging from 0 Hz to 1000 Hz . However, the band frequency of SEMG, which includes significant information, ranges from 20 Hz to 500 Hz . Raw SEMG signals have low amplitude; thus, the SEMG signal can be affected by many types of noises such as ambition noise or combines with them [46].

The impedance of the body skin reduces the amplitude of SEMG signals and induces noise. The noise generated from the skin is caused by fat between the muscle and skin and the blood flow in minuscule vessels under the skin [21]. Other powerful noises include environmental noise that mainly comes from the environment, as well as electromagnetic radiation sources, electrical power wires, and fluorescent lamps during recording . Various significant noises that affect SEMG are from the subcutaneous tissue layers , the spread of the innervation zone (IZ) , crosstalk from neighbouring muscles , electrode size, and electrode position [27]. Electrode position can significantly mislead the description of a statistical and spectral factor of SEMG, thus affecting SEMG evaluation [29,30].

MUSCLE PHYSIOLOGY:

The muscles of the human body are divided into three categories, namely, skeletal, cardiac, and smooth muscles; each muscle group has its own characteristics . Smooth muscles are non-striated and self-acting because humans cannot control their movements. Smooth muscles are tissues that basically form supporting blood vessels and the walls of hollow organs, such as the stomach . Cardiac muscle or heart muscle is one of the major muscle groups, which is independent of the neural network . The heart muscle is contracted automatically in the walls and histological foundation . The most important muscle category consists of skeletal muscles that are found in the majority of muscle tissues . These muscle groups are attached by the tendon to the bone [36]. In contrast to cardiac and smooth muscles, skeletal muscles are known as the voluntary muscle group. Humans can control skeletal

muscles to make movements for daily living because these muscles are under the control of the nervous system .

Skeletal muscles generate force and movement. Their structural unit is the muscle fibre [38]. The construction group of muscle fibres is muscle myofiber or muscle cell. A myofiber has an approximately cylindrical shape with a diameter a few microns meters (10-100 μm) and a few millimetres to a few centimetres in length (1.5 mm to 30 cm) . Many myofiber bundles or fascicules are spliced by tissue in the muscle. The fascicule arrangement in a muscle is associated with muscle power and its motion limitation. The muscle fibres contract to move or produce a force.

Muscle origin is the attachment of the muscle to the bone, which is fixed and does not move during contraction. Muscle origin typically has more mass, and it is more stable when the muscle is contracted compared with the other muscle end. The skeletal muscles are connected to the bone by the tendon in an area called insertion zone. Movements occur at the joint muscles; thus, the insertion zone is usually distant from the distal portion of the muscle about the muscle origin to facilitate the movement . Tendon is a strong band tissue connection, which usually links one end of the skeletal muscle to a joint or bone and is capable of tolerating the tension. Furthermore, the tendon has been considered to transmit forces. This link allows tendons to modulate forces reactively during movements and provide stability when muscles are in the rest mode [46].

Tendons are nonessential in performing the same practical role, with some tendons typically positioned in the limbs. Moreover, tendons can save and regain energy during high performance. For example, when a human walk, the Achilles tendon stretches and the joint ankle flexes. After this action, the stored elastic energy will be released when the foot plantar flexes. The stretching of the tendon allows the muscle to increase its force when the muscle acts with less or without any change in length [57]. The nervous system controls each muscle function in the muscle IZ. Involuntary muscles, such as heart muscles, have IZ by the autonomic nervous system and skeletal muscles by the external. The point at the end of the nervous system (innervation point of voluntary muscles) is called the motor unit (MU) . MU includes a fibre of the motor nerve, and all of the fibres of the muscle have their innervate point.

There are over 600 skeletal muscles in the human body but, do not worry, you do not need to know them all. Most of the muscles you are required to know are shown in Fig You will be

able to see that most of these muscles extend from one bone to another, are attached in at least two places and cross at least one joint. From our knowledge of the skeletal system, we know that muscles are attached to bones by tendons. These points of attachment at either end of the muscle form the origin and the insertion. It is important to remember that muscles can only pull, they can never push. When a muscle contracts, the pulling of one bone towards another across a movable joint causes movement.

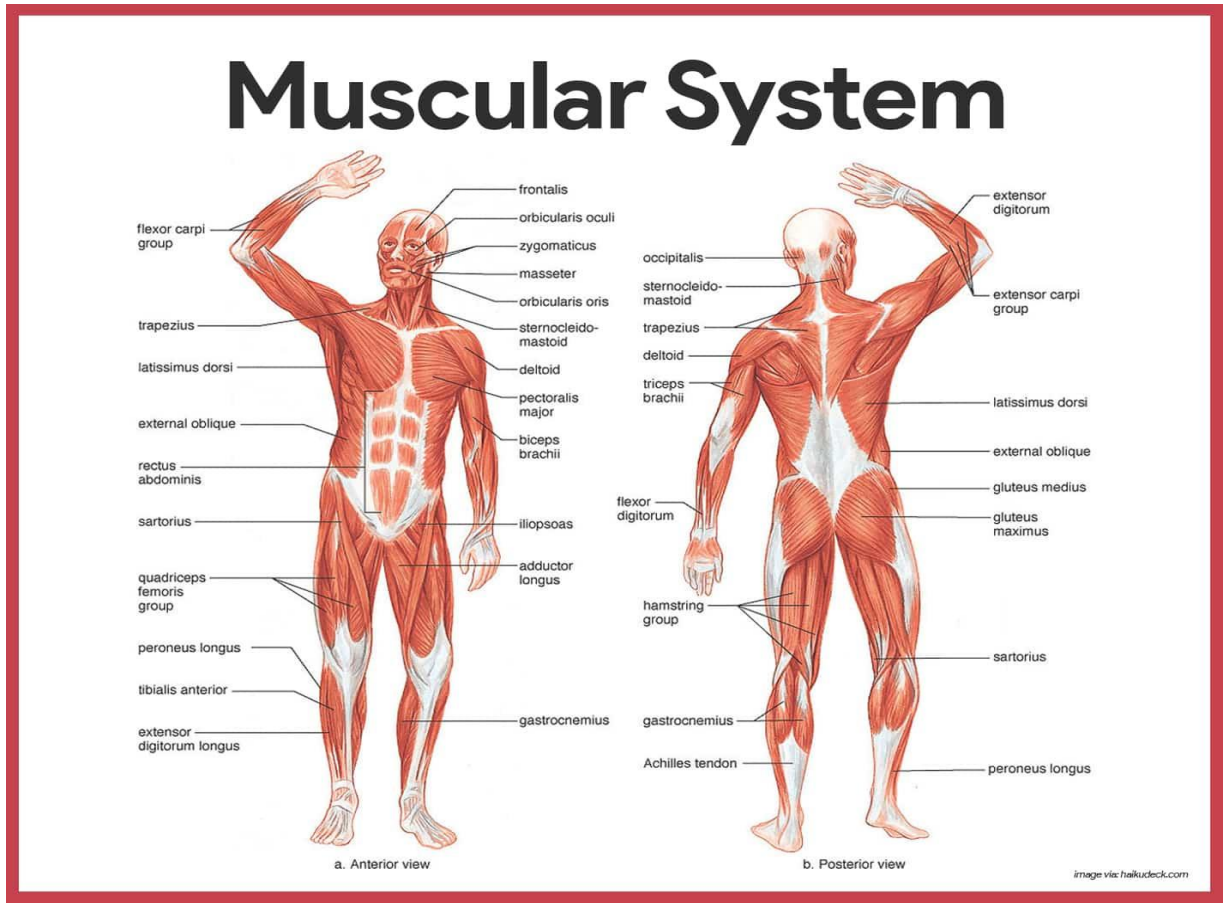

Fig 1.3 Muscular system

TYPES OF MUSCLES:

There are over 600 muscles in the human body, and they make up about 40-50% of the weight of the body. Muscle tissue is soft tissue and is one of the four fundamental types of tissue present in animals. There are three types of muscle tissue recognized in vertebrates:

Skeletal muscle:

Skeletal muscle is anchored by tendons (or by aponeuroses at a few places) to the bone and is used to effect skeletal movement such as locomotion and in maintaining posture. Though this

postural control is generally maintained as an unconscious reflex, the muscles responsible react to conscious control like non-postural muscles. An average adult male has 42% of skeletal muscle and an average adult female is has 36% body mass.

Smooth muscle:

The arrectorpili found in the skin and Smooth muscle or "involuntary muscle" is found in the walls of organs and structures such as the oesophagus, stomach, intestines, bronchi, bladder, blood vessels in which it controls the erection of body hair.

Cardiac muscle:

Cardiac muscle (myocardium), is also an "involuntary muscle" but is highly akin in structure to skeletal muscle.

Fig 1.4 Type of muscle

STRUCTURE OF MUSCLE CELLS:

A muscle cell, known technically as a myocyte, is a specialized animal cell that can shorten its length. While several associated proteins help, actin and myosin form thick and thin filaments which slide past each other to contract small units of a muscle cell. These units are called sarcomeres, and many of them run end-to-end within a larger fibre called a myofibril. A muscle cell is a long cell compared to other forms of cells, and many muscle cells connect with each other to form the long fibres found in muscle tissue.

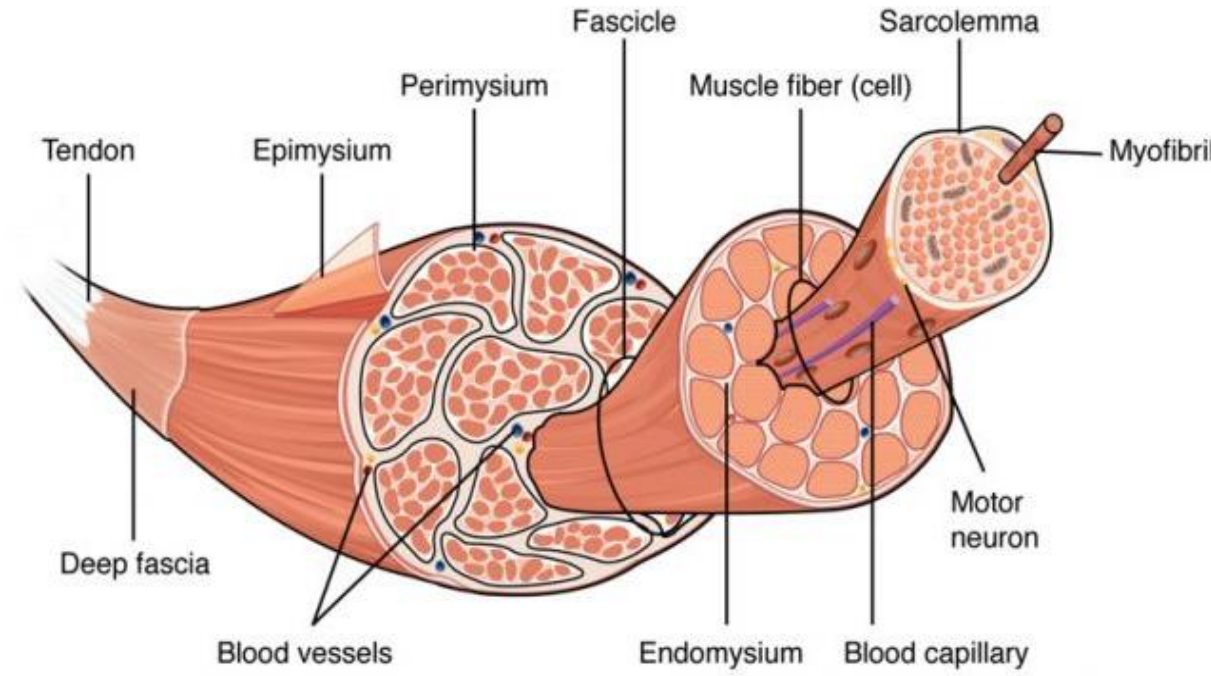

Fig 1.5 The Three Connective Tissue Layers: Bundles of muscle fibres, called fascicles, are covered by the perimysium. Muscle fibres are covered by the endomysium.

Inside each skeletal muscle, muscle fibres are organized into bundles, called fascicles, surrounded by a middle layer of connective tissue called the perimysium. This fascicular organization is common in muscles of the limbs; it allows the nervous system to trigger a specific movement of a muscle by activating a subset of muscle fibres within a fascicle of the muscle. Inside each fascicle, each muscle fibre is encased in a thin connective tissue layer of collagen and reticular fibres called the endomysium. The endomysium surrounds the extracellular matrix of the cells and plays a role in transferring force produced by the muscle fibres to the tendons.

In skeletal muscles that work with tendons to pull on bones, the collagen in 3 connective tissue layers intertwines with the collagen of a tendon. Tendon's other end it fuses with the periosteum coating the bone. The tension created by contraction of the muscle fibres is then transferred through the connective tissue layers, to the tendon, and then to the periosteum to pull on the bone for movement of the skeleton. As shown in the image below, a muscle cell is a compact bundle of many myofibrils. Each myofibril is made of many sarcomeres bundled together and attached end-to-end. A specialized form of the endoplasmic reticulum, known as the sarcoplasmic reticulum, extends in and around these myofibril bundles. The sarcoplasmic reticulum (SR for short) concentrates a chemical needed for the muscle cells to contract and is activated by signals from nerve cells. The signals travel through the transverse tubules (T

tubules in the picture below) after being received from a nerve and activate the SR. Mitochondria are densely packed throughout the muscle cells, to provide a constant flow of ATP. The entire cell is covered in a specialized cell membrane known as the sarcolemma. The sarcolemma has a special opening which allows nerve impulses to be passed from transverse tubules[38,40].

The plasma membrane of muscle fibres is called the sarcolemma (from the Greek sarco, which means "flesh") and the cytoplasm is referred to as sarcoplasm (Fig below). Within a muscle fibre, proteins are organized into structures called myofibrils that run the length of the cell and contain sarcomeres connected in series. Because myofibrils are only approximately 1.2μm in diameter, hundreds to thousands (each with thousands of sarcomeres) can be found inside one muscle fibre. The sarcomere is the smallest functional unit of skeletal muscle fibre and is a highly organized arrangement of contractile, regulatory, and structural proteins. It is the shortening of these individual sarcomeres that lead to the contraction of individual skeletal muscle fibres (and ultimately the whole muscle)[16].

A sarcomere is defined as the region of a myofibril contained between two cytoskeletal structures called Z-discs (also called Z-lines), and the striated appearance of skeletal muscle fibres is due to the arrangement of the thick and thin myofilaments within each sarcomere . The dark striated A band is composed of the thick filaments containing myosin, which span the centre of the sarcomere extending toward the Z-discs. The thick filaments are anchored at the middle of the sarcomere (the M-line) by a protein called myomesin. The lighter I band regions contain thin actin filaments anchored at the Z-discs by a protein called α-actinin. The thin filaments extend into the A band toward the M-line and overlap with regions of the thick filament. The A band is dark because of the thicker myosin filaments as well as overlap with the actin filaments. The H zone in the middle of the A band is a little lighter in colour because the thin filaments do not extend into this region.

Because a sarcomere is defined by Z-discs, a single sarcomere contains one dark A band with half of the lighter I band on each end. During contraction, the myofilaments themselves do not change length but actually slide across each other so the distance between the Z-discs shortens. The length of the A band does not change (the thick myosin filament remains a constant length), but the H zone and I band regions to shrink. These regions represent areas where the filaments do not overlap, and as filament overlap increases during contraction these regions of no overlap decrease[17].

THE FUNCTION OF A MUSCLE CELL:

The thin filaments are composed of two filamentous actin chains (F-actin) comprised of individual actin proteins . These thin filaments are anchored at the Z-disc and extend toward the centre of the sarcomere. Within the filament, each globular actin monomer (G-actin) contains a myosin binding site and is also associated with the regulatory proteins, troponin and tropomyosin. The troponin protein complex consists of three polypeptides. Troponin I (TnI) binds to actin, troponin T (TnT) binds to tropomyosin, and troponin C (TnC) binds to calcium ions. Troponin and tropomyosin run along the actin filaments and control when the actin binding sites will be exposed for binding to myosin.

Thick myofilaments are composed of myosin protein complexes, which are composed of six proteins: two myosin heavy chains and four light chain molecules. The heavy chains consist of a tail region, a flexible hinge region, and globular head which contains an Actin-binding site and a binding site for the high energy molecule ATP. The light chains play a regulatory role at the hinge region, but the heavy chain head region interacts with actin and is the most important factor for generating force. Hundreds of myosin proteins are arranged into each thick filament with tails toward the M-line and heads extending toward the Z-discs.

Other structural proteins are associated with the sarcomere but do not play a direct role in active force production. Titin, which is the largest known protein, helps align the thick filament and adds an elastic element to the sarcomere. Titin is anchored at the M-Line, runs the length of myosin, and extends to the Z disc. The thin filaments also have a stabilizing protein, called nebulin, which spans the length of the thick filaments[60].

To activate a muscle, the brain sends an impulse down a nerve. The nerve impulse travels down the nerve cells to the neuromuscular junction, where a nerve cell meets a muscle cell. The impulse is transferred to the nerve cell and travels down specialized canals in the sarcolemma to reach the transverse tubules. The energy in the transverse tubules causes the SR to release of the Ca2+ it has built up, flooding the cytoplasm with calcium. The Ca2+ has a special effect on the proteins associated with actin.

Troponin, when not in the presence of Ca2+, will bind to tropomyosin and cause it to cover the myosin-binding sites on the actin filament. This means that without Ca2+ the muscle cell will be relaxed. When Ca2+ is introduced into the cytosol, troponin will release tropomyosin and tropomyosin will slide out of the way. This allows the myosin heads to attach to the actin

filament. Once this happens, myosin can use the energy gained from ATP to crawl along the actin filament. When many sarcomeres are doing this at the same time, the entire muscle contract.

While only a small percentage of the heads are attached at any one time, the many heads and continual use of ATP ensures a smooth contraction. The myosin crawls until it reaches the Z plate, and full contraction has been obtained. The SR is continually removing Ca2+ from the cytoplasm, and concentration falls below a certain level troponin rebinds to tropomyosin and the muscle releases.

While the above model is a generalized version in skeletal muscle, similar processes control the contractions of cardiac and smooth muscle. In cardiac muscle, the impulses are in part controlled by pacemaker cells that release impulses regularly. Smooth muscle is different from skeletal muscle that actin and myosin filament is not organized in convenient bundles. While they are organized differently, smooth muscle still operates on the function of myosin and actin. Smooth muscle can obtain a signal to contract from different sources, including the nervous system and environmental cues the cells receive from different parts of the body[62].

ELECTROCARDIOGRAPHY (ECG):

ECG is the process of recording the electrical activity of the heart using electrodes placed on the skin of the body. These electrodes detect the small electrical changes on the skin which arise from the heart muscle's electrophysiological pattern of depolarizing and repolarising during each heartbeat. It is a very commonly performed cardiology test.

THE NORMAL ECG:

A normal ECG contains intervals, waves, segments and one complex, as defined below.

Wave: A positive or negative deflection from the baseline that indicates a specific electrical event. The waves on an ECG include the P wave, R wave, Q wave, S wave, T wave.

Interval: The time between two specific ECG events. The intervals commonly measured on an ECG include the QRS interval (also called QRS duration), PR interval, QT interval and RR interval.

Segment: The length between two different points on an ECG that are supposed to be at the baseline amplitude (not negative or positive). The segments on an ECG include the PR segment, TP segment, and ST segment.

Complex: The combination of many waves grouped together. The only one main complex on an ECG is QRS complex.

Point: There is only one point on an ECG which is known as the J point, which is where the QRS complex ends and the ST segment begins.

A typical ECG wave cycle has some marking point P, R, S, Q and T. These markings are clearly shown in figure 1.6. Using these points several other features further derived, namely peaks or waves, intervals, segments and complex etc. The features are shown in figure 1.7and figure 1.6.

One of the most important of these is the QRS complex. Which has a very high R peak, two other Q and S inverted peak? Detecting a QRS complex is a very useful step towards others feature extraction of an ECG. The lead II is generally used for QRS complex detection due to its best prominence of QRS complex.

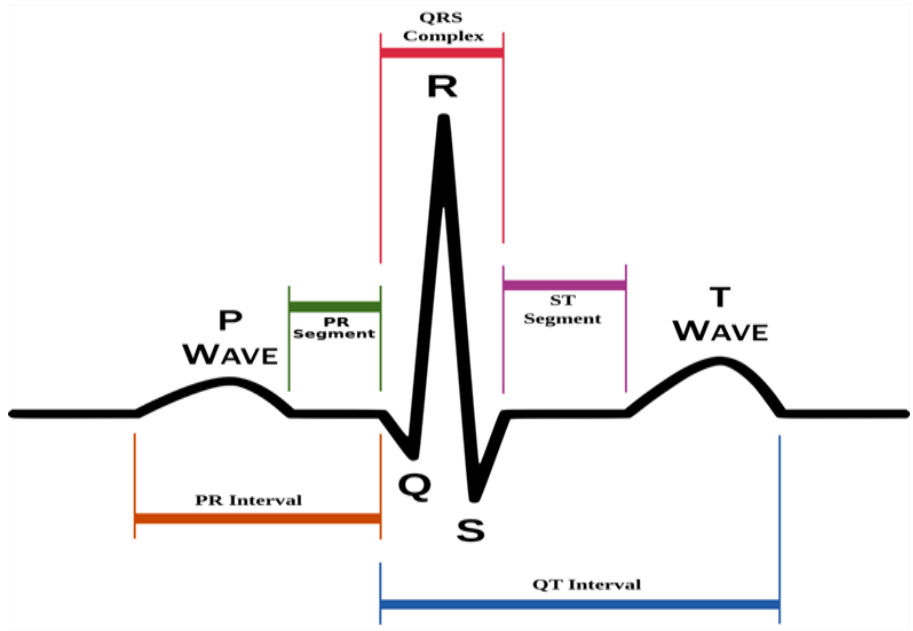

Fig 1.6 QRS complex waveform

A brief description of some of the import has been given below:

P-wave: P wave is the first small peak of the ECG signal, which is caused by the depolarization of the atrial muscle prior to contraction. The atria contain very little muscle and so the voltage generated during this is quite small.

QRS complex: The QRS complex comes just after the P wave with a comparatively very high R peaks with two inverted small peaks Q and S at each side of it. It is caused by the ventricular depolarization. Although atrial repolarisation occurs simultaneously, as the amplitude generated by this is very low its effect is not visible.

T-wave: Afterward the QRS complex part again a small peak can be seen in a typical ECG tracing. It is caused by ventricular repolarization. The time between ventricular contractions, during which ventricular filling occurs, is referred to as the diastole.

PR Interval: The time interval between the occurrence of P peak and R peak in an ECG waveform. It should be 0.12s – 0.40s normally.

QT Interval: The time interval between Q point in an ECG waveform and the T point. It should be less the 0.40s normally.

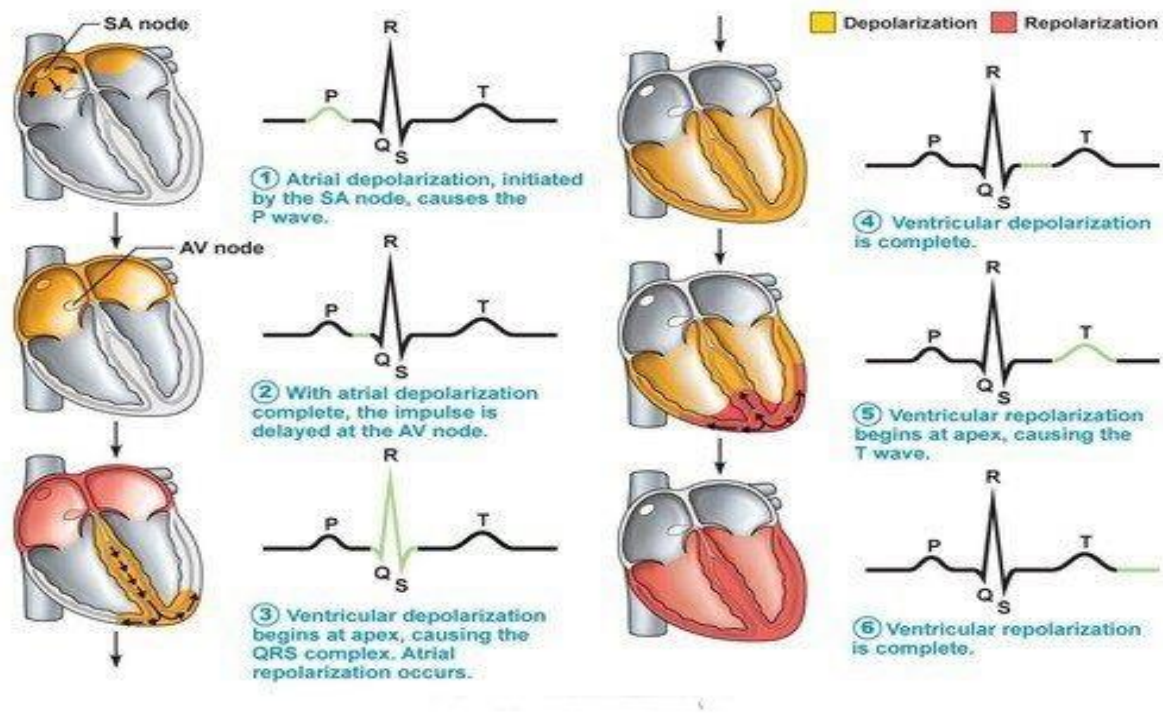

Fig 1.7 P,Q,R,S,T formation

Although generally, the R-peak has the largest amplitude components, the morphology of a healthy ECG tracing can vary greatly from patient to patient with the P- or T-waves dominating or merging at times[65].

Heart Cycle is to be detected to measure the heart rate variability in it. We define a heart cycle by the segment between two consecutive normal components. For convenience, the R wave is taken as the normal component. So in an ECG data stream, the R peaks are to be detected to form RR time series. Processing those RR intervals in the RR time series the HRV parameters are obtained.

Heart Rate Variability (HRV) means the variations in interbeat intervals of the heart rhythms or the variations in instantaneous heart rate. This variation has been found to be mainly caused by the sympathetic and parasympathetic nervous system. So HRV has the potential to be a good measure of sympathovagal balance. Researchers and physiologists for the last few decades have been trying to develop a standardized protocol to use it as a biomarker of diseases and other cardiovascular and psychological conditions. It is needed to find the instantaneous heart rate so that the variability in it can be detected[68,69].

ANATOMY OF CARDIOVASCULAR SYSTEM:

The cardiovascular system can be thought of as the transport system of the body. This system has three main components: the heart, the blood vessel and the blood itself. The heart is the system's pump and the blood vessels are like the delivery routes. Blood can be thought of as a fluid which contains the oxygen and nutrients the body needs and carries the wastes which need to be removed. The following information describes the structure and function of the heart and the cardiovascular system as a whole.

The heart's job is to pump blood around the body. The heart is located between the two lungs. It lies left of the middle of the chest.

STRUCTURE OF THE HEART:

The heart is a muscle about the size of a fist and is roughly cone-shaped. It is about 12cm long, 9cm across the broadest point and about 6cm thick. The pericardium is a fibrous covering which wraps around the whole heart. It holds the heart in place but allows it to move as it beats. The wall of the heart itself is made up of a special type of muscle called cardiac muscle.

CHAMBERS OF THE HEART:

The heart has two sides, the right side and the left side. The heart has four chambers. The left and right side each have two chambers, a top chamber and a bottom chamber. The two top chambers are known as the left and right atria (singular: atrium). The atria receive blood from different sources. The left atrium receives blood from the lungs and the right atrium receives blood from the rest of the body. The bottom two chambers are known as the left and right ventricles. The ventricles pump blood out to different parts of the body. The right ventricle pumps blood to the lungs while the left ventricle pumps out blood to the rest of the body. The ventricles have much thicker walls than the atria which allows them to perform more work by pumping out blood to the whole body.

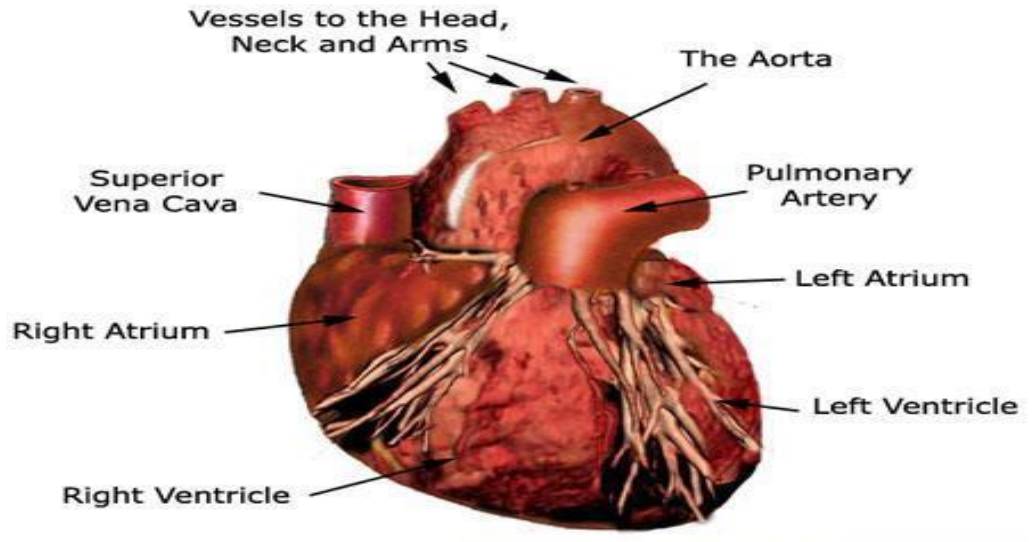

Fig 1.8 Anatomy of the heart

BLOOD VESSELS:

Blood Vessel is tubes which carry blood. Veins are blood vessels which carry blood from the body back to the heart. Arteries are blood vessels which carry blood from the heart to the body. There are also microscopic blood vessels which connect arteries and veins together called capillaries. There are a few main blood vessels which connect to different chambers of the heart. The aorta is the largest artery in our body. The left ventricle pumps blood into the aorta which then carries it to the rest of the body through smaller arteries. The pulmonary trunk is the large artery which the right ventricle pumps into. It splits into pulmonary arteries which take the blood to the lungs. The pulmonary veins take blood from the lungs to the left

atrium. All the other veins in our body drain into the inferior vena cava (IVC) or the superior vena cava (SVC). These two large veins then take the blood from the rest of the body into the right atrium.

VALVES:

Valves are fibrous flaps of tissue found between the heart chambers and in the blood vessels. They are rather like gates which prevent blood from flowing in the wrong direction. They are found in a number of places. Valves between the atria and ventricles are known as the right and left atrioventricular valves, otherwise known as the tricuspid and mitral valves respectively. Valves between the ventricles and the great arteries are known as the semilunar valves. The aortic valve is found at the base of the aorta, while the pulmonary valve is found the base of the pulmonary trunk. There are also many valves found in veins throughout the body. However, there are no valves found in any of the other arteries besides the aorta and pulmonary trunk.

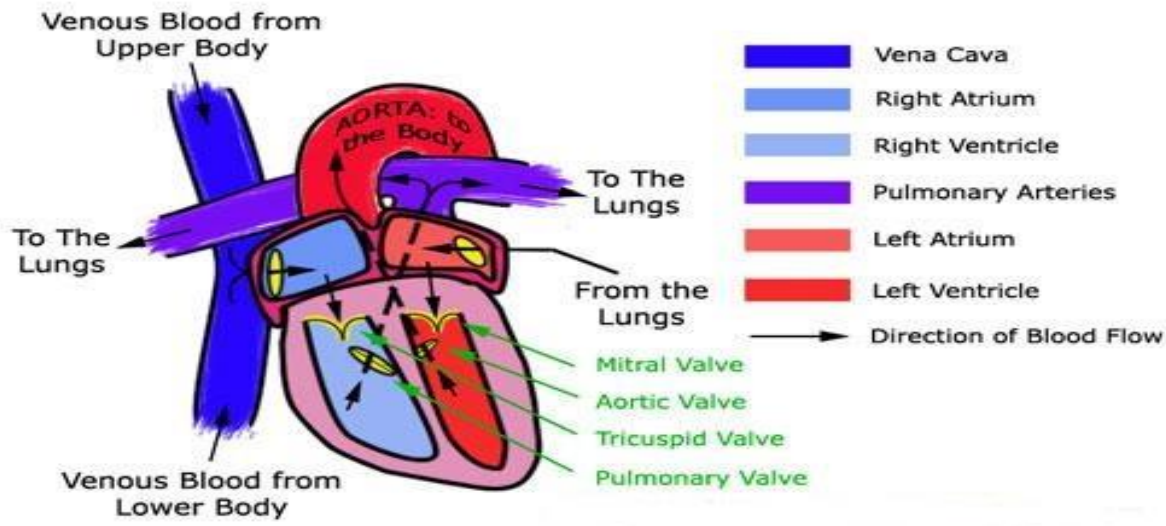

Fig 1.9 Heart chambers and valve.

The cardiovascular system refers to the heart, blood vessels and the blood. Blood contains oxygen and other nutrients which your body needs to survive. The body takes these essential nutrients from the blood. At the same time, the body dumps waste products like carbon dioxide, back into the blood, so they can be removed. The main function of the cardiovascular system is, therefore, to maintain blood flow to all parts of the body, to allow it to survive. Veins deliver used blood from the body back to the heart. Blood in the veins is

low in oxygen (as it has been taken out by the body) and high in carbon dioxide (as the body has unloaded it back into the blood). All the veins drain into the superior and inferior vena cava which then drain into the right atrium. The right atrium pumps blood into the right ventricle. Then the right ventricle pumps blood to the pulmonary trunk, through the pulmonary arteries and into the lungs. In the lungs, the blood picks up oxygen that we breathe in and gets rid of carbon dioxide, which we breathe out. The blood becomes rich in oxygen which the body can use. From the lungs, blood drains into the left atrium and is then pumped into the left ventricle. The left ventricle then pumps this oxygen-rich blood out into the aorta which then distributes it to the rest of the body through other arteries. The main arteries which branch off the aorta and take blood to specific parts of the body are:

- Carotid arteries, which take blood to the neck and head
- Coronary arteries, which provide blood supply to the heart itself
- Hepatic artery, which takes blood to the liver with branches going to the stomach
- Mesenteric artery, which takes blood to the intestines
- Renal arteries, which takes blood to the kidneys
- Femoral arteries, which take blood to the legs

The body is then able to use the oxygen in the blood to carry out its normal functions. This blood will again return back to the heart through the veins and the cycle continues.

COMPONENTS OF THE HEARTBEAT:

The adult heart beats around 70 to 80 times a minute at rest. When you listen to your heart with a stethoscope you can hear your heartbeat. The sound is usually described as “lubb-dupp”. The “lubb” also known as the first heart sound, is caused by the closure of the atrioventricular valves. The “dupp” sound is due to the closure of the semilunar valves when the ventricles relax (at the beginning of ventricular diastole). Abnormal heart sounds are known as murmurs. Murmurs may indicate a problem with the heart valves, but many types of murmur are no cause for concern. (For more information see: (see Valvular Heart Disease)

ELECTROCARDIOGRAM LEADS:

As the heart undergoes depolarization and repolarization, electrical currents spread throughout the body because the body acts as a volume conductor. The electrical currents generated by the heart are commonly measured by an array of electrodes placed on the body

surface and the resulting tracing is called an electrocardiogram (ECG, or EKG). By convention, electrodes are placed on each arm and leg (standard and augmented limb leads), and six electrodes are placed at defined locations on the chest (precordial leads). These electrode leads are connected to a device that measures potential differences between selected electrodes to produce the characteristic ECG tracings.

Some of the ECG leads are bipolar leads (e.g., standard limb leads) that utilize a single positive and a single negative electrode between which electrical potentials are measured. Unipolar leads (augmented leads and chest leads) have a single positive recording electrode and utilize a combination of the other electrodes to serve as a composite negative electrode. Normally, when an ECG is recorded, all leads are recorded simultaneously, giving rise to what is called a 12-lead ECG[69].

Three types of ECG leads are:

- Limb Leads (Bipolar)
- Augmented Limb Leads (Unipolar)
- Chest Leads (Unipolar)

LITERATURE REVIEW

EMG FORCE AND MUSCLE:

Electromyography is the signal generated by the muscles during contraction of the muscle fibers with respond to a certain stimulus or physical activity. The rate of activation of muscle fibers depends on the firing rate of the motor unit action potentials (MUAP) [73]. The theory behind activation of muscle fibres can be interpreted as follows: The group of motorneurons located in the spinal cord activates the muscle fibers and hence lead to contraction of muscles responsible for doing musculoskeletal movements. Motorneurons that are active simultaneously generate action potentials that are mostly independent of action potentials of other motorneurons. There is some level of synchronization of motorneuron action potentials in limb muscles that likely result from common input sources [74,75]. The train of motor unit action potentials emanating at the skin surface during contraction of a muscle is collected through the differential input electrodes placed at specific active locations. The metal plate electrodes collect the surface potential difference and are plotted as an output of the instrumentation amplifier with differential amplification technology after requisite filtering and smoothing.

A lot of attempts have been made in the recent past regarding establishment of an EMG-force relationship under various circumstances. The features and quantities mined from SEMG gives useful information about the physiology and muscle activation patterns. The information obtained from EMG reflects the forces that will be generated by the muscles and the intervention timing of motor commands [73]. For example, quite a lot of studies have investigated the relationship between surface electromyography (EMG) and torque exerted about a human joint [76,77,78]. The relation of surface EMG to torque makes EMG an attractive alternative to direct muscle tension measurements, necessary in many physical assessments.

The inter-relation of the acquired EMG signal and muscle tension on mutual physiological factors gives way to conduct research work to develop mathematical models relating EMG to Force/torque and joint dynamics. The experimental studies have explored both linear and nonlinear models to achieve better accuracy [79,80].

EMG FORCE APPLICATION:

EMG-Force relationship could prove to be a highly useful model to predict and determine fatigue point, endurance level, rate of MUAP activation, condition monitoring of the performance of neuromuscular system, rehabilitation and recovery [78,80]. The estimation of a parameter which follows the trend line of the EMG signal generation rate has always been a matter of interest among the researchers working with EMG and its related fields. This is still an open area of research until a successful model is established which can predict and determine physiological conditions of the neuromuscular system.The force produced by the muscle is directly proportional to Vrms value.

DENOISING:

In the time of signal acquisition there might be some types of noise present there like Contact noise (This is happened when the electrode for a instants out of contact) ,Motion noise(this is due to the movement of subject electrode moves from skin position) or Electromagnetic nose(this is due to electromagnetic component activation).

So the acquired signal needs to be denoised as they have very lower value. The biosignals (EMG) are non-stationary in nature so fourier transformation for denoising has major drawback so wavelet based denoising can be done.[] Since 1990 the wavelet based research most widely used. For wavelet thresholding can be done by manually or by run a suitable program. The discrete wavelet transform mostly used rather than continuous wavelet transform.[45,46]

EMG SIGNAL AND MULTICHANNEL APPLICATION FOR WEIGHT LIFTING:

Now a day's new development for multichannel detection of EMG signals for different locating muscle groups. Which provide huge space of determination of various muscle groups condition at the same with various working condition.

EMG signal analysis was attempted to find the muscle activation or force produced by muscles during lifting heavy load. Different muscle groups reaction with load are varies from each other. To improve joint or back pain this study was established as a proper guidance [47,48]. The muscle force with various weights can help to improve muscle pain reduction

using devices. The weight variation can be used for better body posture conception during this type of work[49] [50] . We can set window to check different muscle activity during no-load , variation of load condition. But this type of work without various age groups could not be fully completed. We can establish a relation between RMS value with time domain as well as with MVC and force .

COMPLEXITY MEASUREMENT:

The EMG force technology has subsequently improved, last few years the complexity measurement on muscle was highly applied. Every biological system including neuromuscular system or cardiovascular are multiscale system, they normally behave with nonlinear , nonstationary and highly complex characteristics. When load is applied on biosystem the complexity changes with time[53]. The complexity determination generally obtained by fractal dimension analysis. A modified method for complexity measurement Higuchi's fractal dimension. Generally when a load is applied on biological system the muscle complexity decreases[55]

FRACTAL:

An important characteristic of all fractal objects is that their measured metric properties, such as length or area, are a function of the scale of measurement. [87] This can be explained by the classic example used by Mandelbrot himself in 1967 to describe the "length" of a coastline (Mandelbrot, 1967). According to Mandelbrot, the length of a coastline depends upon the length of the ruler used to measure the coastline. By using a large scale, the intricate details of the coastline cannot be captured. On the other hand, using an infinitely small scale, the length of the coastline will be infinitely large. When measured at a given spatial scale d, the total length of a crooked coastline L(d) is estimated as a set of N straight-line segments of the length d. Since, the small details of the coastline not recognized at lower spatial resolutions but become apparent at higher spatial resolutions, the measured length L(d) increases as the scale of measurement of increases. This, in fractal geometry, the Euclidean concept of "length" becomes a process rather than an event, and this process is controlled by a constant parameter[31,37].

EFFECT OF YOGA:

Any type of physical exercise induces the variation in the Autonomic nervous system (ANS) to maintain the physiological homeostasis behaviour. The parasympathetic changes causes a significant variation on muscles or cardiovascular system.The yoga exercise always interact with physical activity as well as respiratory system exercise as a result the effect is much more higher on ANS. The nolinear chaotic and frequency domain analysis induced a clear rhythmic pattern. The exercise also causes change of the heart rate value. The statistical value could not reveal any significance if parasympathetic of sympathetic component present.The heart rate variability also changes due to yoga exercise[25].

HEART RATE VARIABILITY (HRV):

Earlier it was believed that the heart beats regularly with a fixed rate. It was after the technological advancement when more precision of measurements of heart rate (HR) were done some amount of variability was observed1. The clinical relevance of heart rate variability (HRV) was first appreciated in 1965 when Hon and Lee [28] observed that fetal distress was preceded by alteration in inter beat intervals before any appreciable changes occur in the actual heart rate. Then Sayers and others had focused attention on the existence of physiological rhythm in beat to beat heart intervals [50]. HRV is basically the fluctuations between R-R intervals. R-R intervals are highly random and complex so some times HRV may not detect in time domain analysis so the nolinear analysis have been introduced to measure the fluctuations. Now a days software tools are developed to measure HRV. Pan Tomkins algorithm most widely used for finding QRS peak detection. Pan Tomkins algorithm introduced digital bandpass filter, which improves the signal to noise ratio and permits the lower threshold. This increases the overall detection sensitivity.

NONLINER BEHAVIOUR – USING HIGUCHI FRACTAL DIMENSION:

Fractal dimension was included into performed analysis because the index ranging from 1(for deterministic curves) to 2(for random series) reflects the complexity of signal.

The problem with fractal dimension lies in the fact that there are several quite different quantities that are called ‘fractal dimension’. Different methods of waveform characterization based on different algorithms of fractal dimension calculations have been proposed. Fractal

dimension of a waveform representing a single in time domain is a measure of the signal's complexity and should not be confused with fractal dimension(e.g. point wise correlation dimension) of an attractor eventually observed when the time series is embedded in so called phase space. The time series is divided into non-overlapping segments of my samples. Consider the samples in the i-th position inside each segment. The distance between those samples can be calculated as their absolute difference. If the normalized sum of all the distances of the samples in the i-th position is calculated for each position, and then averaged, the result is a measure of the length of the time series. The Higuchi's algorithm involves computing the length of the time series over a certain range m. The slope of the line fitting the log-log plot of the lengths as a function of 1/m gives a measure of the fractal dimension of the time series, i.e. how the length of the time series scales. In the literature many other algorithms are available for the estimation of the fractal dimension of a time series, although Higuchi's is one of the most used in the biomedical domain[38]. Because a simple curve has Euclidean dimension equal 1 and a plane has dimension equal 2 value of Higuchi fractal dimension (D) is always between 1.0 (for a straight line or a simple Euclidean curve) and 2.0. This method is basically nonlinear analysis which indicates the complexity measurement of any biological system[38,76,80].

TOOLS AND TECHNIQUES

EMG RMS:

The EMG signal acquisition purpose we used the RMS 4 channel ALERON 401 EMG machine and for data conversion, we have checked have used RMS EMG SALUS software version. Here the surface electrodes are used. The sampling frequency of this EMG system is 4600Hz/sec.

ECG RMS:

Similarly when ECG signal was taken the acquisition process was bye RMS Vesta 121i ELECTROCARDIOGRAPH Machine with RMS active software. The ECG machine gives the flexibility of 12leads, 6leads, 3leads ECG signal acquisition. We can also set various data storage time according to our requirement. We can also set high pass, low pass frequency with a notch. The flexible Gain and sweep set up also present in this system.

MATLAB:

The MATLAB® (matrix laboratory) is a multi-paradigm numerical computing environment. It is a proprietary programming language, which has been developed by MathWorks. MATLAB allows users to manipulate, plotting of functions and data, algorithms implementation, user interfaces (UI) creation. Programs written in other languages, such as C, C++, C#, Java, Fortran and Python can be interfaced using MATLAB. Although it is developed primarily for numerical computing, an optional toolbox with MuPAD symbolic engine is there. Which allows the user to access the symbolic computing abilities. For dynamic and embedded systems there is an additional package, Simulink. It adds graphical multi-domain simulation and model-based design features

For EMG based application we used the following parameter

I. RMS value
II. Higuchi fractal dimension(HFD)
III. PSD plot

For denoising, we used the wavelet transform technique. Since biosignal is a very low range of amplitude it needs to be noise free properly.

WAVELET:

Fourier analysis has a serious drawback. In transforming to the frequency domain, time information is lost. When looking at a Fourier transform of a signal, it is impossible to tell when a particular event took place. If a single doesn't change much over time – that is, if it is what is called a stationary signal – this drawback isn't very important.

Therefore, to overcome the drawbacks in the analysis of multi-resolution non-stationary signals different techniques evolved. Although the first significant development in this field was done with the introduction of the windowing techniques suggested by Denis Gabor (1946) is short time Fourier transform or STFT algorithm. The STFT is based on Fourier transform of smaller section of a signal a time, which is known as windowing. It maps a signal into a two-dimensional function of time and frequency. The main drawback in this method is about the choice of the window length since once a window length is selected it remains fixed for all the other frequency components of the signal. Many a time it is required for a more flexible approach especially in case of physiological signals. The next logical step to overcome the limitations of STFT was the wavelet analysis which is based on the windowing technique with variable sized regions. It is to be noted that wavelet analysis does not incorporate the Time-Frequency region rather it is based on Time-Scale region, shown below. Before we move to further discussion on wavelet transform and analysis, we need to investigate the sense of scale in case of 1D signal analysis. Here we used wavelet discrete wavelet (DWT) transform because continuous wavelet transforms (CWT) produces the redundant signal representation, while DWT critically sampling with a great reduction in dilation and shift[77-78].

Signal and image can be analyzed in Wavelet Toolbox™. The toolbox includes algorithms for continuous wavelet analysis, wavelet coherence, synchro squeezing, and data- adaptive time-frequency analysis. The toolbox also includes apps and functions for decimated and non-decimated discrete wavelet analysis of signals and images, including wavelet packets and dual-tree transforms.

It can explore how spectral features evolve over time, identify common time-varying patterns in two signals, and perform time-localized filtering using continuous wavelet analysis. Discrete wavelet analysis can be used to analyse signals and images at different resolutions to detect change points, discontinuities, and other events not readily visible in raw data. Signal

statistics on multiple scales can be compared and fractal analysis of data can be performed to reveal hidden patterns. With Wavelet Toolbox user can obtain a sparse representation of data, useful for denoising or compressing the data while preserving important features.

The Wavelet Toolbox^{TM} GUI can be accessed by typing the command 'wavemenu' in the MATLAB command line.

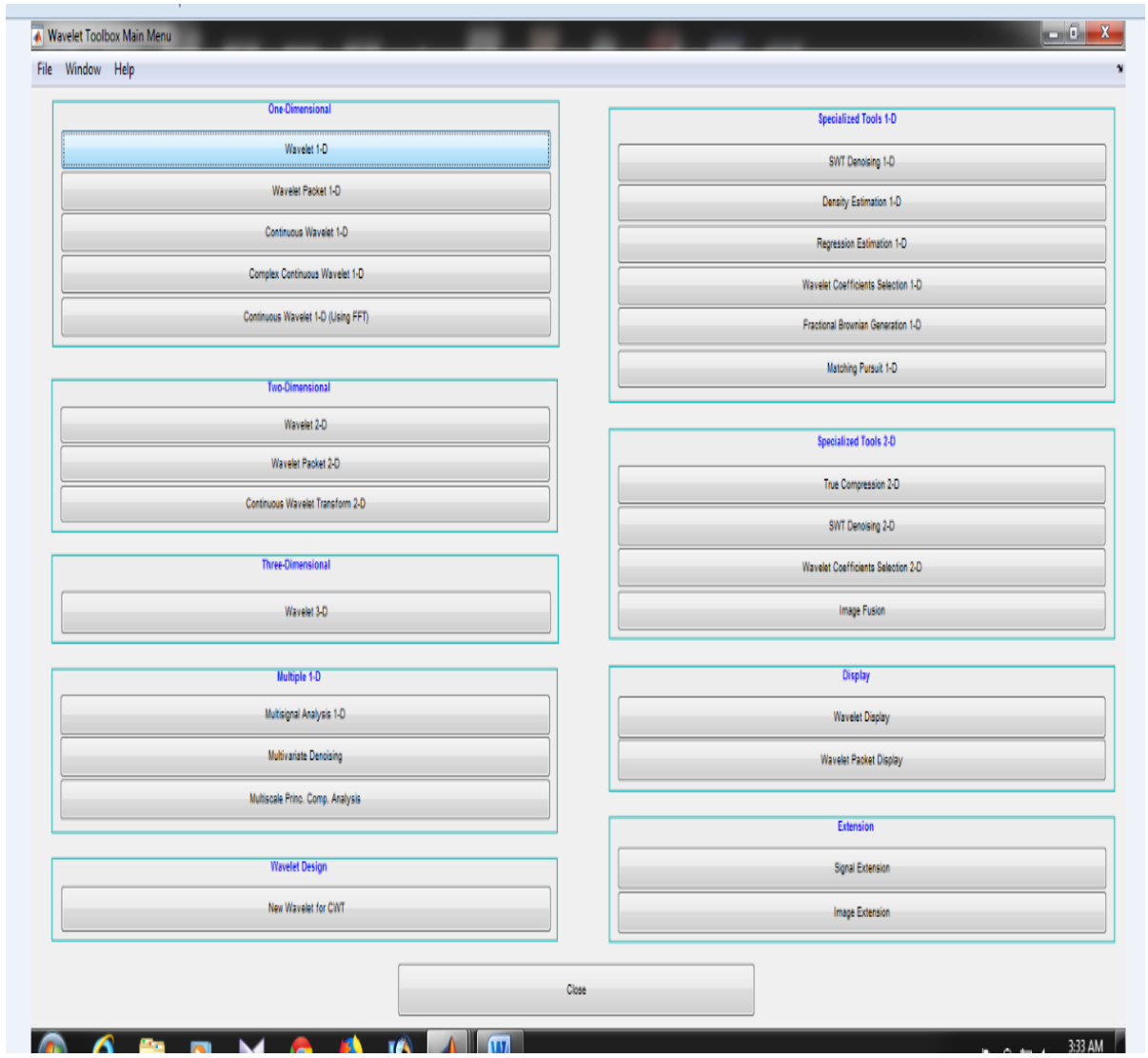

Fig3.1: Wavelet toolbox.

RMS VALUE:

The amplitude of the EMG signal is stochastic (random) with a Gaussian distribution which ranges from 0 to 10 mV (peak to peak). The RMS represents the square root of the average power of the EMG signal for a given period of time. It is known as a time domain variable because the amplitude of the signal is measured as a function of time.

$$x_{\text{rms}} = \sqrt{\frac{1}{T_2 - T_1}\int_{T_1}^{T_2} [f(t)]^2 \, dt}$$

Applications of the EMG Variables :

- To determine the activation timing of a muscle (on and off) - use raw EMG signal
- To determine the degree of activation - use RMS
- To estimate force produced by a muscle - use RMS.

FRACTAL ANALYSIS:

The term "fractal" was first used introduced by mathematician Benoit Mandelbrot in 1975 and is derived from the Latin word *frāctus* which means "broken" or "fractured" and used it to describe objects whose complex geometry cannot be characterized by an integral dimension. [30,31] The main attraction of fractal geometry lies in its ability to describe the irregular or fragmented shape of natural features as well as other complex objects that traditional Euclidean geometry fails to analysis.

HIGUCHI'S FRACTAL ANALYSIS METHODE:

Higuchi's fractal dimension (HFD) used to measure the complexity of the biological system

Higuchi's fractal dimension (HFD) is effective in that aspect as this method gives an idea about the complexity of the system [58,59].This method calculates the fractal dimension of a time series directly in the time domain. For a time series expressed as *X(1), X(2),... X(N)* the algorithm first constructs k new time series as:

$$X_m^k : X(m), X(m = k), X(m = 2 * k) \dots \dots \dots, X\left(\left[m\frac{N-k}{k}\right] . k\right)$$

$$m = 1,2,3 \dots k$$

From=1,2,.....k. Here *m* is the initial time, *k* is the interval time, *int(r)* is the integer part of a real number *r*. Then 'length' Lm of each curve is expressed as:

$$Lm(k) = \frac{\frac{1}{k}\left[\sum_{i=1}^{int(\frac{N-m}{k})} |X(m + i.k) - X(m + (i-1).k)\right] * \frac{N-1}{int(\frac{N-m}{k}).k}}{k}$$

Where N is the total number of samples and $int\left(\frac{N-m}{k}\right).k$ is the normalization factor.

Finally, *L(k)* is plotted with time interval k as the average value of k. the fractal dimension can be obtained by logarithmic plotting of L(k) against the different value of k ranging to Kmax.

The curve of fractal follows the given equation:

$L(k) \propto k^{-D}$

D is the fractal dimension obtains from the curve.

The appropriate value of Kmax is determined by initially plotting values of the fractal dimension(FD) for different values of k. The k value which after the FD is saturated, called as Kmax value[36].

When we entered into ECG based approach the followings tools and technique were used for analysis:

ECG PEAK DETECTION: PAN TOMPKINS ALGORITHM:

The QRS peak detection algorithm introduced by Jaipur Pan and Willis J. Tompkins is most widely used and often cited algorithm for the extraction of QRS complexes from electrocardiograms, [79] ECG is first passed through a series of low-pass and high-pass filters. Then the filtered signal is passed through derivative, squaring and window integration phases. Finally, a thresholding technique is applied, and the R-peaks are detected.

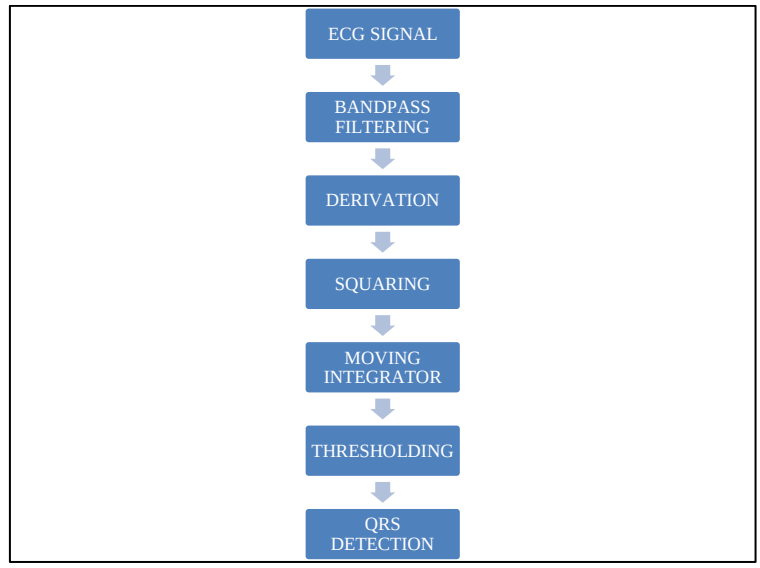

Fig 3.2-Pan Tompkins QRS detection algorithm follow chart

The purpose of the bandpass filtering is to isolate the predominant QRS energy centred at 10 Hz and to attenuate the low frequencies characteristic of P and The waves and baseline drift, and also remove higher frequencies associated with muscle noise and power line interference. The next processing step is differentiation, which is a standard technique for finding high slopes that distinguish the QRS complexes from other ECG components. All of the above processes are accomplished using linear filters. Next is a nonlinear transformation that consists of point-by-point squaring of the signal samples. This is done to make all the data positive prior to subsequent integration, and also makes the higher frequencies in the signal obtained from the differentiation process more conspicuous. These higher frequencies are normally characteristic of the QRS complex. The squared waveform passes through a moving window integrator. This integrator sums the area under the squared waveform over a 150-ms interval, then moves forward by one sample interval, and then integrates the new 150-ms window. The windows width is chosen to be long enough to include the time duration of extended abnormal QRS complexes, but short enough so that it does not overlap both a QRS complex and a T wave. Adaptive amplitude threshold applied to the bandpass- filtered waveform and to the moving integration waveform is based on continuously updated estimates of the peak signal level and the peak noise. After preliminary detection by the adaptive thresholds, decision processes make the final determination as to whether or not a detected event was a QRS complex. A measurement algorithm calculates the QRS duration for QRS detection. From this algorithm RR intervals and the QRS detection process can be done[70,71].

LOMB -SCARGLE PERIODOGRAM:

RR tachogram is developed by sampling the heart (ECG signal) once per beat, which is thus uneven in time. Since the Fourier transform algorithm requires even sampling, it is necessary to re-sample the tachogram using interpolation. However, this approach has its own sets of problems: for example, linear interpolation is a poor approximation, and cubic splines create unacceptable oscillations when one RR interval is unusually longer than its predecessor. In order to avoid the drawbacks of interpolation, one method is to compute the Fourier spectrum directly from the unevenly sampled tachogram. The Lomb periodogram is an excellent method for the operation since it weights the data on a point-by-point basis rather than on a per-interval basis. It has been shown that the Lomb periodogram can provide a more accurate

estimate of a tachogram's power spectral density (PSD) than interpolation followed by a regular Fourier transform. [80].

The Lomb-Scargle periodogram (Lomb 1976; Scargle 1982) is a well -known algorithm for detecting and characterizing periodicity in unevenly sampled time-series. The Lomb-scargle method works directly with the nonuniform samples and thus makes it unnecessary to resample or interpolate. [72].

The periodogram at frequency f is determined by:

$$Pls\ (f) = \frac{1}{2a^2} \quad \{\frac{[\sum_i X_i \cos\ \omega(t_i - T)]^2}{\sum_i cos^2\ \omega(t_i\ - T)} + \frac{[\sum_i X_i \sin\ \omega(t_i - T)]^2}{\sum_i sin^2\ \omega(t_i\ - T)}\}$$

Here the term T is the time delay, which is estimated by the following formula:

$$\tan 2\omega T = \frac{\sum_i sin2\omega t_i}{\sum_i cos2\omega t_i}$$

Thus, spectral estimation of HRV data, which is non-uniformly sampled in time, can be computed using Lomb-Scargle periodogram. The Lomb-Scargle periodogram is computed using the function *plomb*. From the obtained periodogram we can calculate the power of spectral bands --- Low-Frequency (LF) band (0.04 to 0.15 Hz) and the High -Frequency (HF) band(0.15 to 0.4 Hz).

HRV parameters reflect the effect of sympathetic and vagal components of the autonomic nervous system (ANS) on the SA rhythm generation. HRV parameters can be classified as:

- Frequency-domain parameters
- Nonlinear dynamic (HFD)
- Time domain parameter

Here we take all normalized value, which is normal to normal value.

SDNN: The standard deviation of the normal to normal (NN) intervals

MEAN: This the mean value of HRV

LF: This is the low-frequency component of HRV

HF: This is the high-frequency component of HRV.

LF-HF ratio: LF component divided by the HF component.

HRV: Fluctuations between RR interval.

METHODOLOGY RESULTS AND DISCUSSION

ESTABLISHMENT OF EMG-FORCE RELATIONSHIP OBTAINED DURING SIMULTANEOUS VOLUNTARY CONTRACTION OF BICEPS AND FLEXOR DIGITORUM PROFUNDUSMUSCLES:

DESIGN OF EXPERIMENT:

We have taken 8 healthy individuals as subjects (5 Female, 3 Male) and their mean age, height and weight are as follows 23.75±1.98 Years, 157.63 ± 5.80 cm, 58 ± 8.70 Kg. The subjects were asked to apply force through a hand dynamometer with %MVC points marked on it on a scale of 1 to 10 as shown in fig.1. The subjects were asked to hold for 3sec in 0%, 20%, 40%, 60%, 80% and 100% MVC points. The transition time from one point to the other was taken as 1 sec. To ensure uniform transition time among subjects each individual was properly trained to work according to the instructions. The total time length of the experiment was 26 sec.

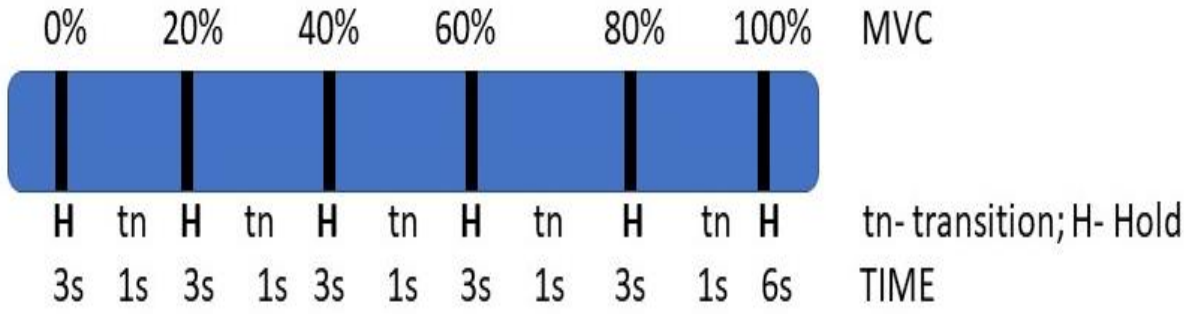

Fig.4.1. MVC scale, time and position details of the hand grip strength dynamometer.

The targeted muscle group in our case was Biceps Brachii and Flexor Digitorum Profundus located on the upper arm and lower arm subsequently. These two muscles of the human arm perform a lot of function which we do with our hand. During the application of the force by the subject on the dynamometer, these two muscles start working in maintaining the desired movement. We have simultaneously recorded their activity while performing the task as shown in fig.2.

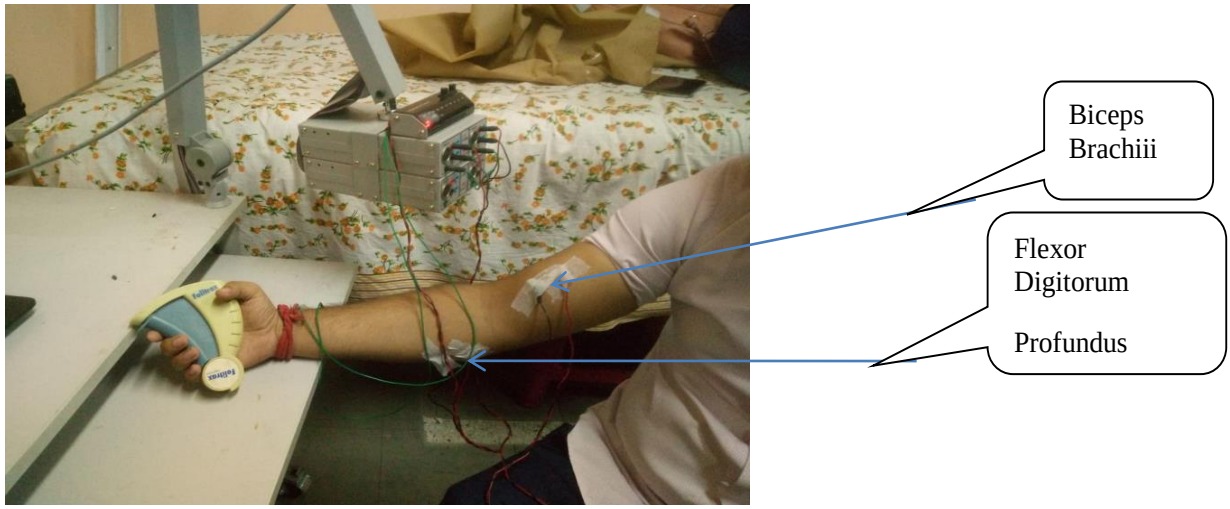

Fig4.2. EMG signal acquisition Protocol

EMG ACQUISITION:

EMG signal from two channels is collected using RMS SALUS EMG, NCV and VEP machine. The 2 Channels for surface EMG signal acquisition collected data simultaneously from two different muscle groups as mentioned earlier. The electrodes used were metal surface disk type, which was attached to the skin surface enclosing the targeted muscle group. To make the signal noise free and ensuring proper contact, a conducting gel is applied over the skin-electrode interface. The gap between the differential input electrodes of each channel was kept between 2 to 3 cm [14]. The ground electrodes were placed over the bony part of the wrist, which served as the active driven ground connection for proper attenuation of common mode signal and high-frequency noises. The filter settings were kept as High Pass cut-off 20Hz and Low Pass cut-off 500Hz. Sensitivity was set at 100 µV. The signal was continuously acquired during the 26 sec time duration of the designed experimental protocol. The amplitude response of the signal for the first 20 seconds is shown in fig.3.

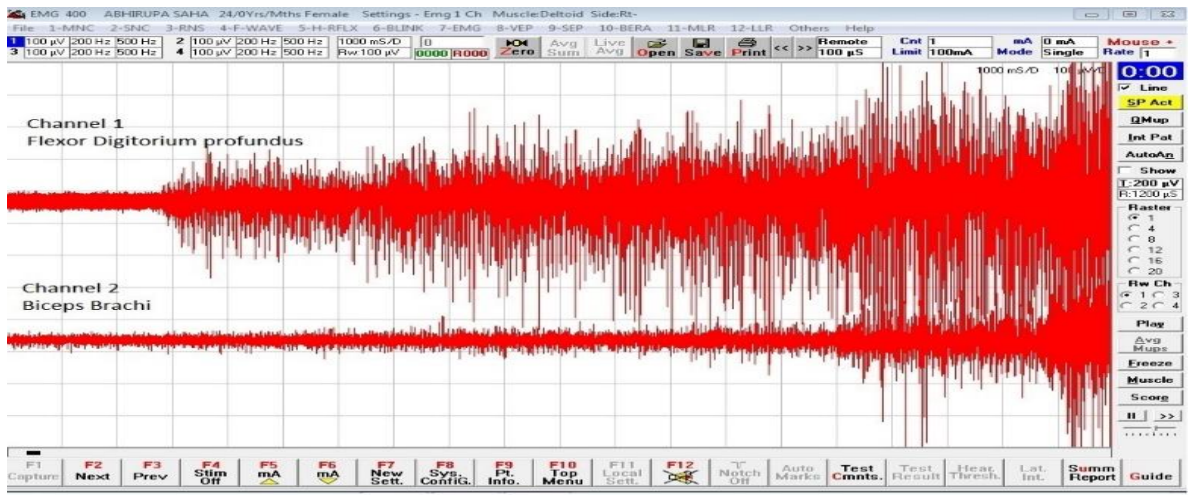

Fig4.3. EMG signal response for 20 sec during Voluntary Contraction of muscles.

ANALYSIS:

The signal is opened in the analysis software of the EMG machine for offline viewing and analyzing. A one-second window is chosen and Vrms along with Vpp is noted for each window. Therefore, we get 4 sets of values for each subject viz. Channel 1 Vpp and Vrms, Channel 2 Vpp and Vrms for each 1-sec window. The whole signal has got 26 windows hence we obtain a matrix of 4x26 dimension for each subject. All the data entries of each subject are made using Microsoft© Excel. The proforma of the data logging sheet is shown in Table 1. Now to obtain a direct relationship between Vrms or Vpp with %MVC, a curve has been plotted. In this curve, the x-axis forms the %MVC values (6 points) and the Y-axis is Vrms or Vpp averaged during each 3 sec time intervals. The 26 points from the matrix is clubbed together (averaging) in the following pattern (3), (3+1), (3+1), (3+1), (3+1), (6+1) to obtain corresponding 6 points of the Y-axis. From the plot of %MVC with Vrms and Vpp curve fitting tool has been applied to obtain a linear approximation of the sparse data. The equations obtained can be used to test its accuracy in predicting fatigue point of the individual person.

Subject 1	Time in Sec	1	2	3	…	…	…	25	26
Channel 1	Vpp								
	Vrms								
Channel 2	Vpp								
	Vrms								

Table 1. The proforma of the data logging sheet of each individual subject.

RESULTS AND DISCUSSION:

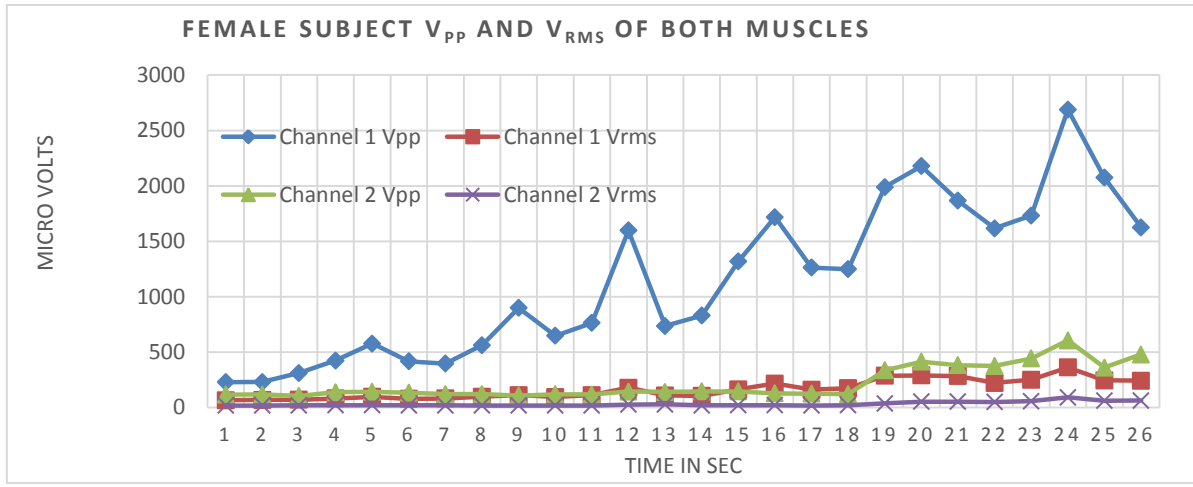

(a)

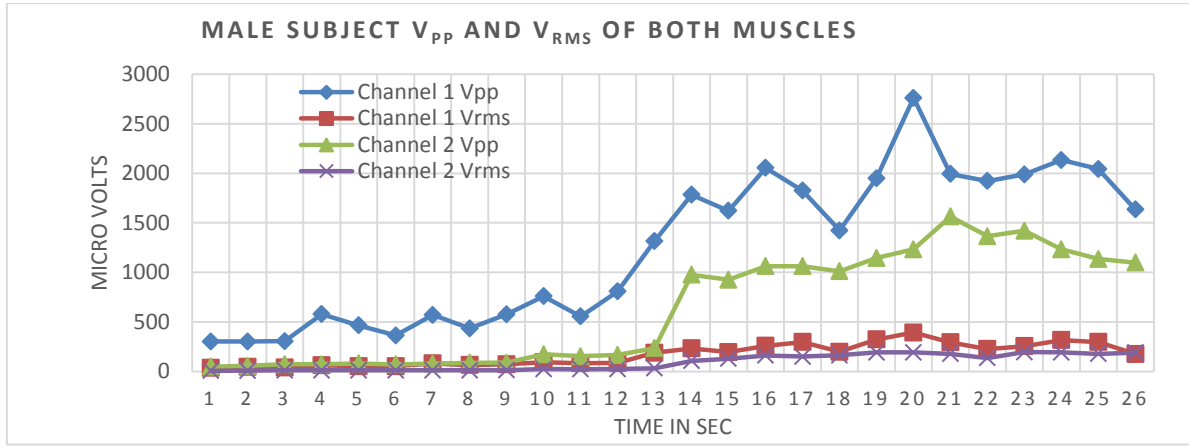

(b)

Fig4.4. (a) Female and (b) Male subjects Vpp and Vrms plot of both the channels w.r.t time in seconds.

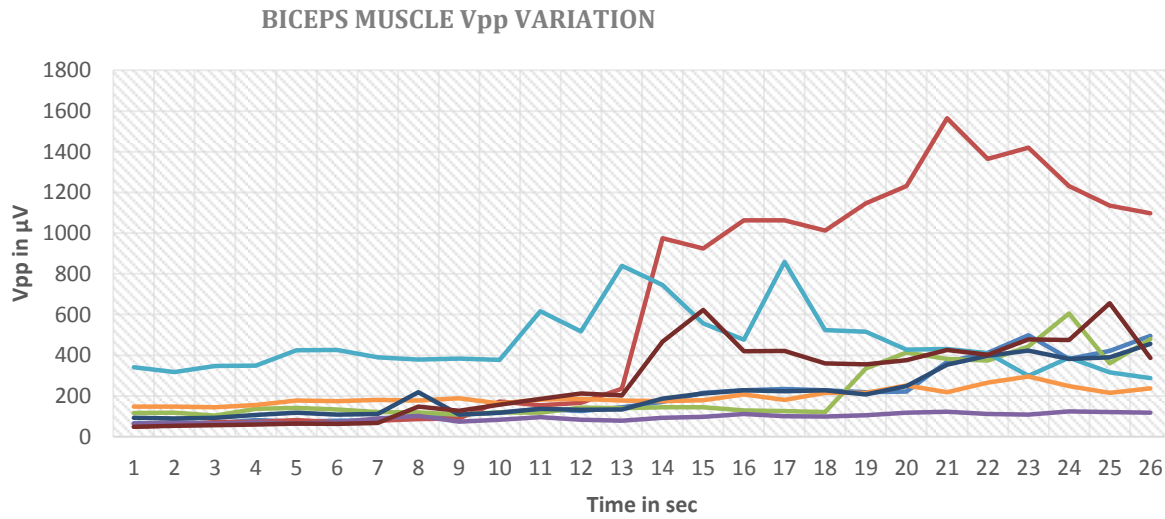

Fig4.5(a). Vpp variation of all the subjects data acquired from Biceps Muscle (Channel 2) w.r.t time in seconds.

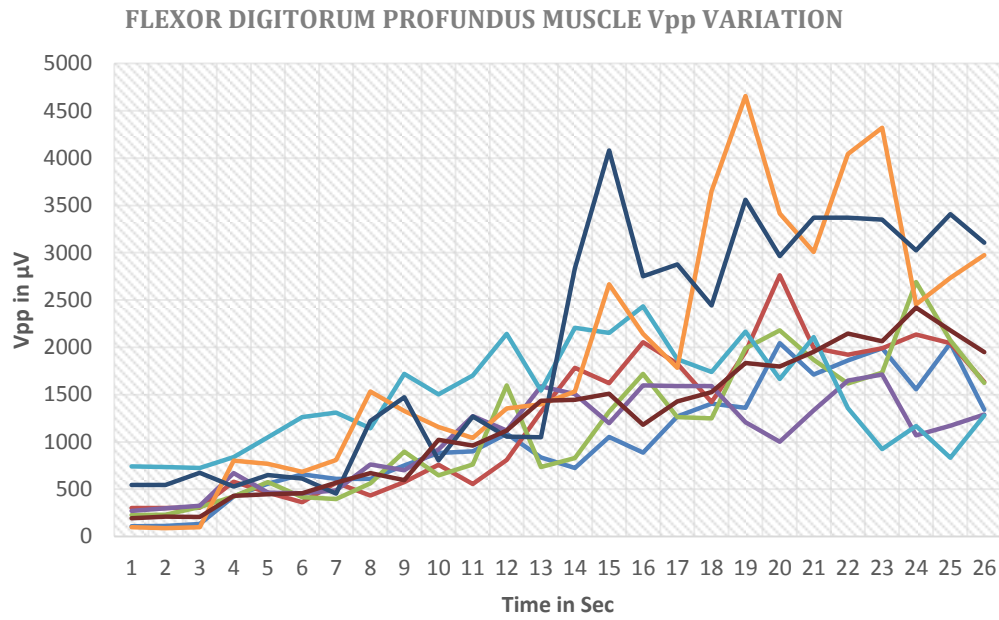

Fig4.5(b). Vpp variation of all the subjects data acquired from Flexor Digitorum Profundus (Channel 1) w.r.t time in seconds.

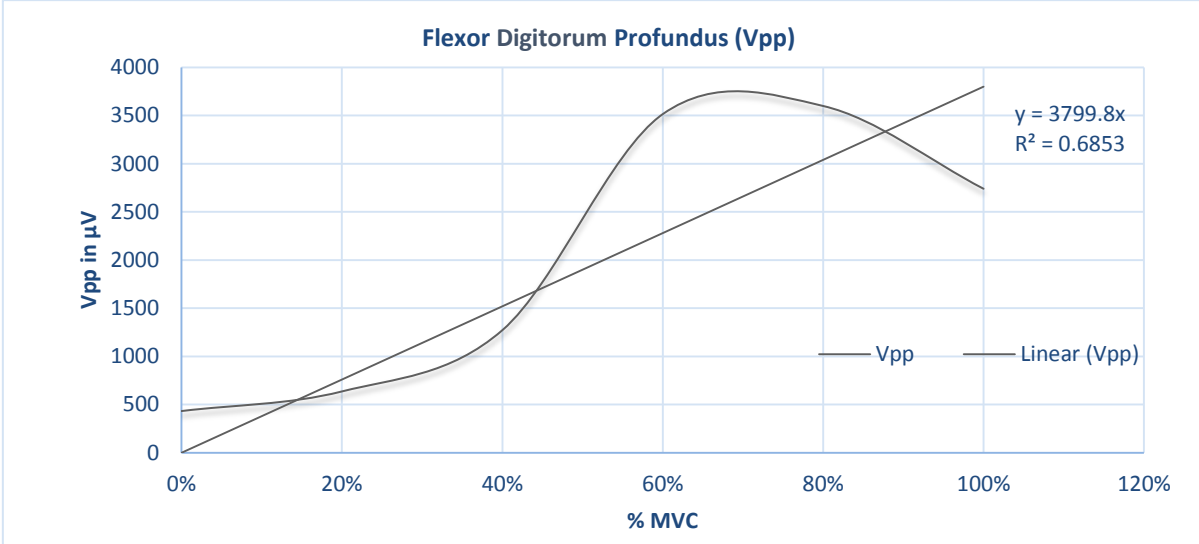

Fig4.6(a). Plot of Flexor DigitorumProfundusVppw.r.t %MVC

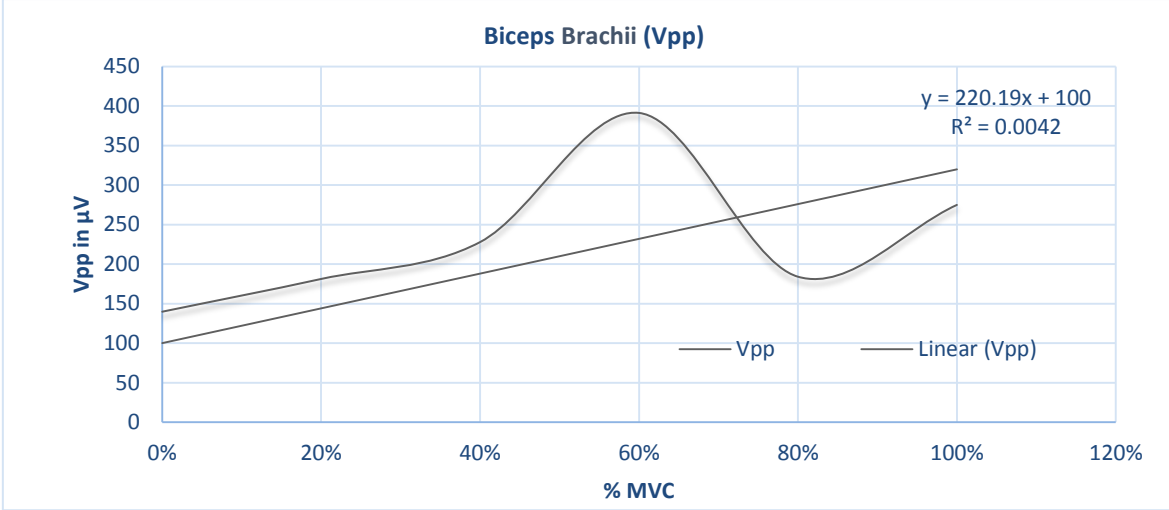

Fig4.6(b). Plot of Biceps Muscle Vpp w.r.t %MVC

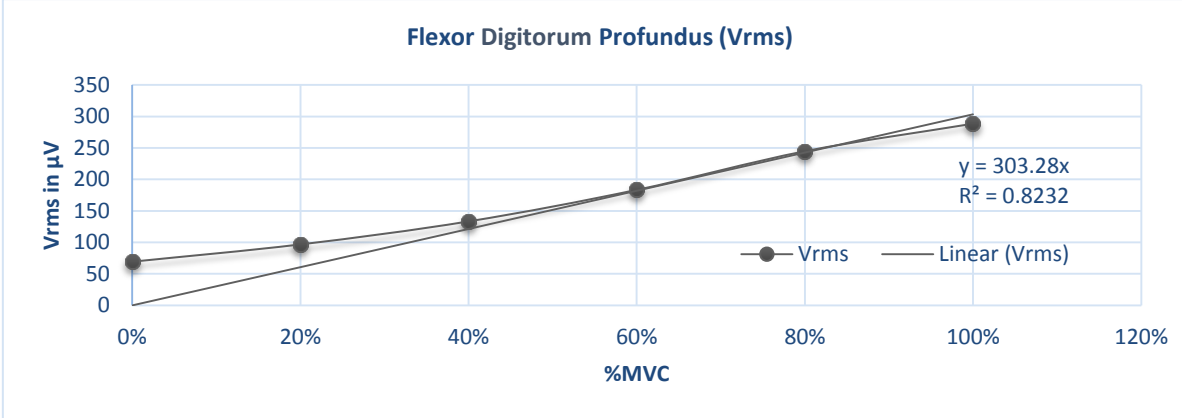

Fig 4.7 – Vrms plot with flexor digitorum profundus.

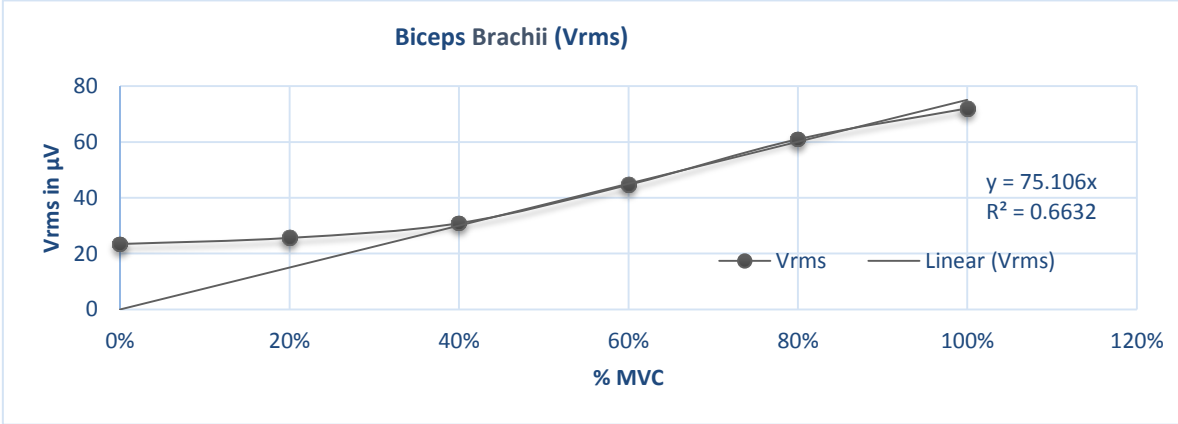

Fig 4.8 – Vrms plot with flexor biceps brachii

DISCUSSION:

The results as obtained are shown in the respective plots constructed using the data collected from the experiments. The first two plots in Fig.4(a) and (b) shows the difference in the variation of all parameters of both the muscles of one female and one male subjects. From these to plots one can infer that, be it male or female the trends from the plotted data suggest that they closely follow each other. The Vpp values of channel 1 have the most fluctuations and higher amplitude, both in case of males and females. The Vrms shows many fluctuations but overall amplitude is less in both the case. Therefore, be it male or female the rate of recruitment of motor units is dependent on the force applied to the hand dynamometer. Moreover, we can see that there is a significant difference in trends obtained from two different channels.

Based on this fact, we have plotted Vrms and Vpp of all the subjects separately for channel 1 and channel 2, as shown in Fig. 5(a) and (b). We have observed that beyond the 13-sec mark, there is a sudden rise in Vpp and Vrms values of nearly all the subjects. This point is the region of60% MVC where the recruitment of motor units rises rapidly.

To establish an EMG-Force relationship, we have separately tested for the values of Vrms and Vpp for both the muscle groups w.r.t the applied force (%MVC). The plots in Fig.6(a) and (b) shows the Vpp v/s %MVC of both the muscles respectively. The plots in Fig.7(a) and (b) shows the relationship between Vrms and %MVC respectively for Flexor DigitorumProfundus and Biceps Brachii.

From % MVC plot we can see that after 60% MVC there is fall in the values of Vpp. The curve obtained has a high degree of non-linearity so a linear approximation of the data distribution is not a feasible option but it is shown to estimate how much deviation it has from the linear trend of the curve. Therefore, we can at least conclude that after 60% MVC the rate of generation of higher peak MUAP begins to reduce since the muscles attain a level of saturation as most or all of the motor units have been employed to bear the tenacity after 60% MVC.

Now as we have also plotted the Vrms v/s %MVC of both the muscle groups, some interesting points about recruitment pattern or firing rate of the motor units have been noticed. We can see that between 40% and 80% MVC is the linear region of the curve. Therefore, we can say that after the application of the force of 40% MVCupto 80% MVC the

rate of generation of MUAP to counter the force is linear, then it slowly starts decreasing. There is always certain residual energy present in the muscles, therefore even at 0% MVC or no contraction, the value obtained is higher than zero.

METHODOLOGY EMG WATER BUCKET LIFTING EMG EXPERIMENT:

In this particular experiment, our goal is to study the effect of load on two muscles groups while carrying the water bucket. The experiment is done with two different human body postures and three types of weight (water bucket load). This work is divided into three stages:

I. Lifting water bucket
II. Holding water bucket
III. Dropping water bucket

Physiological Event: The physiological event for this experiment is shown below:

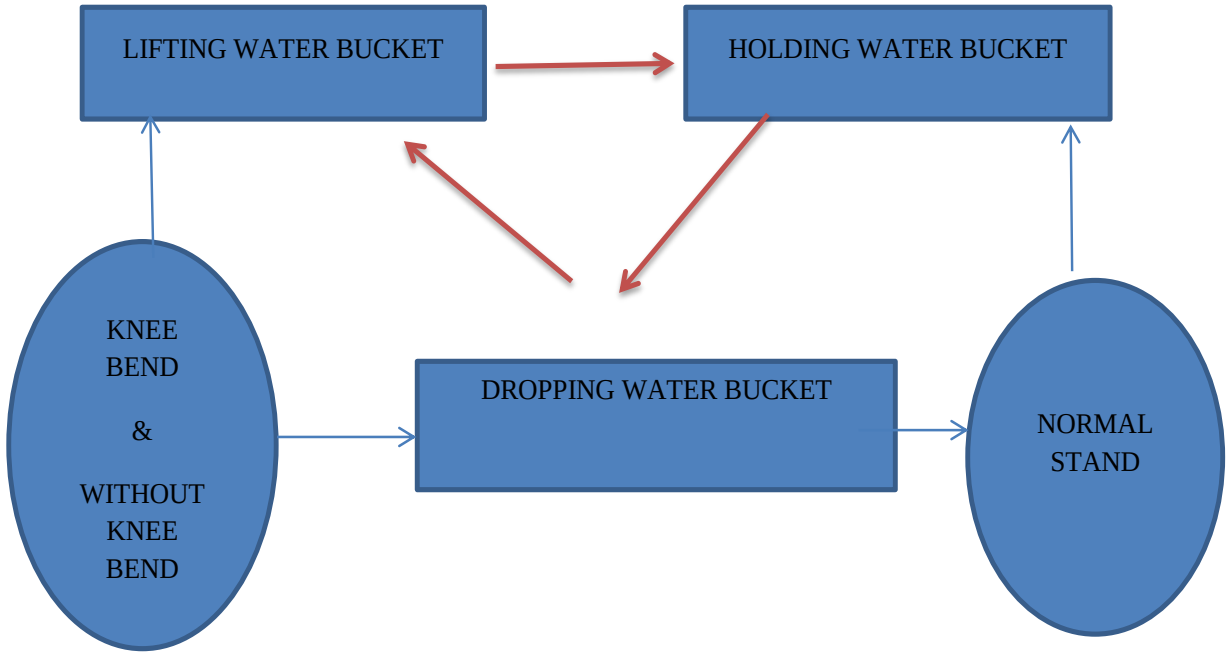

Fig4.9. Physiological event on water bucket lifting holding and dropping back

EXPERIMENTAL PROTOCOL:

The subjects are given two body postures condition while lifting and dropping back the water bucket :

I) Knee Bend

II) Without Knee Bend

While in all cases in the time of holding water bucket subjects were asked to stand normally. Here during the exercise three water bucket is used (15kg, 10kg, 5kg).

At first, the subjects were asked to lift the 5kg water bucket with knee bending body within 5 seconds posture and hold it at normal standing position. Finally after 50 seconds of holding they were asked to drop down water bucket within 5seconds.

After 2 minutes rest, they had done the same work with a 10kg load of the water bucket. Finally, after 2min same process was followed with 15kg of water bucket load.

When the knee band condition is done the subjects repeated the same protocol without knee bend body posture.

KNEE BENDING AND WITHOUT KNEE BENDING :

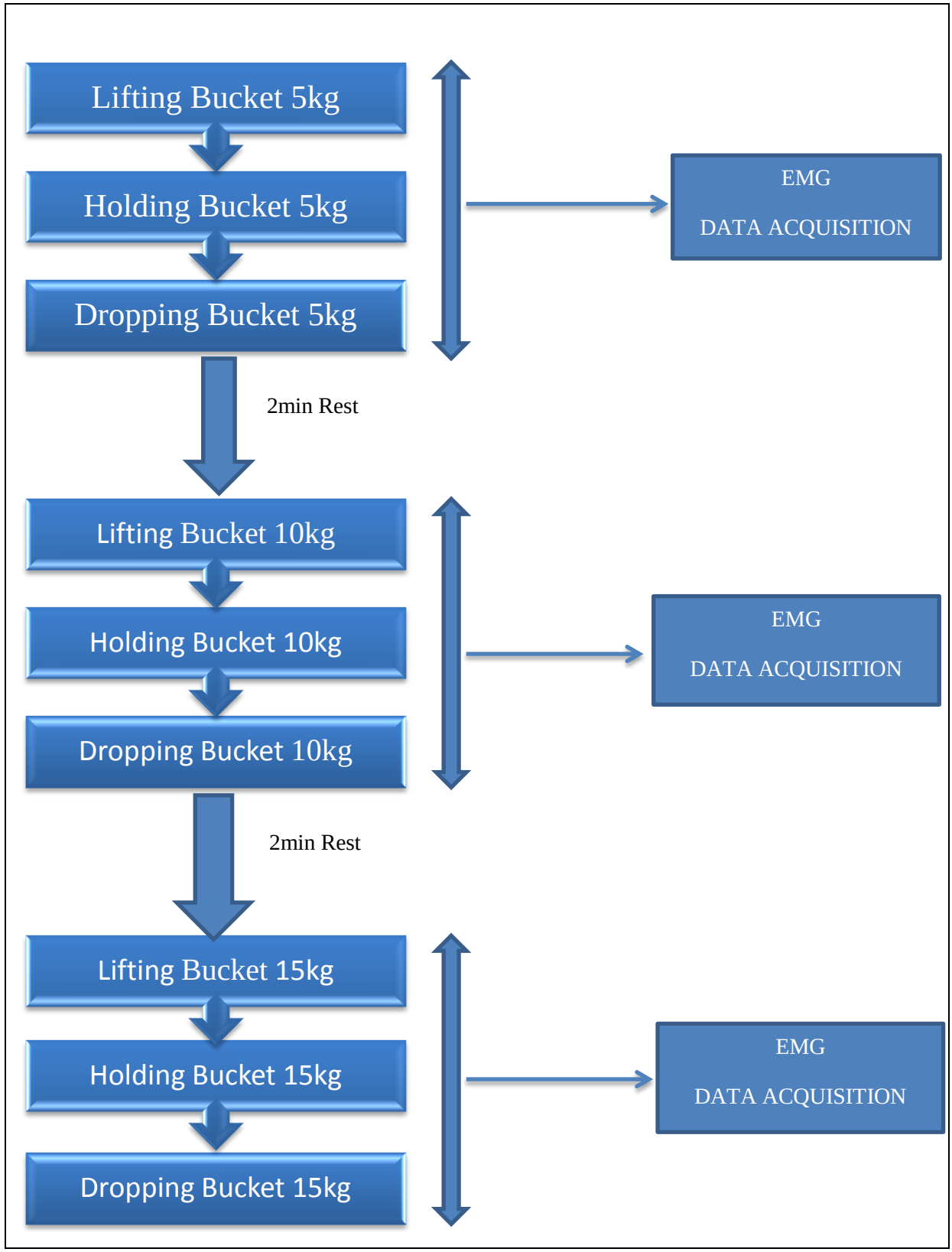

ACQUISITION AND PROCESSING EMG SIGNAL:

The EMG signal was recorded by RMS 4 channel EMG system with RMS SALUS software system. The system provides unparalleled flexibility to target maximum four muscles group at a time with user customized preset test libraries and a wide range of signal analysis applications.

Here during the whole work, two muscle groups were targeted. These two muscles group are so involved in water bucket lifting, holding and dropping back process. The EMG channels were attached to those two muscles group as:

I) Channel1 was collecting EMG signal from shoulder muscle Trapezius(shoulder muscle)
II) While Channel2 was collecting EMG signal from Triceps muscle. (shown in fig.)

Here we used metal surface disk type electrodes which were attached to the surface of the targeted muscles group. The skin was cleaned by 70% Ethyl Alcohol cleanser and also a conduction gel was applied over the electrodes to make noise free and proper contact. The gap of active and reference electrodes of each channel was kept between 2cm to 3cm. High pass filter of the system was set at 20Hz and Low pass filter was set at 500Hz. The sensitivity was maintained at 100 µv. The total duration of signal for particular bucket work was 1min 7 sec(For 5kg knee bend condition work time 1min 7sec, same time for the 10kg 15kg load. Also same time of signal acquisition for without knee bend condition was recorded).

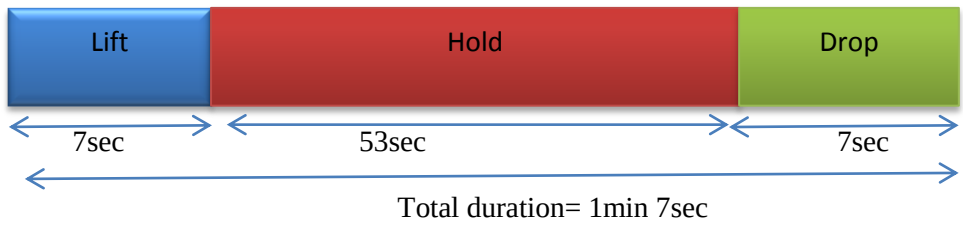

Fig 4.10 – EMG acquisition time

PROCESSING AND ANALYSIS:

For EMG signal process was done by MATLAB. Before import, the data in MATLAB the raw signal was converted into a comma separated value (.csv) value by RMS EMG ALERON

software, which gave the value in Microsoft Excel. The excel data then was imported in MATLAB and followed the given steps:

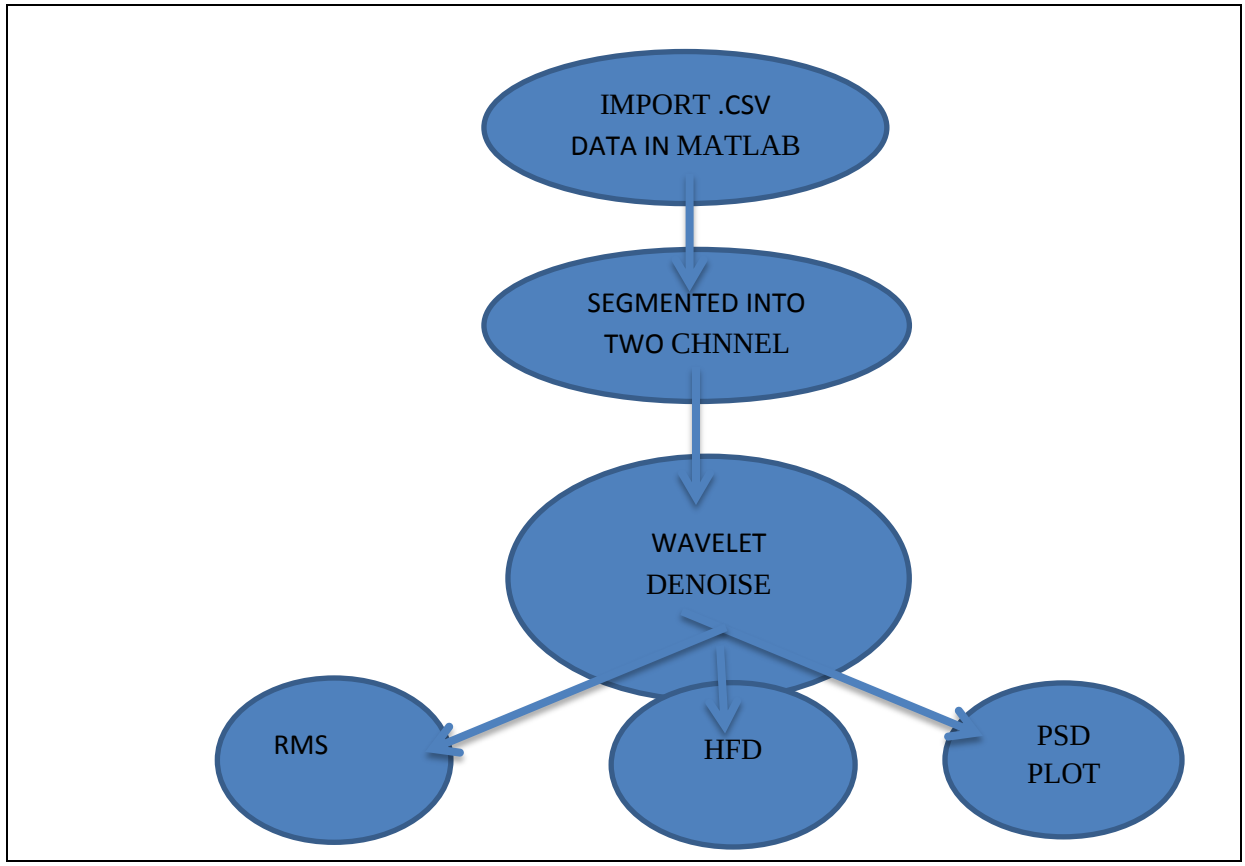

Fig 4.11- EMG bucket lifting analysis

The biosignals have a low range so the effect of noise on biosignals is higher so we used Wavelet denoising process

Vrms value gives us the clear picture determines the degree of activation and also estimate force produced by the muscle.

The complexity of the muscular system during this whole work was determined by the Higuchi fractal dimension (HFD) technique.

Wavelet denoising was done by wavelet 1-D. for manual thresholding was processed by using Daubechies6 (DB6) level 9.

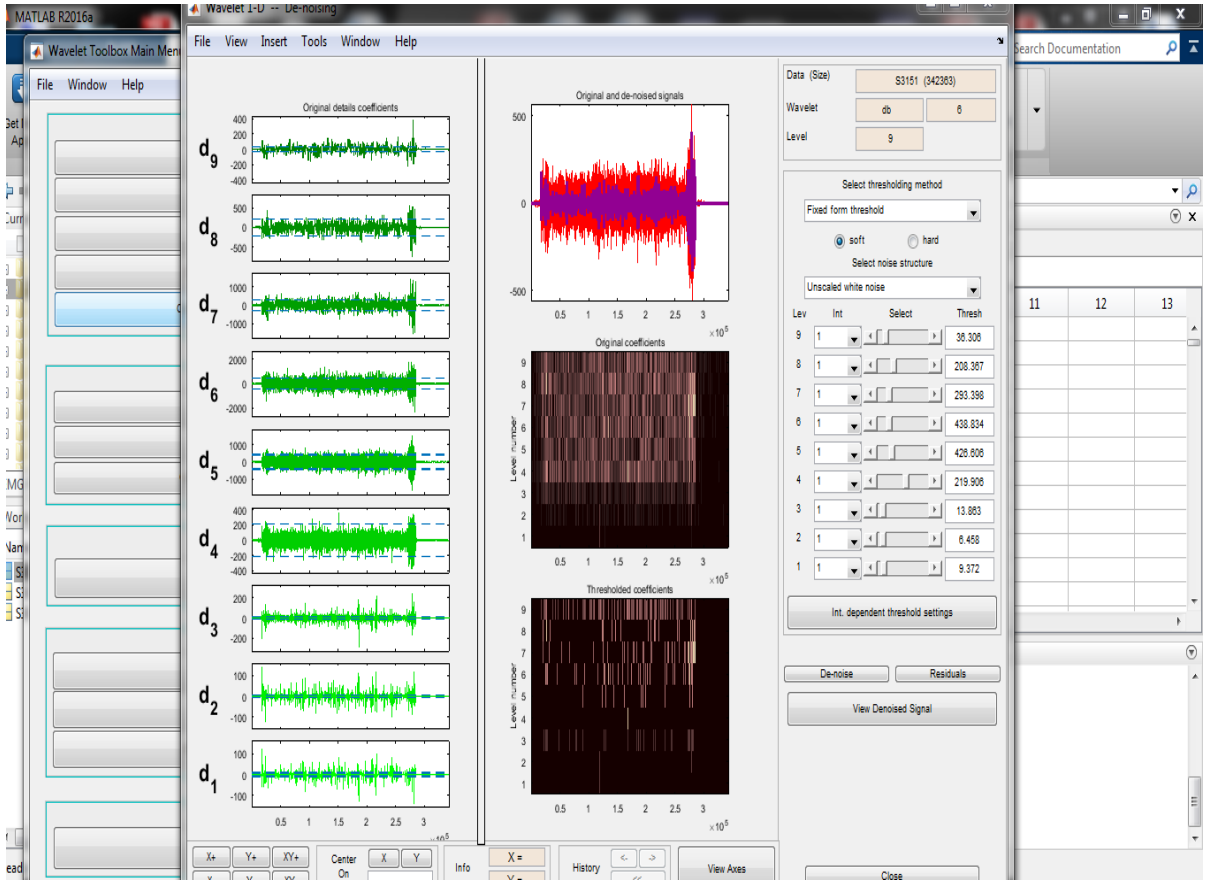

Fig 4.12 Wavelet denoising thresholding.

PSD PLOT:

The power spectral density plot was done by Welch's power estimation tool. Power Spectral Density (PSD) estimation of the waves. PSD estimation the calculated using Welch Power Spectral Density. The periodogram is not a consistent estimator of the true power spectral density of the wide-sense stationary process. Welch's technique to reduce the variance of the periodogram breaks the time series into segments, usually overlapping. Welch's method computes a modified periodogram for each segment and then averages these estimates to produce the estimate of the power special density. Because the process is wide-sense stationary and Welch's method uses PSD estimates of different segments of the time series, the modified periodogram represent approximately uncorrelated estimates of the true PSD and averaging reduces the variability. The segments are typically multiplied by a window function, such as a Hamming window so that Welch's method amounts to averaging modified periodogram.

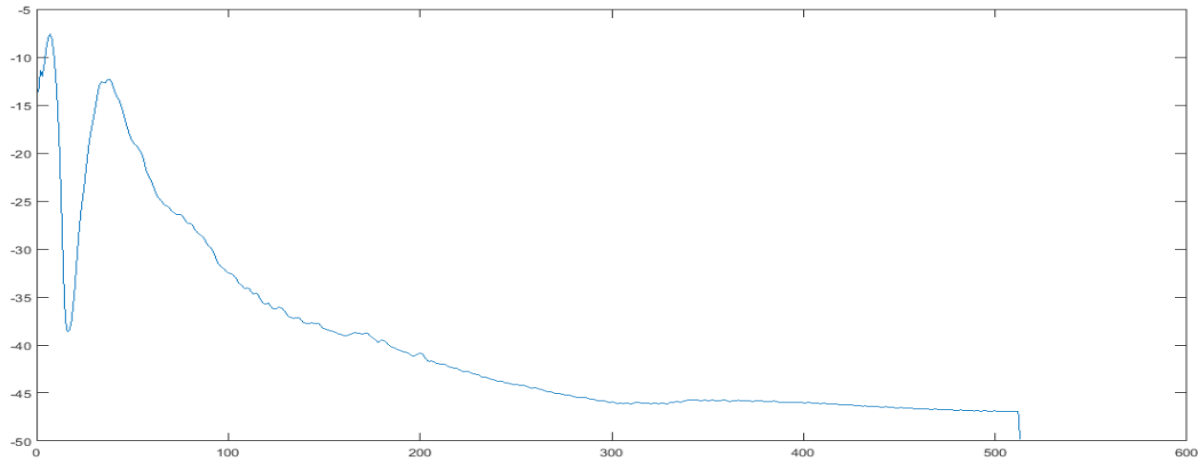

Fig 4.13: PSD plot.

RESULTS AND DISCUSSION:

In this experiment, there are three variables –

I. Muscle
II. Weight
III. Posture

COMPARISON OF MUSCLE:

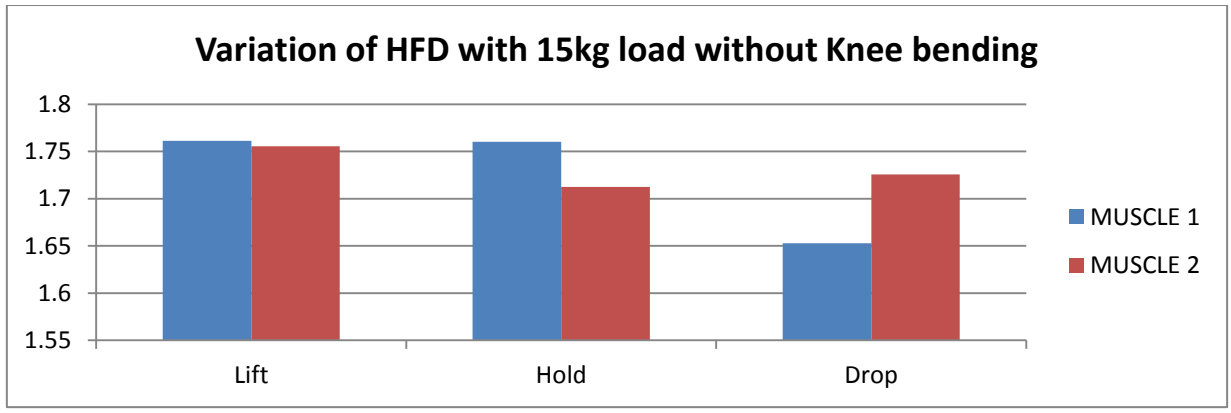

Fig 4,14. Variation of HFD with the 15kg load without Knee bending (Comparison of muscle)

HDF max value and HDF min value comparison:

Muscles	HFD max	HFD min
Muscl1	Lift	Drop
Muscle2	Lift	Hold

At all stage (Lifting, holding, dropping) muscle comparison:

Lift		Hold		Drop	
Higher value	**Lower value**	**Higher value**	**Lower value**	**Higher value**	**Lower value**
Muscle1	Muscle2	Musle1	Muscle2	Muscle2	Muscle1

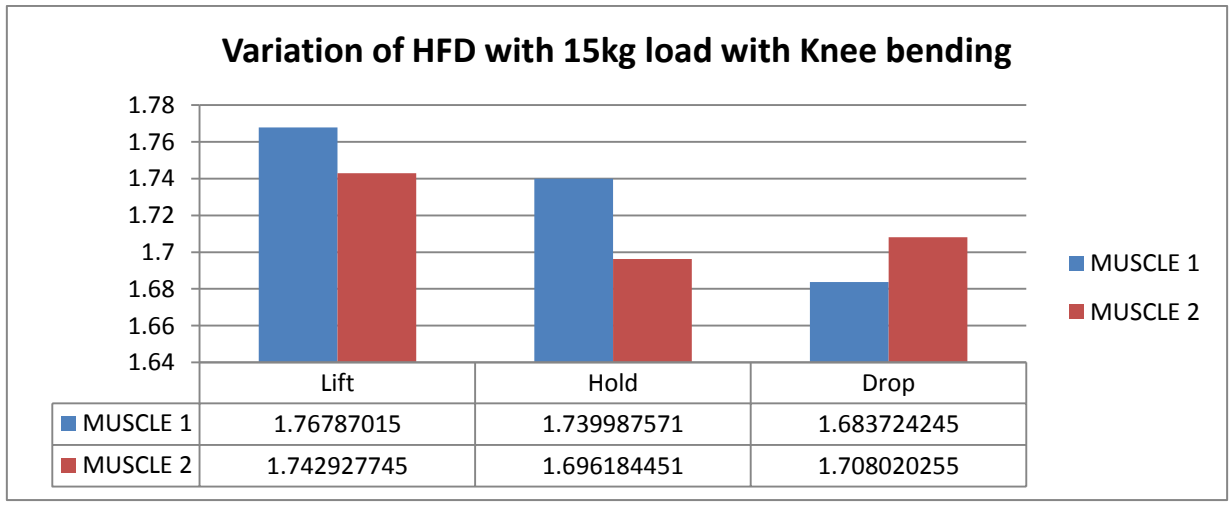

Fig4.15 Variation of HFD with 15kg load with Knee bending (Comparison of muscle)

HDF max value and HDF min value comparison:

Muscles	HFD max	HFD min
Muscl1	Lift	Drop
Muscle2	Lift	Hold

At all stage (Lifting, holding, dropping) muscle comparison:

Lift		Hold		Drop	
Higher value	**Lower value**	**Higher value**	**Lower value**	**Higher value**	**Lower value**
Muscle1	Muscle2	Musle1	Muscle2	Muscle2	Muscle1

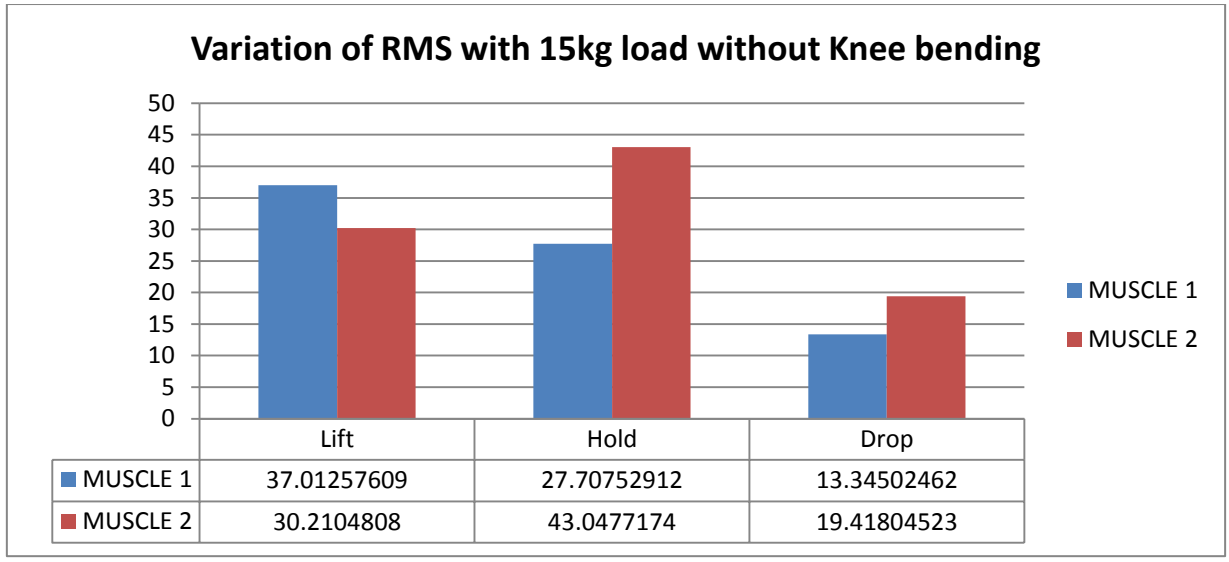

Fig4.16 Variation of RMS with the 15kg load without Knee bending (Comparison of muscle)

RMS max value and RMS min value comparison:

Muscles	**RMS max**	**RMS min**
Muscl1	Lift	Drop
Muscle2	Hold	Drop

At all stage (Lifting, holding, dropping) muscle comparison:

Lift		**Hold**		**Drop**	
Higher value	**Lower value**	**Higher value**	**Lower value**	**Higher value**	**Lower value**
Muscle1	Muscle2	Musle1	Muscle2	Muscle2	Muscle1

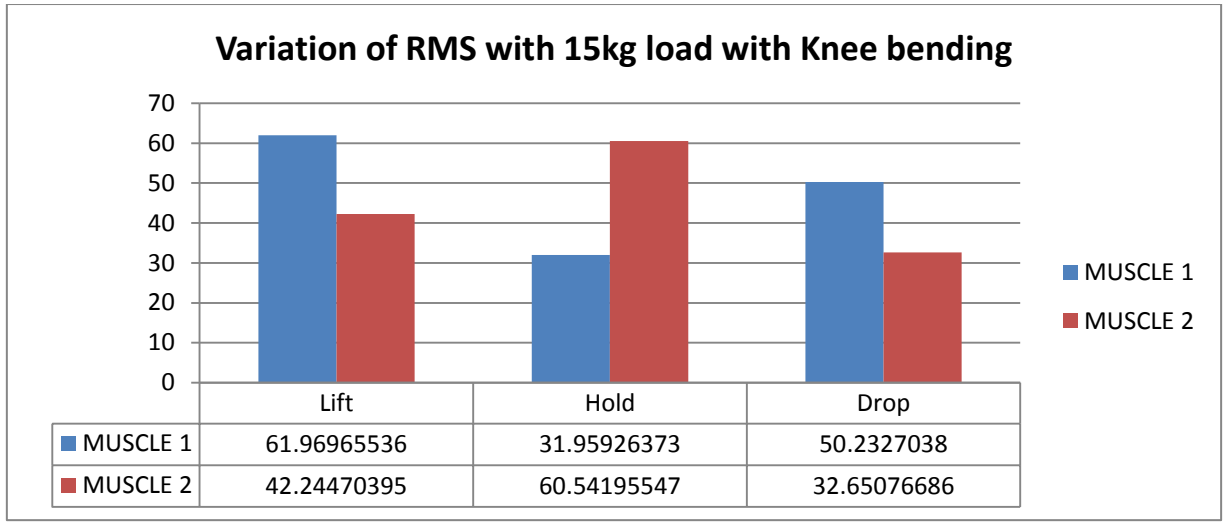

Fig 4.17 Variation of RMS with 15kg load with Knee bending(Comparison of muscle)

RMS max value and RMS min value comparison:

Muscles	RMS max	RMS min
Muscl1	Lift	Hold
Muscle2	Hold	Drop

At all stage (Lifting, holding, dropping) muscle comparison:

Lift		Hold		Drop	
Higher value	**Lower value**	**Higher value**	**Lower value**	**Higher value**	**Lower value**
Muscle1	Muscle2	Muscle2	Muscle1	Muscle1	Muscle2

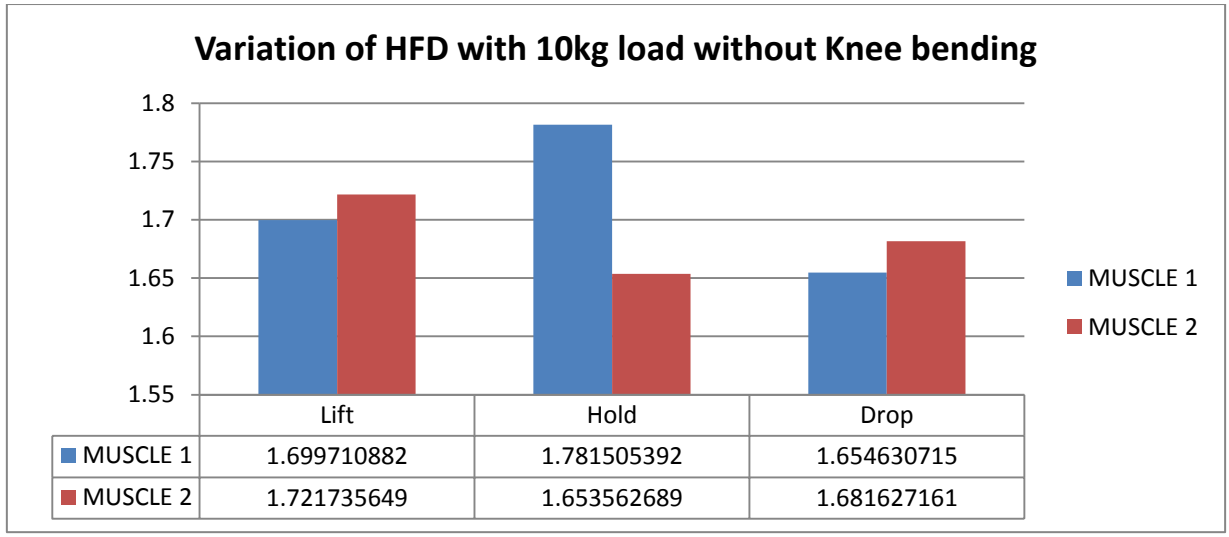

Fig 4.18 Variation of HFD with the 10kg load without Knee bending (Comparison of muscle)

HFD max value and HFD min value comparison:

Muscles	**HFD max**	**HFD min**
Muscl1	Hold	Drop
Muscle2	Lift	Hold

At all stage (Lifting, holding, dropping) muscle comparison:

Lift		**Hold**		**Drop**	
Higher value	**Lower value**	**Higher value**	**Lower value**	**Higher value**	**Lower value**
Muscle2	Muscle1	Muscle1	Muscle2	Muscle2	Muscle1

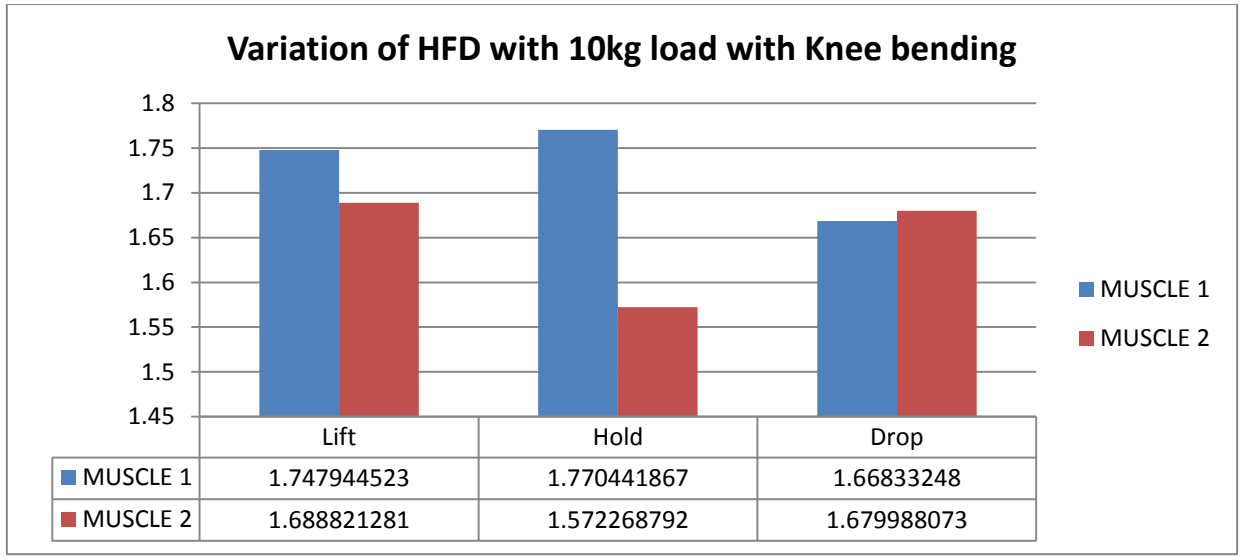

Fig 4.19 Variation of HFD with 10kg load with Knee bending(Comparison of muscle)

HFD max value and HFD min value comparison:

Muscles	HFD max	HFD min
Muscl1	Hold	Drop
Muscle2	Lift	Drop

At all stage (Lifting, holding, dropping) muscle comparison:

Lift		Hold		Drop	
Higher value	Lower value	Higher value	Lower value	Higher value	Lower value
Muscle1	Muscle2	Muscle1	Muscle2	Muscle2	Muscle1

- For knee bend at dropping period the HFD value for muscle1 and muscle 2 almost remain the same. But for without knee bend HFD value changes significantly.

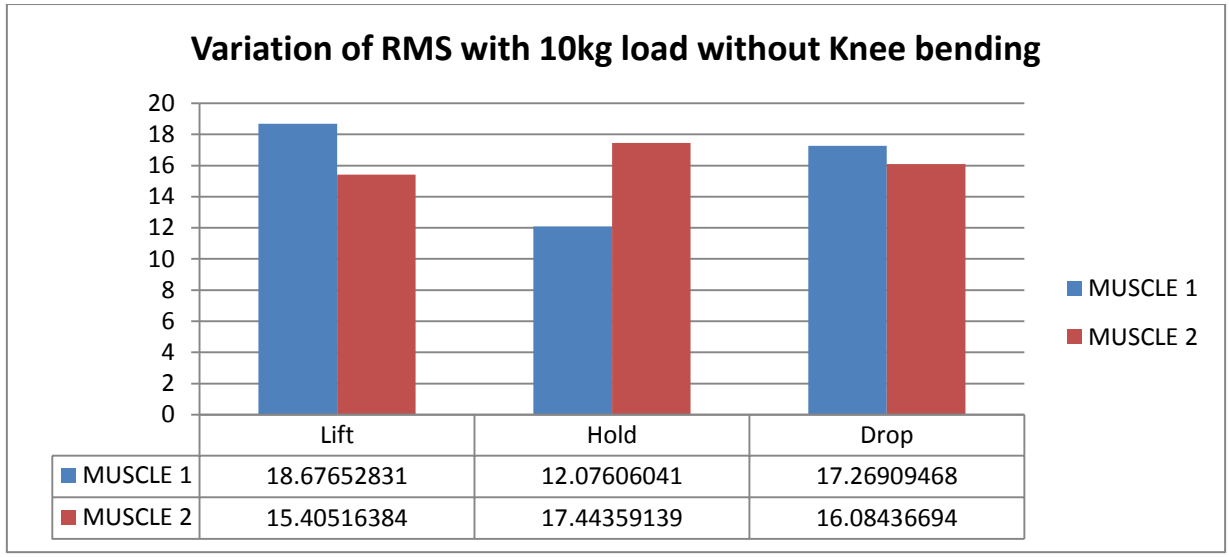

Fig 4.20 Variation of RMS with the 10kg load without Knee bending (Comparison of muscle)

RMS max value and RMS min value comparison:

Muscles	**RMS max**	**RMS min**
Muscl1	Lift	Hold
Muscle2	Hold	Lift

At all stage (Lifting, holding, dropping) muscle comparison:

Lift		**Hold**		**Drop**	
Higher value	**Lower value**	**Higher value**	**Lower value**	**Higher value**	**Lower value**
Muscle1	Muscle2	Muscle2	Muscle1	Muscle1	Muscle2

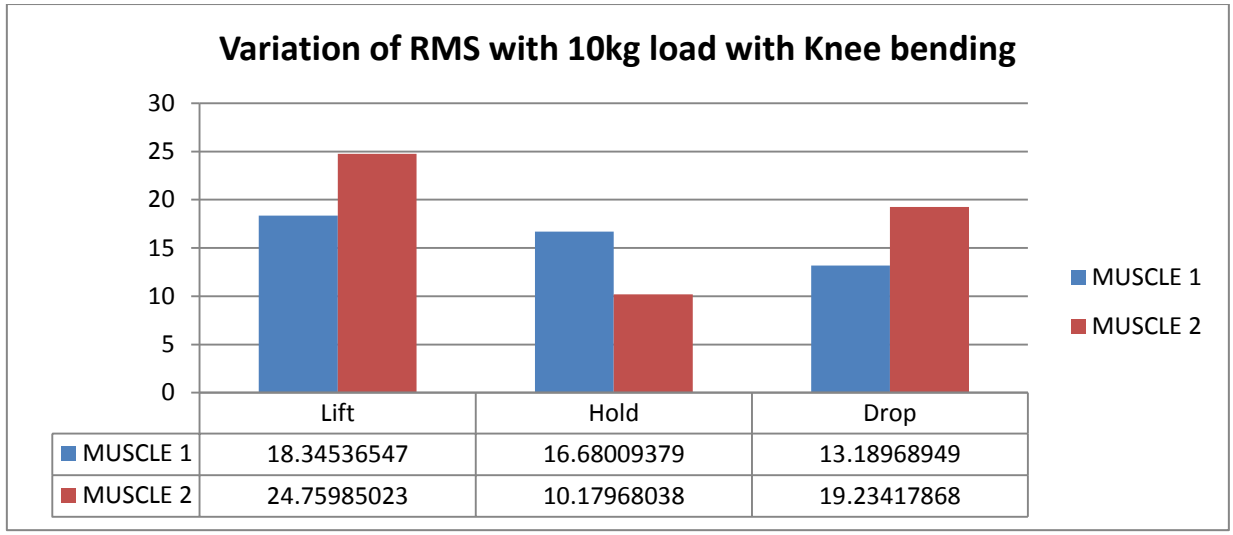

Fig.4.21 Variation of RMS with 10kg load with Knee bending (Comparison of muscle)

Muscles	RMS max	RMS min
Muscl1	Lift	Drop
Muscle2	Lift	Hold

At all stage (Lifting, holding, dropping) muscle comparison:

Lift		Hold		Drop	
Higher value	**Lower value**	**Higher value**	**Lower value**	**Higher value**	**Lower value**
Muscl2	Muscl1	Muscl1	Muscl2	Muscl2	Muscl1

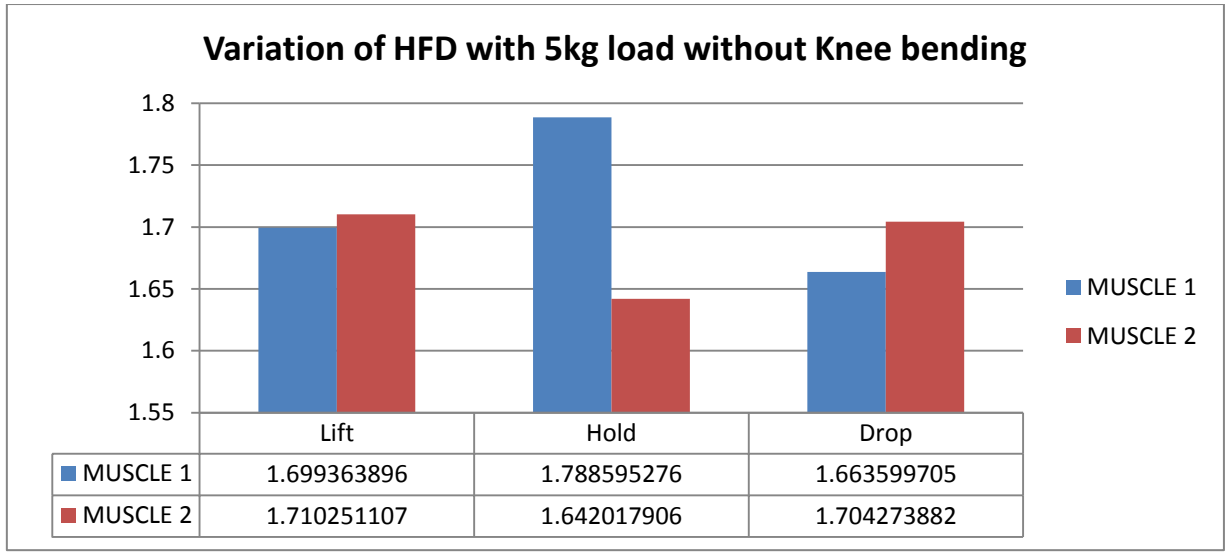

Fig 4.22. Variation of HFD with the 5kg load without Knee bending (Comparison of muscle)

HFD max value and HFD min value comparison:

Muscles	HFD max	HFD min
Muscl1	Hold	Drop
Muscle2	Lift	Hold

- For muscle2 HFD value of lifting and dropping period almost the same

At all stage (Lifting, holding, dropping) muscle comparison:

Lift		Hold		Drop	
Higher value	**Lower value**	**Higher value**	**Lower value**	**Higher value**	**Lower value**
Muscle2	Muscle1	Muscle1	Muscle2	Muscle2	Muscle1

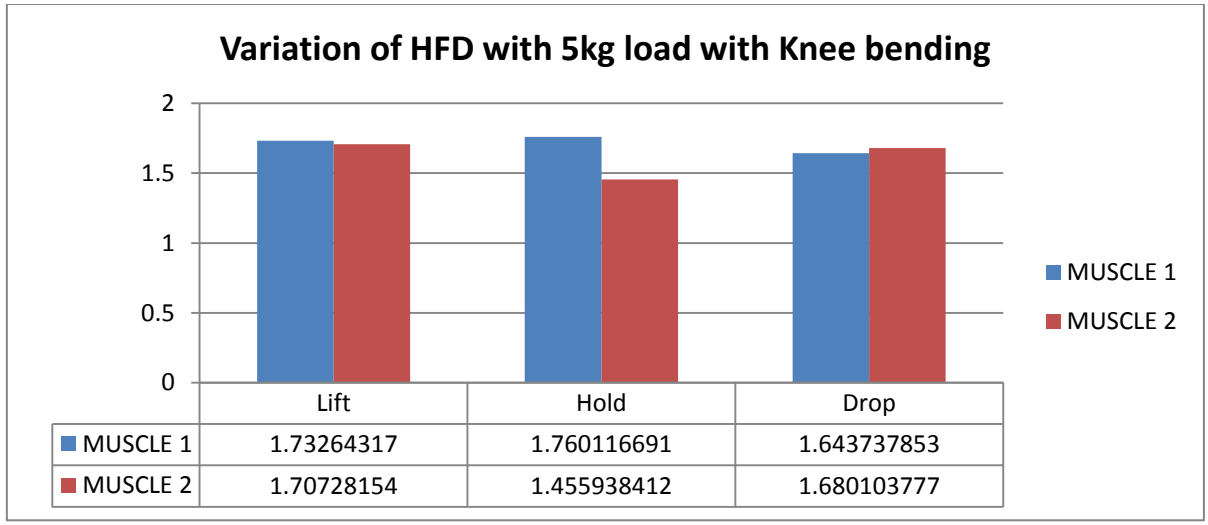

Fig 4.23 Variation of HFD with 5kg load with Knee bending(Comparison of muscle)

HFD max value and HFD min value comparison:

Muscles	**HFD max**	**HFD min**
Muscl1	Hold	Drop
Muscle2	Lift	Hold

At all stage (Lifting, holding, dropping) muscle comparison:

Lift		**Hold**		**Drop**	
Higher value	**Lower value**	**Higher value**	**Lower value**	**Higher value**	**Lower value**
Muscle1	Muscle2	Muscle1	Muscle2	Muscle2	Muscle1

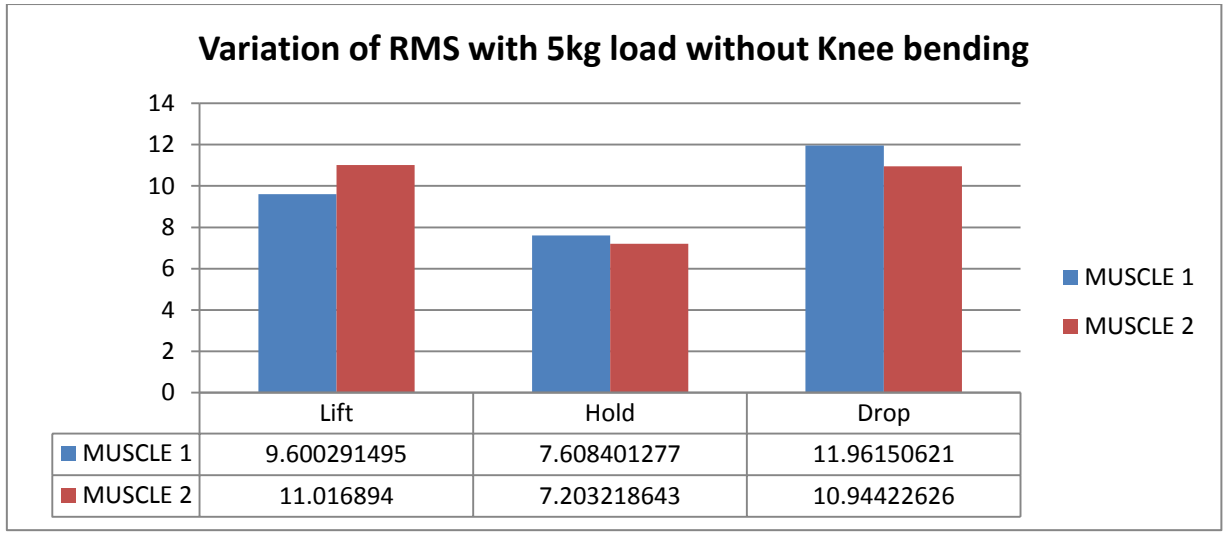

	Lift	Hold	Drop
MUSCLE 1	9.600291495	7.608401277	11.96150621
MUSCLE 2	11.016894	7.203218643	10.94422626

Fig 4.24 Variation of RMS with the 5kg load without Knee bending(Comparison of muscle)

RMS max value and RMS min value comparison:

Muscles	RMS max	RMS min
Muscl1	Drop	Hold
Muscle2	Lift	Hold

At all stage (Lifting, holding, dropping) muscle comparison:

Lift		Hold		Drop	
Higher value	Lower value	Higher value	Lower value	Higher value	Lower value
Muscles2	Muscle1	Muscle2	Muscle1	Muscle1	Muscle2

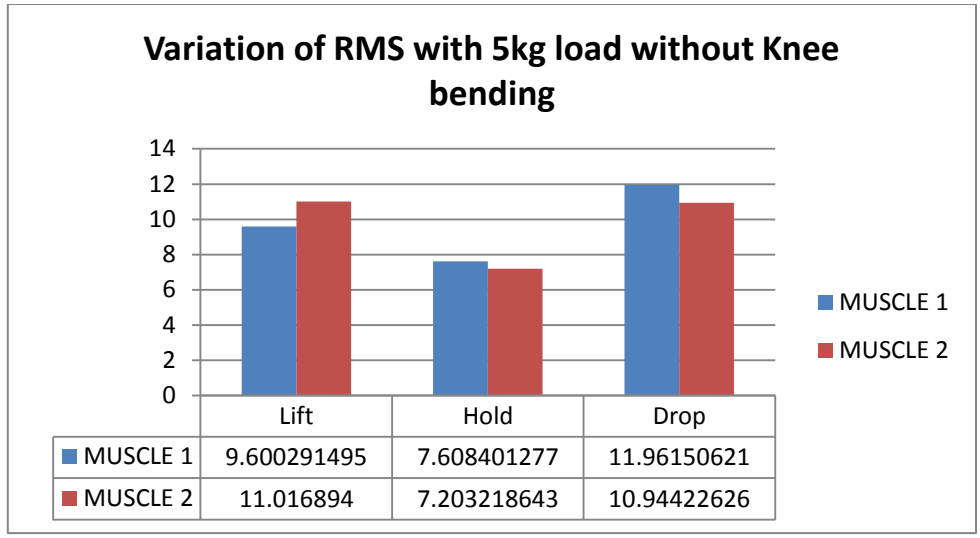

Fig 4.25 Variation of RMS with 5kg load with Knee bending(Comparison of muscle)

RMS max value and RMS min value comparison:

Muscles	**RMS max**	**RMS min**
Muscle1	Drop	hold
Muscle2	Lift	Hold

At all stage (Lifting, holding, dropping) muscle comparison:

Lift		**Hold**		**Drop**	
Higher value	**Lower value**	**Higher value**	**Lower value**	**Higher value**	**Lower value**
Muscle2	Muscle1	Muscle1	Muscle2	Muscle1	Muscle2

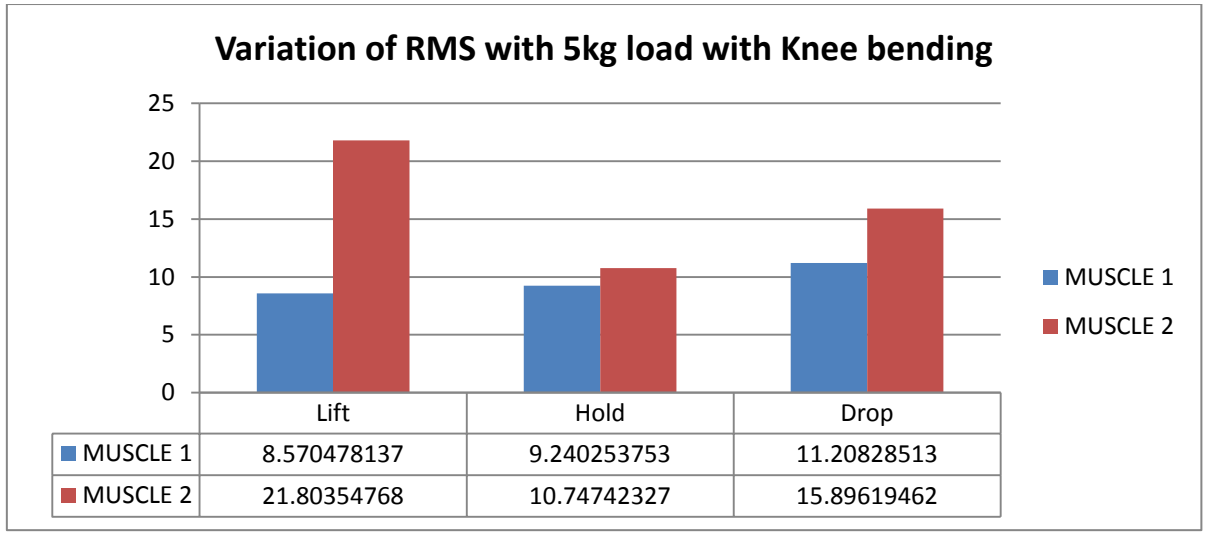

Fig 4.26 Variation of RMS with 5kg load with Knee bending(Comparison of muscle)

RMS max value and RMS min value comparison:

Muscles	**RMS max**	**RMS min**
Muscl1	Drop	Hold
Muscle2	Lift	Hold

At all stage (Lifting, holding, dropping) muscle comparison:

Lift		**Hold**		**Drop**	
Higher value	**Lower value**	**Higher value**	**Lower value**	**Higher value**	**Lower value**
Muscle2	Muscle1	Muscle2	Muscle1	Muscle2	Muscle1

COMPARISON OF POSTURE:

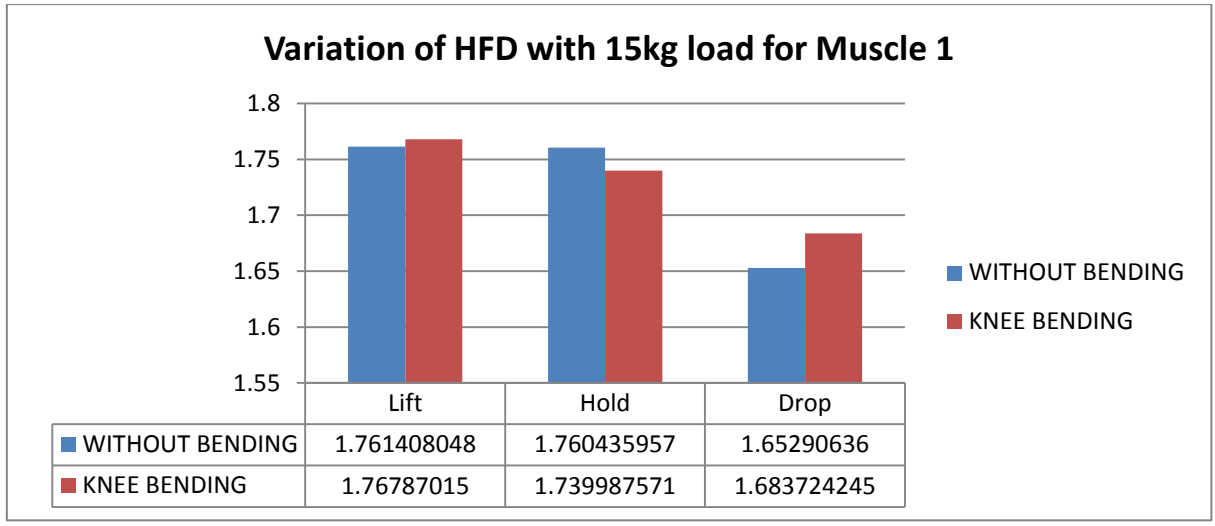

	Lift	Hold	Drop
WITHOUT BENDING	1.761408048	1.760435957	1.65290636
KNEE BENDING	1.76787015	1.739987571	1.683724245

Fig 4.27 Variation of HFD with 15kg load for Muscle 1 (Comparison of posture)

- Without knee bending HFD is maximum at lifting and minimum at Dropping. But at holding and lifting the HFD value almost the same.
- With knee bending the HFD is maximum at lifting and minimum at dropping. For the HFD for lifting and holding significantly different value.
- At lifting or dropping for knee bending HFD is higher, while at dropping HFD for without knee bending is higher than with knee bending.

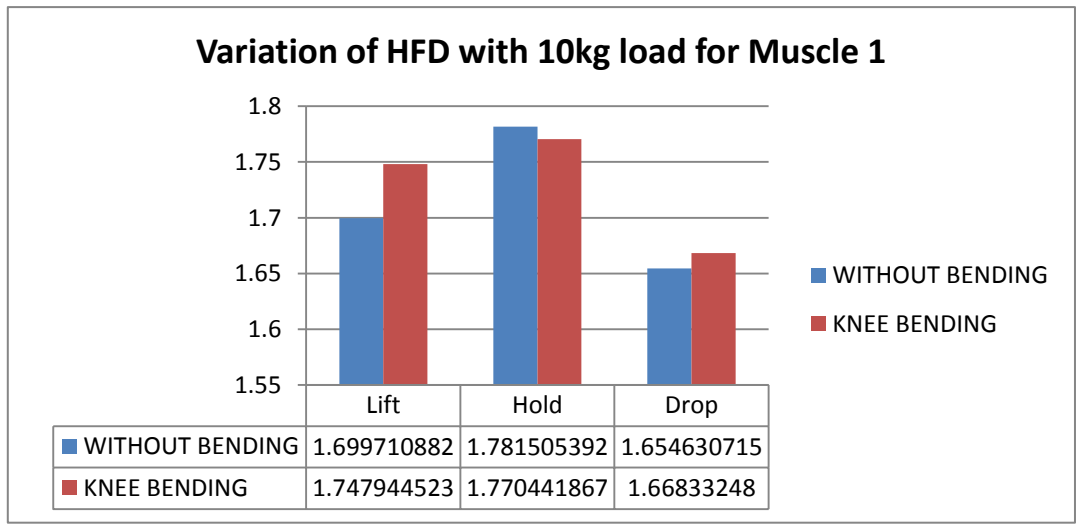

	Lift	Hold	Drop
WITHOUT BENDING	1.699710882	1.781505392	1.654630715
KNEE BENDING	1.747944523	1.770441867	1.66833248

Fig 4.28 Variation of HFD with 10kg load for Muscle 1 (Comparison of posture)

- For 10kg without knee bending, HFD is maximum at holding and minimum at dropping
- For 10kg with knee bending HFD maximum at holding and minimum at dropping.
- At lifting or dropping for knee bending HFD is higher, while at dropping HFD for without knee bending is higher than with knee bending.

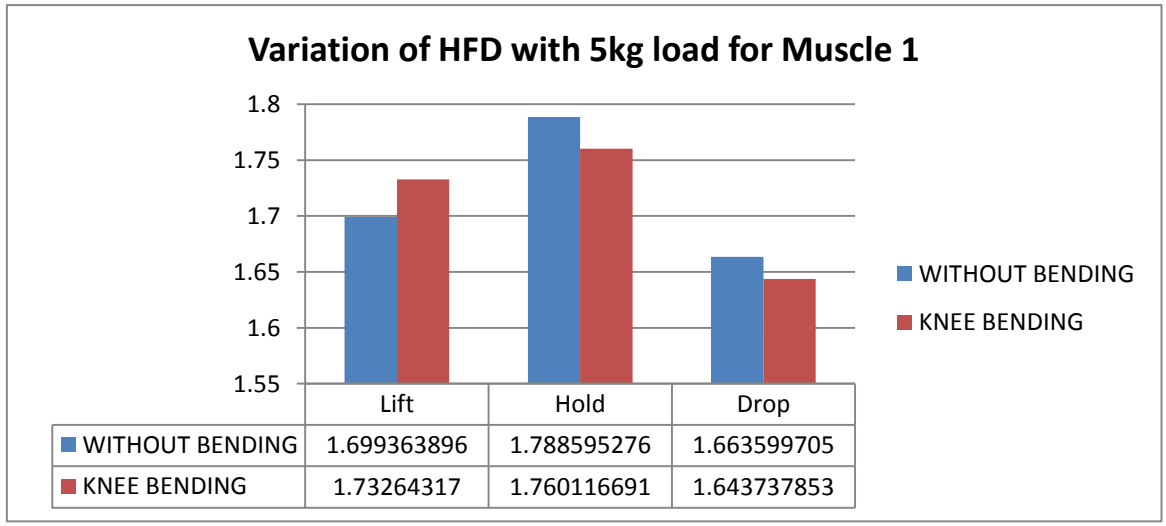

	Lift	Hold	Drop
WITHOUT BENDING	1.699363896	1.788595276	1.663599705
KNEE BENDING	1.73264317	1.760116691	1.643737853

Fig 4.29 Variation of HFD with 5kg load for Muscle 1 (Comparison of posture)

- For 5kg without knee bending, HFD is maximum at holding and minimum at dropping.
- For 5 kg with knee bending HFD maximum at holding and minimum at dropping.
- At every stage (lifting, holding and dropping) the HFD for without knee bending is higher.

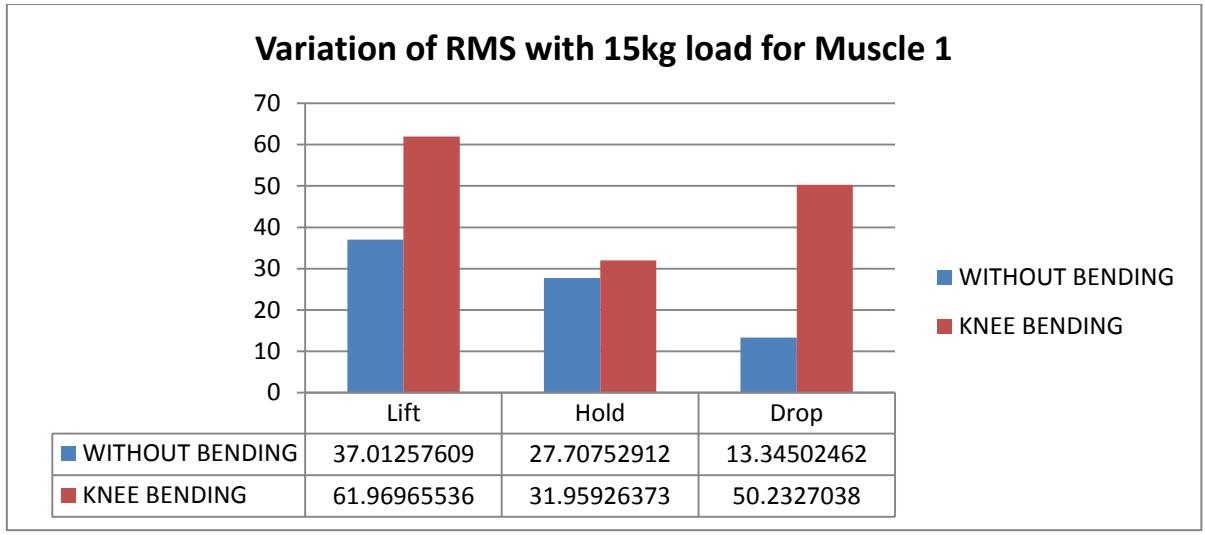

	Lift	Hold	Drop
WITHOUT BENDING	37.01257609	27.70752912	13.34502462
KNEE BENDING	61.96965536	31.95926373	50.2327038

Fig 4.30 Variation of RMS with 15kg load for Muscle 1(Comparison of posture)

- For 15kg without knee bending RMS is maximum at lifting and minimum at dropping.
- For 15kg with knee bending RMS is maximum at lifting and minimum at holding.
- Here at all stage RMS for knee bending is much more higher than without knee bending posture.

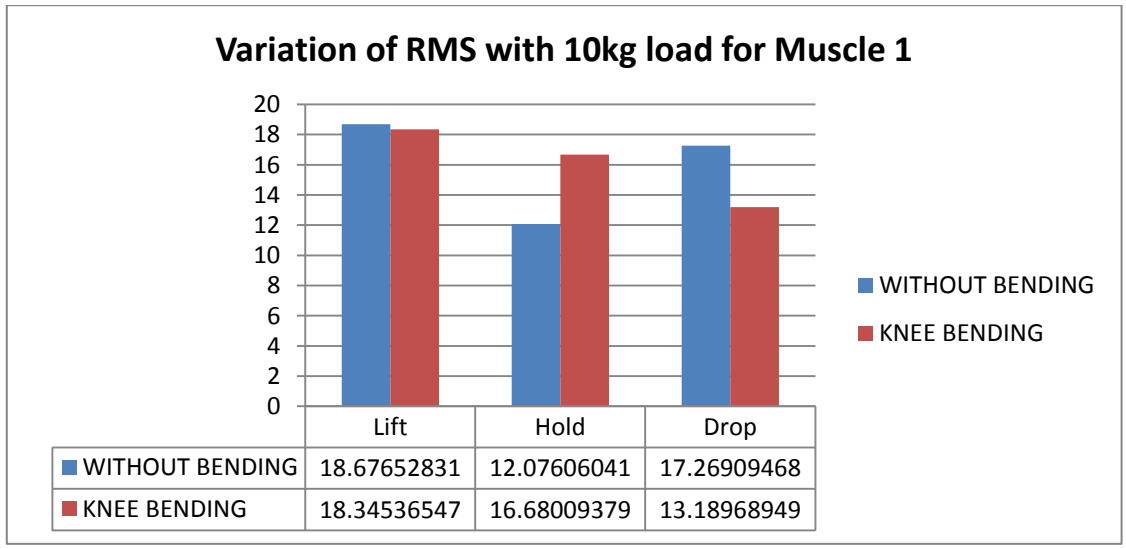

	Lift	Hold	Drop
WITHOUT BENDING	18.67652831	12.07606041	17.26909468
KNEE BENDING	18.34536547	16.68009379	13.18968949

Fig 4.31 Variation of RMS with 10kg load for Muscle 1(Comparison of posture)

- For 10kg without knee bending RMS is maximum at lifting and minimum at holding.
- For 10kg with knee bending RMS is maximum at lifting and minimum at dropping.

- At lifting or dropping RMS for without knee bending is higher, while at holding opposite phenomena is found.

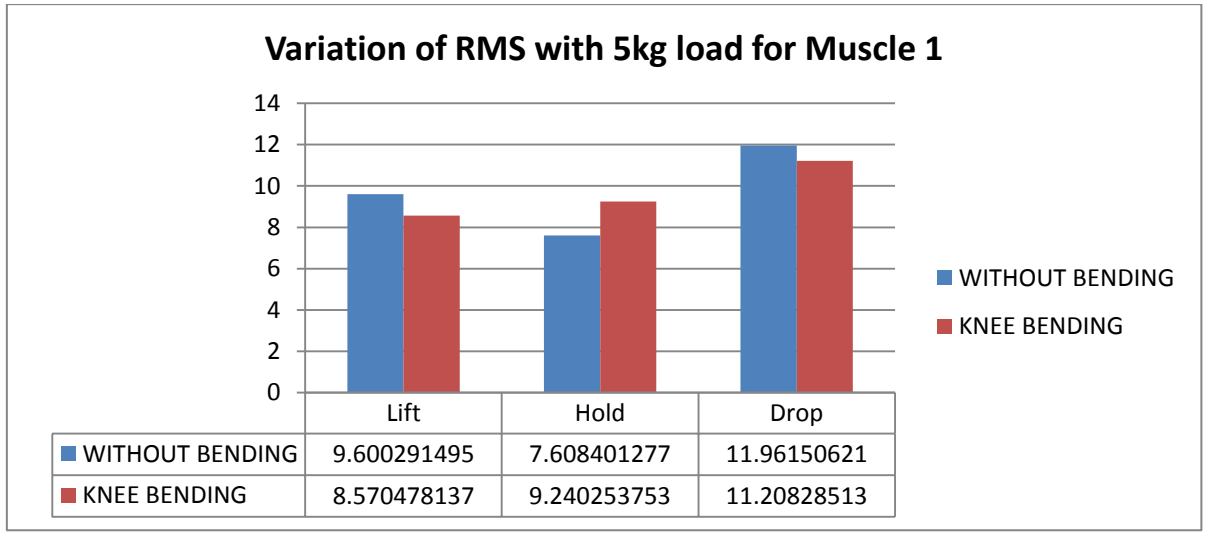

	Lift	Hold	Drop
WITHOUT BENDING	9.600291495	7.608401277	11.96150621
KNEE BENDING	8.570478137	9.240253753	11.20828513

Fig 4.32 Variation of RMS with 5kg load for Muscle 1(Comparison of posture)

- For 5kg without knee bending RMS is at dropping and minimum at holding.
- For 5kg with knee bending RMS is maximum at dropping and minimum at lifting.
- At lifting or dropping RMS for without knee bending is higher, while at holding opposite phenomena is found.

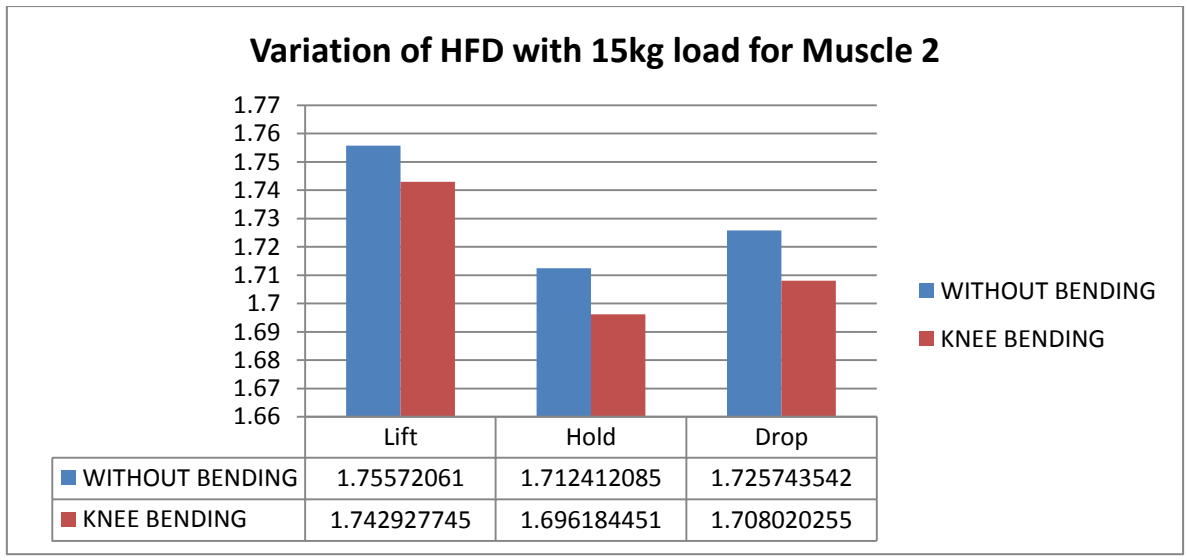

	Lift	Hold	Drop
WITHOUT BENDING	1.75572061	1.712412085	1.725743542
KNEE BENDING	1.742927745	1.696184451	1.708020255

Fig 4.33 Variation of HFD with 15kg load for Muscle 2 (Comparison of posture)

- For 15kg without knee bending, HFD is maximum at lifting and minimum at holding.

- For 15kg with knee bending, HFD is maximum at lifting and minimum at holding.
- Here for all stage, HFD without knee bending is higher than compared to HFD with knee bending.

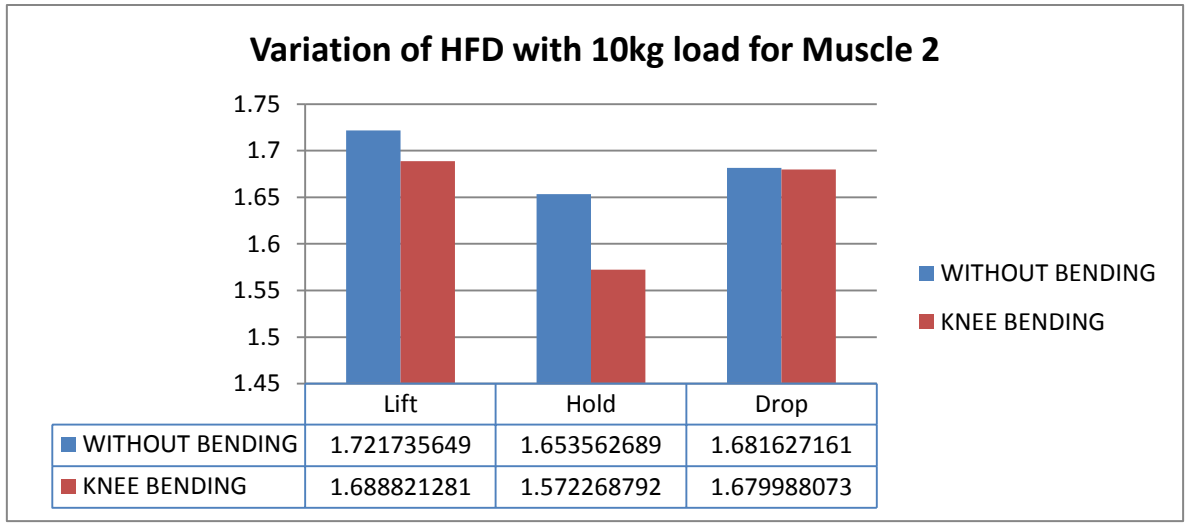

	Lift	Hold	Drop
WITHOUT BENDING	1.721735649	1.653562689	1.681627161
KNEE BENDING	1.688821281	1.572268792	1.679988073

Fig 4.34 Variation of HFD with 10kg load for Muscle 2 (Comparison of posture)

- For 10kg without knee bending, HFD is maximum at lifting and minimum at holding.
- For 10kg with knee bending, HFD is maximum at lifting and minimum at holding.
- Here for all stage, HFD without knee bending is higher than compared to HFD with knee bending.

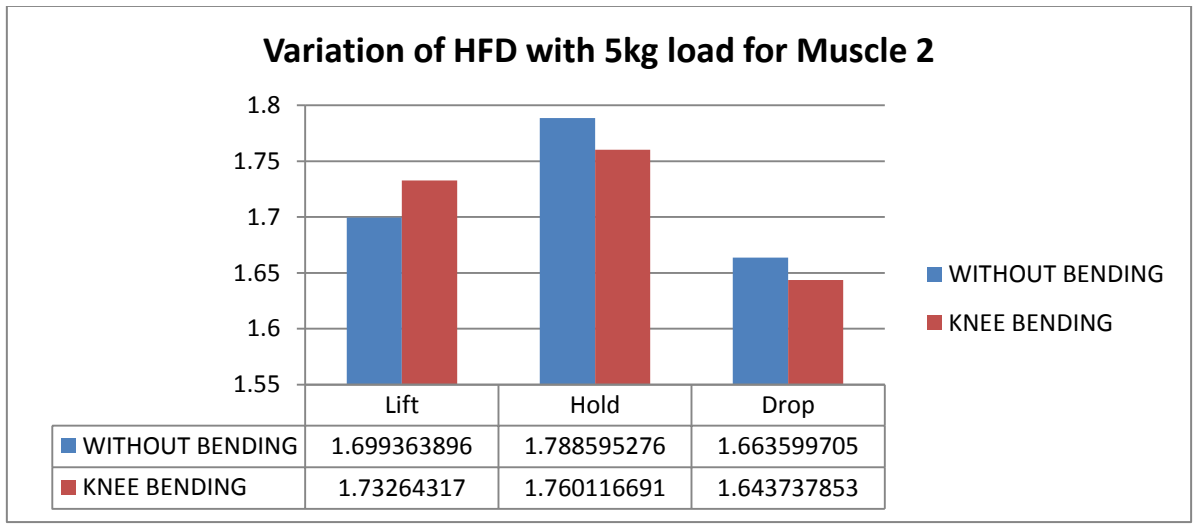

	Lift	Hold	Drop
WITHOUT BENDING	1.699363896	1.788595276	1.663599705
KNEE BENDING	1.73264317	1.760116691	1.643737853

Fig 4.35 Variation of HFD with 5kg load for Muscle 2 (Comparison of posture)

- For 5kg without knee bending, HFD is maximum at holding and minimum at dropping.
- For 5kg with knee bending, HFD is maximum at holding and minimum at dropping.
- At holding or dropping HFD without knee bending is higher, while at lifting opposite phenomena is found.

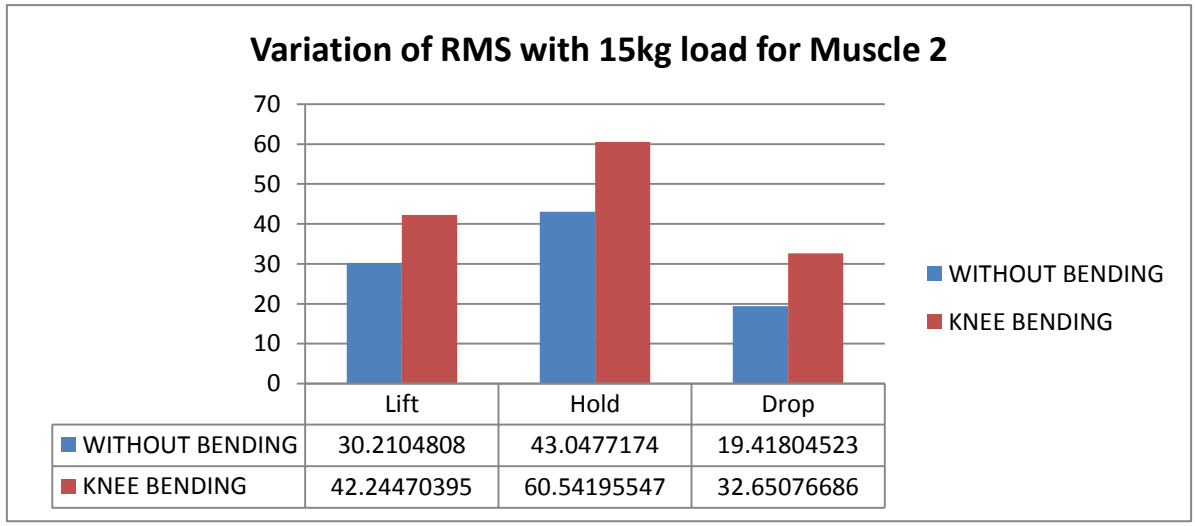

	Lift	Hold	Drop
WITHOUT BENDING	30.2104808	43.0477174	19.41804523
KNEE BENDING	42.24470395	60.54195547	32.65076686

Fig 4.36 Variation of RMS with 15kg load for Muscle 2 (Comparison of posture)

- For 15kg without knee bending RMS is maximum at holding and minimum at dropping.
- For 15kg without knee bending RMS is maximum at holding and minimum at dropping.
- Here at all stage RMS with knee bending is much more higher than without knee bending posture.

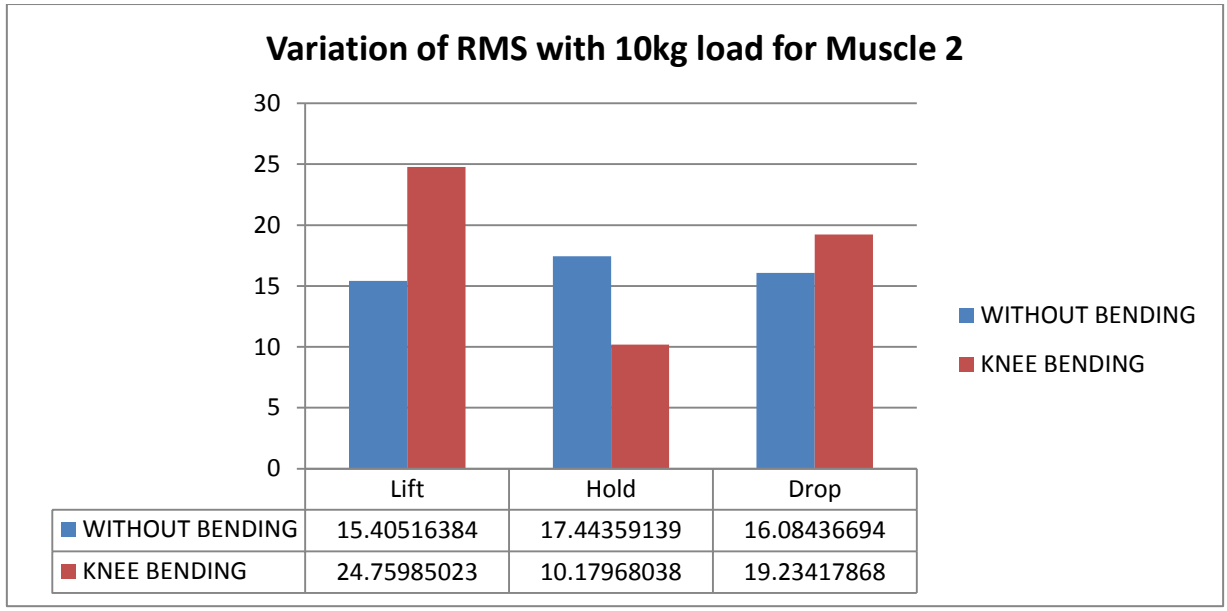

	Lift	Hold	Drop
WITHOUT BENDING	15.40516384	17.44359139	16.08436694
KNEE BENDING	24.75985023	10.17968038	19.23417868

Fig 4.37 Variation of RMS with 10kg load for Muscle 2 (Comparison of posture)

- For 10kg without knee bending RMS is maximum at lifting and minimum at holding.
- For 10kg with knee bending RMS is maximum at lifting and minimum at holding.
- Here at lifting or dropping RMS is higher, while at holding opposite phenomena is found.

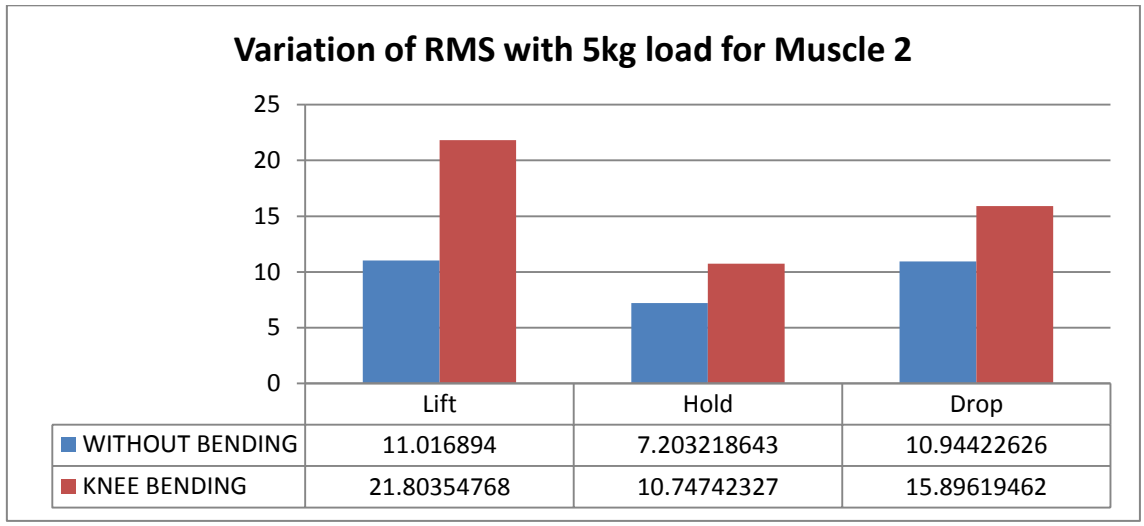

	Lift	Hold	Drop
WITHOUT BENDING	11.016894	7.203218643	10.94422626
KNEE BENDING	21.80354768	10.74742327	15.89619462

Fig 4.38 Variation of RMS with 5kg load for Muscle 2 (Comparison of posture)

- For 5kg without knee bending RMS is maximum at lifting and minimum at holding.
- For 5kg with knee bending RMS is maximum at lifting and minimum at holding.
- Here at all stage RMS with knee bending is much more higher than without knee bending posture.

COMPARISON OF WEIGHT:

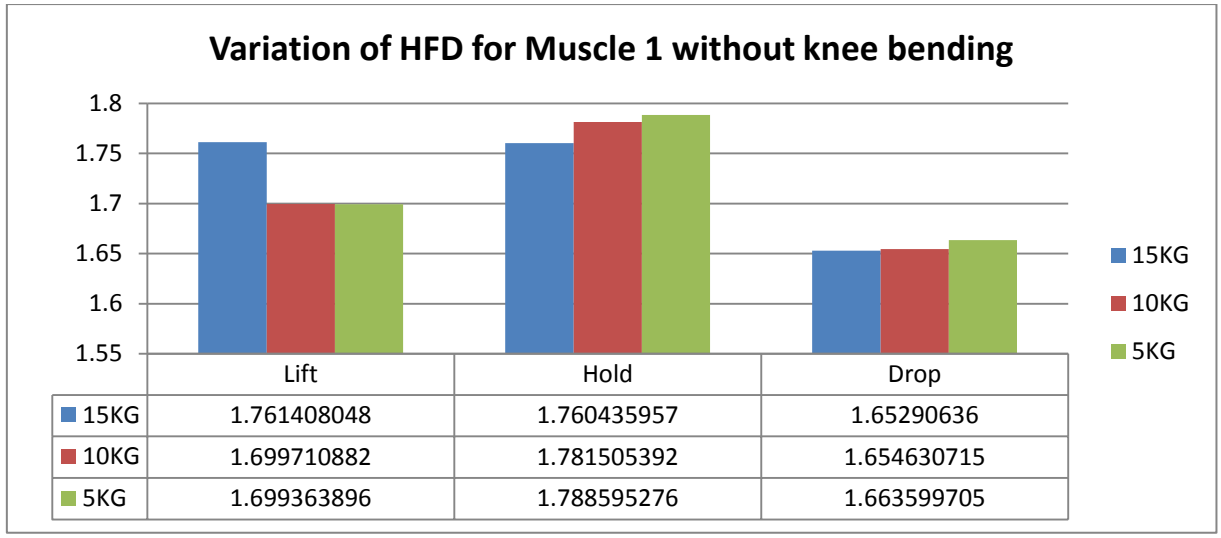

	Lift	Hold	Drop
15KG	1.761408048	1.760435957	1.65290636
10KG	1.699710882	1.781505392	1.654630715
5KG	1.699363896	1.788595276	1.663599705

Fig 4.39 Variation of HFD for Muscle 1 without knee bending (Comparison of weight)

WEIGHTS	**HFD (at a different time)**	
	MAX	**MIN**
15KG	Lift	Drop
10KG	Hold	Drop
5KG	Hold	Drop

- Here at lifting time, the HFD value is highest for 15kg. While for 10kg or 5kg HFD value almost remain the same
- At holding the HFD increases with decreasing weight. So complexity decreases with increasing weight
- Same phenomena are observed at dropping time. But HFD values are less compared to holding or lifting time.

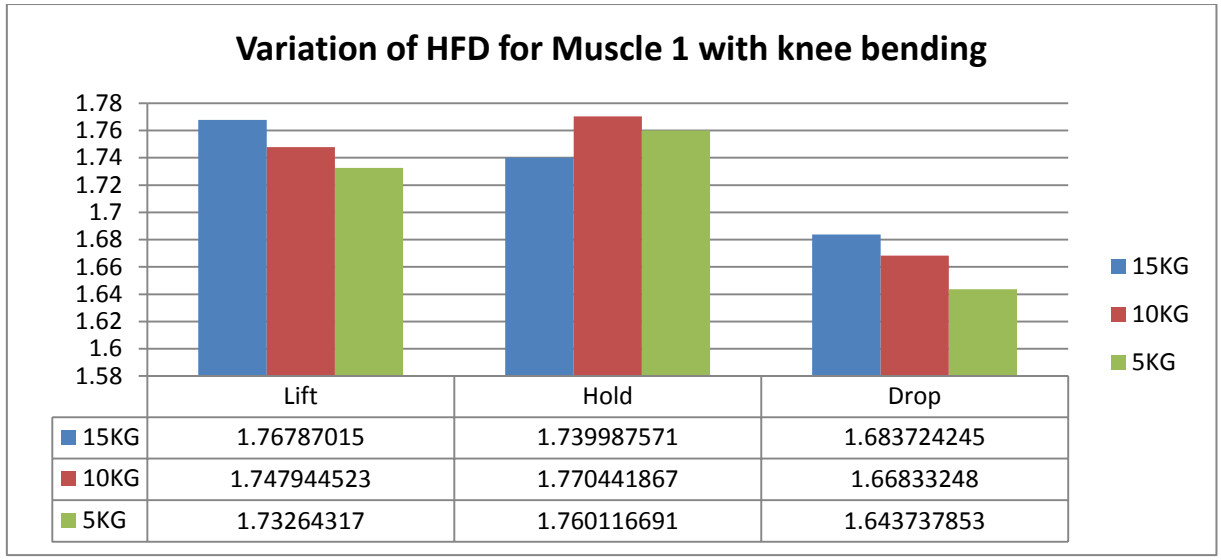

	Lift	Hold	Drop
15KG	1.76787015	1.739987571	1.683724245
10KG	1.747944523	1.770441867	1.66833248
5KG	1.73264317	1.760116691	1.643737853

Fig 4.40 Variation of HFD for Muscle 1 with knee bending (Comparison of weight)

WEIGHTS	**HFD (at different time)**	
	MAX	**MIN**
15KG	Lift	Drop
10KG	Hold	Drop
5KG	Hold	Drop

- At lifting the HFD value decreases with decreasing weight. The changes in HFD are significant with weight changing.
- At holding The HFD is highest for 10kg, while the lowest value of HFD is found for 15kg. Here the HFD for 10kg or 5kg almost same.
- At dropping the HFD decreases with decreasing weight. But here HFD values for all weight are lesser compared to lifting or holding time

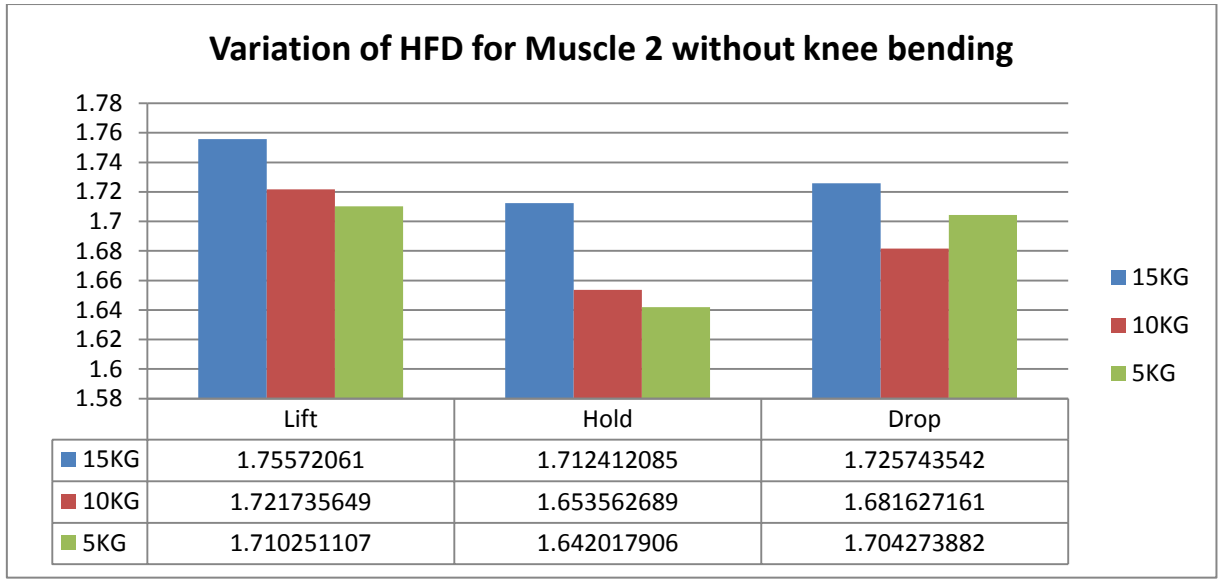

	Lift	Hold	Drop
15KG	1.75572061	1.712412085	1.725743542
10KG	1.721735649	1.653562689	1.681627161
5KG	1.710251107	1.642017906	1.704273882

Fig 4.41 Variation of HFD for Muscle 2 without knee bending (Comparison of weight)

WEIGHTS	HFD (At different time)	
	MAX	MIN
15KG	Lift	Hold
10KG	Lift	Hold
5KG	Lift	Hold

- At Lifting the HFD decreases with decreasing weight.
- At holding HFD also decreases with decreasing weight.
- At dropping HFD is highest for 15 kg, while the lowest for 10kg.
- Here HFD values are maximum at lifting time, while minimum values are found at holding.

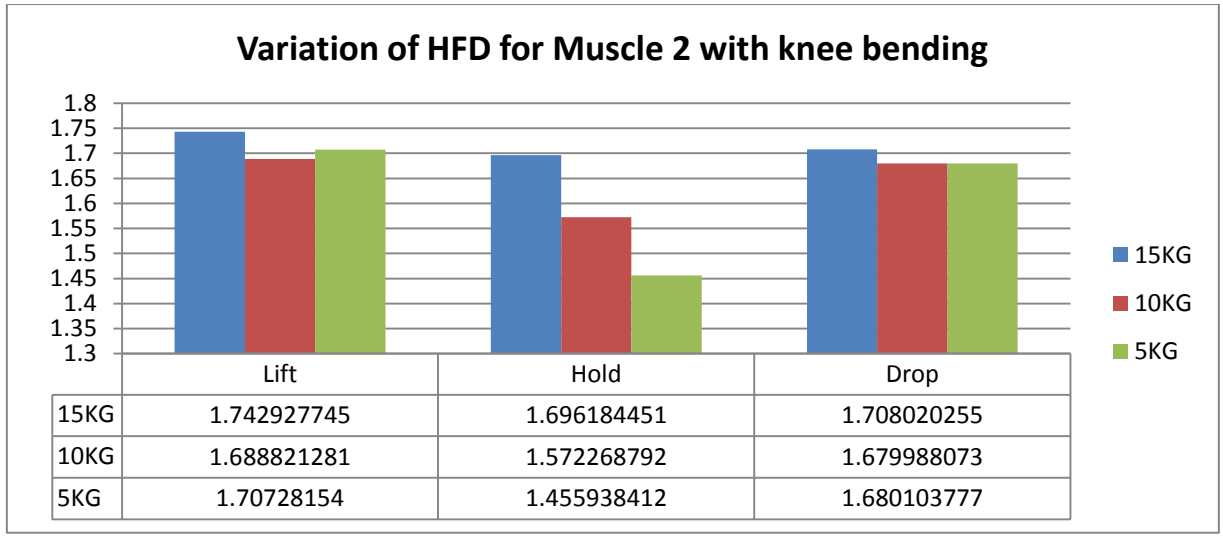

	Lift	Hold	Drop
15KG	1.742927745	1.696184451	1.708020255
10KG	1.688821281	1.572268792	1.679988073
5KG	1.70728154	1.455938412	1.680103777

Fig 4.42 Variation of HFD for Muscle 2 with knee bending (Comparison of weight)

WEIGHTS	**HFD (At different time)**	
	MAX	**MIN**
15KG	Lift	Hold
10KG	Lift	Hold
5KG	Lift	Hold

- At lifting HFD for 15kg is highest, while HFD is lowest for 10kg. But for 10kg and 5kg there is no significant change in HFD.
- At holding HFD significantly decreases with decreasing weight.
- At dropping HFD is highest for 15 kg and lowest for 10kg. But HFD of 10kg or 5kg almost same.
- HFD values for all three weight have a maximum at Lifting and minimum at holding.

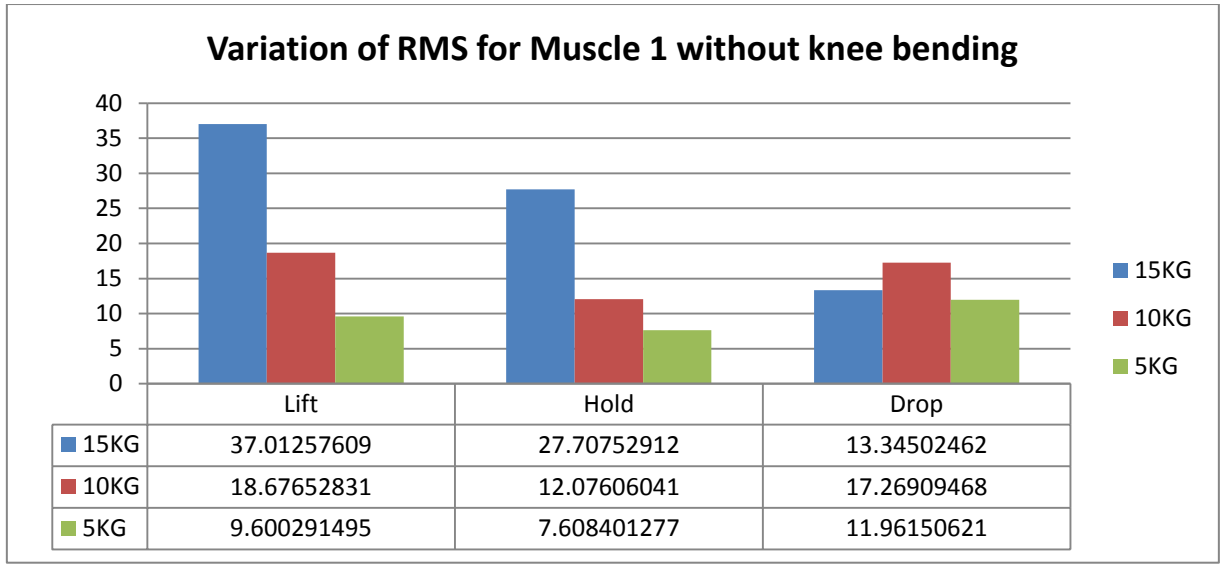

	Lift	Hold	Drop
15KG	37.01257609	27.70752912	13.34502462
10KG	18.67652831	12.07606041	17.26909468
5KG	9.600291495	7.608401277	11.96150621

Fig 4.43 Variation of RMS for Muscle 1 without knee bending (Comparison of weight)

WEIGHTS	**RMS(At different time)**	
	MAX	**MIN**
15KG	Lift	Drop
10KG	Lift	Hold
5KG	Drop	Hold

- At lifting RMS value decreases with decreasing weight.
- At holding also RMS decreases with decreasing weight.
- At dropping RMS decreases for 10kg to the 5kg weight change. But for 15kg to 10 kg change, RMS increases.
- For 15kg and 10kg, RMS is maximum at lifting. But for 5kg the maximum value of RMS is at dropping
- For 15kg RMS minimum value is at dropping, while for 10kg or 5kg at holding RMS is minimum.

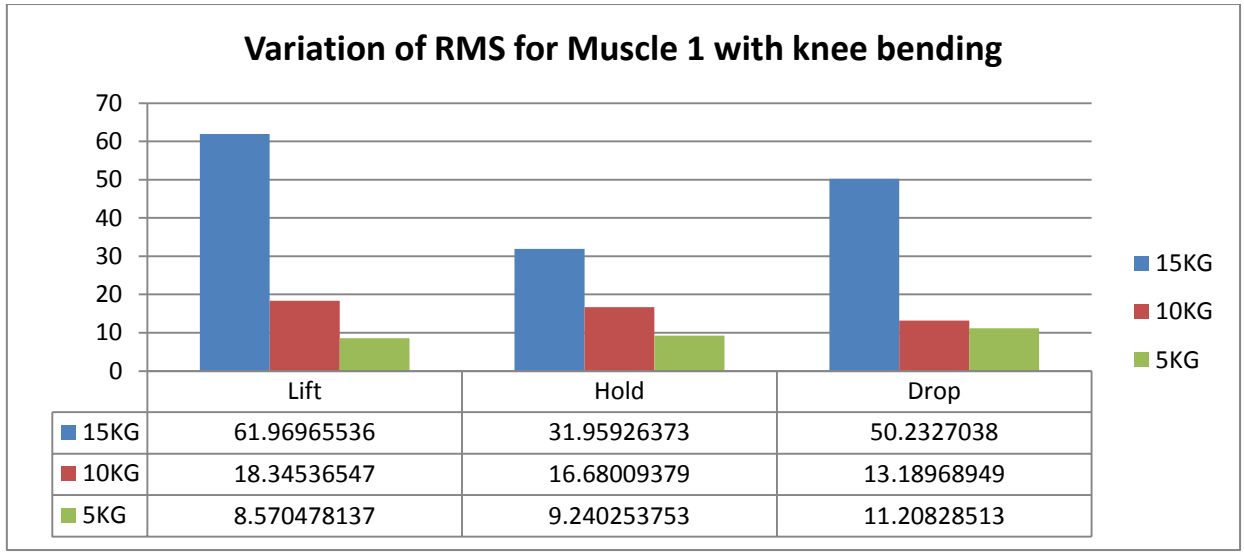

	Lift	Hold	Drop
15KG	61.96965536	31.95926373	50.2327038
10KG	18.34536547	16.68009379	13.18968949
5KG	8.570478137	9.240253753	11.20828513

Fig 4.44 Variation of RMS for Muscle 1 with knee bending (Comparison of weight)

WEIGHTS	**RMS(At different time)**	
	MAX	**MIN**
15KG	Lift	Hold
10KG	Lift	Drop
5KG	Drop	Lift

- At lifting or holding or dropping time the RMS decreases with decreasing time.
- The RMS value variation also increases with increasing weight i.e. for 15kg the variation or RMS value difference is much more higher than 10kg or 5kg.
- For 15kg or 10kg RMS is maximum at lifting, While for 5kg maximum RMS occurs at dropping.
- For minimum RMS for 15kg is at holding, while for 10kg RMS minimum is found at dropping and for 5kg at lifting.

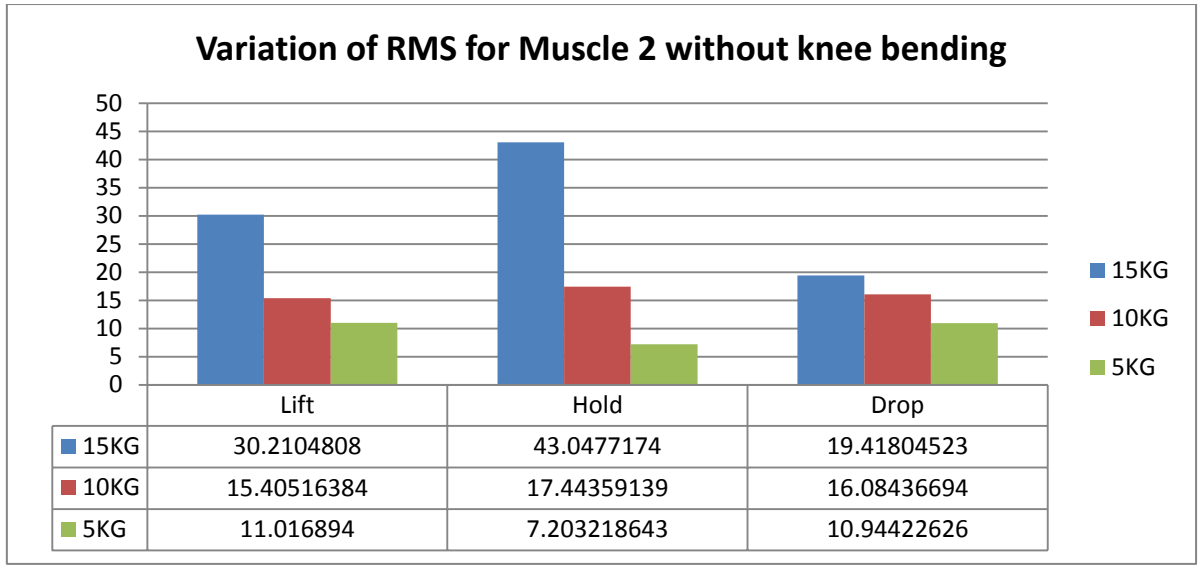

	Lift	Hold	Drop
15KG	30.2104808	43.0477174	19.41804523
10KG	15.40516384	17.44359139	16.08436694
5KG	11.016894	7.203218643	10.94422626

Fig 4.45 Variation of RMS for Muscle 2 without knee bending (Comparison of weight)

WEIGHTS	**RMS(At different time)**	
	MAX	**MIN**
15KG	Hold	Drop
10KG	Hold	Lift
5KG	Lift	Hold

- At lifting or holding or dropping time the RMS decreases with decreasing time.
- For 15g or 10kg, the maximum RMS is at holding, while 5kg the maximum RMS is at lifting.
- For 15kg minimum RMS is at dropping, for 10kg minimum RMS at lifting and for 5kg minimum, RMS is at holding.
- Here also it is observed that the difference between RMS for different stage increases with increasing weight.

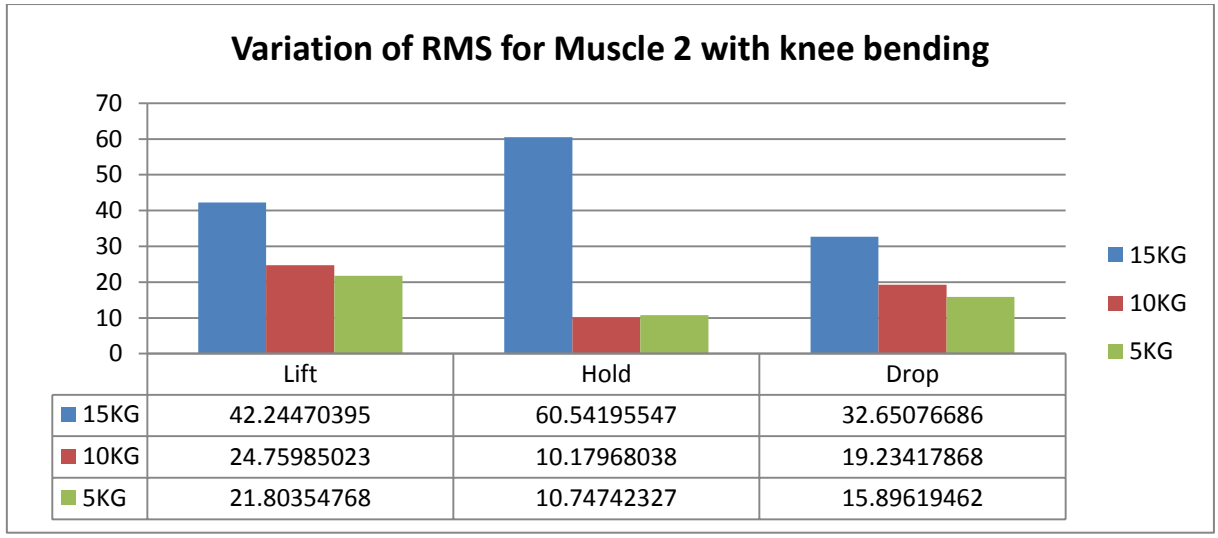

	Lift	Hold	Drop
15KG	42.24470395	60.54195547	32.65076686
10KG	24.75985023	10.17968038	19.23417868
5KG	21.80354768	10.74742327	15.89619462

Fig 4.46 Variation of RMS for Muscle 2 with knee bending (Comparison of weight)

WEIGHTS	**RMS(At different time)**	
	MAX	**MIN**
15KG	Hold	Drop
10KG	Lift	Hold
5KG	Lift	Hold

- Here at lifting or dropping the RMS decreases with decreasing weight, while at holding the RMS decreases with decreasing weight but 10kg and 5kg the RMS value almost the same
- For 10kg or 5kg, the RMS is maximum at lifting, while for 15kg it is at holding.
- For 10kg or 5kg, the minimum RMS is at holding V while for 15kg it is at dropping.

TRANSITION PERIOD COMPARISON:

Here we plot the HFD and RMS value for two transition period. Higuchi fractal dimension (HFD) indicates the complexity of muscles. The higher value of HFD means the complexity is higher.

While the Root means square (RMS) value indicates the determine degree of activation or force produced by the muscle.

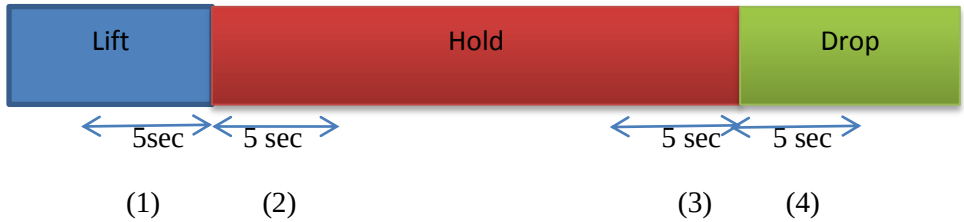

Transition1= changes from data point 1 to data set point 2
Transition2 = changes from data point 3 to data set point4

VARIATION OF HFD FOR MUSCLE1 AT TRANSITION WITHOUT KNEE BENDING

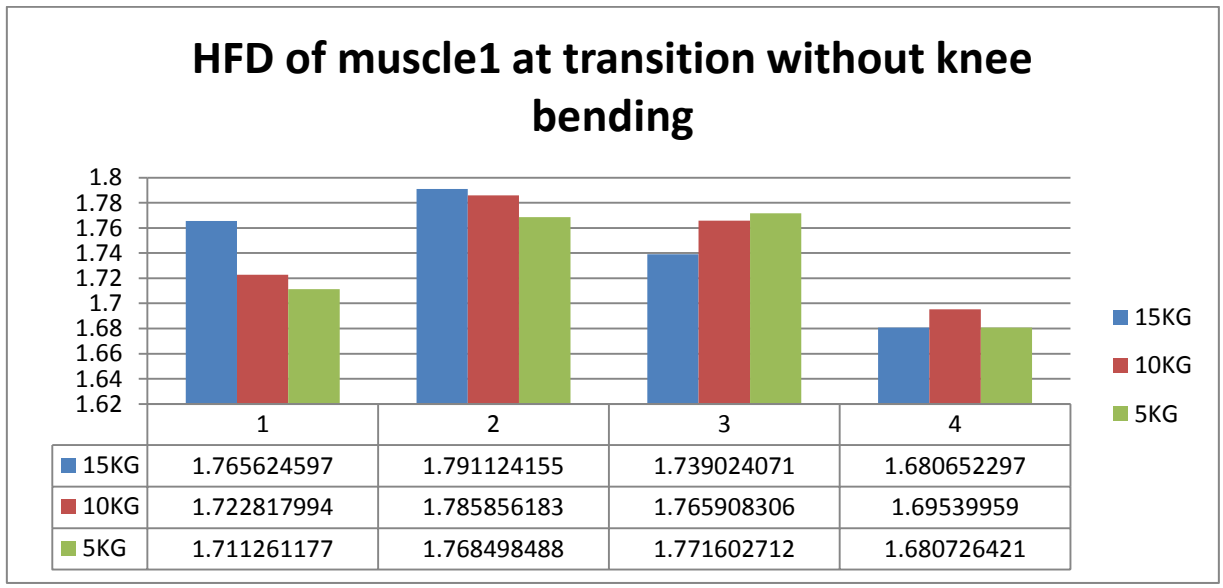

	1	2	3	4
15KG	1.765624597	1.791124155	1.739024071	1.680652297
10KG	1.722817994	1.785856183	1.765908306	1.69539959
5KG	1.711261177	1.768498488	1.771602712	1.680726421

Fig 4.47 HFD of muscle1 at transition without knee bending(transition)

- At transition1 each HFD value for different weight increases from point 1 to point 2. Which indicate that complexity increases.
- At transistion2 each HFD value for different weight decreases from point 3 to point 4

  So the complexity of muscle decreases.
- Here it is clear from point2 and point3, due to long holding time the complexity decreases from point2 to point 3. Also, the difference of complexity changes decreases with decreasing weight(i.e. for 15kg difference ofHFD from 2 3 is highest, next for 10kg and at last for 5kg)

VARIATION OF HFD FOR MUSCLE1 AT TRANSITION WITH KNEE BENDING

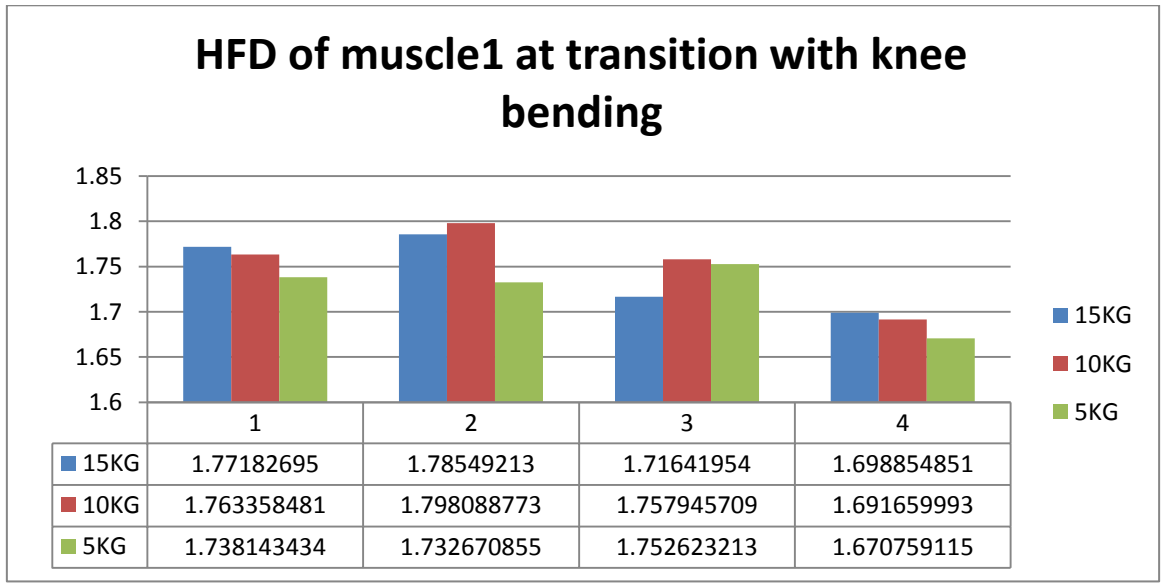

	1	2	3	4
15KG	1.77182695	1.78549213	1.71641954	1.698854851
10KG	1.763358481	1.798088773	1.757945709	1.691659993
5KG	1.738143434	1.732670855	1.752623213	1.670759115

Fig 4.48 Plot HFD for muscle1 at transition with knee bending(transition)

- At transition1 the HFD for 15kg or 10kg increases i.e. complexity increases, while for 5kg HFD almost remain the same.
- At transitrion2 each HFD value decreases I.e. the complexity decreases.
- From point 2 to point 3 the HFD for 15kg or 10kg decreases, while for 5kg HFD slightly increases.

VARIATION OF HFD FOR MUSCLE2 AT TRANSITION WITHOUT KNEE BENDING

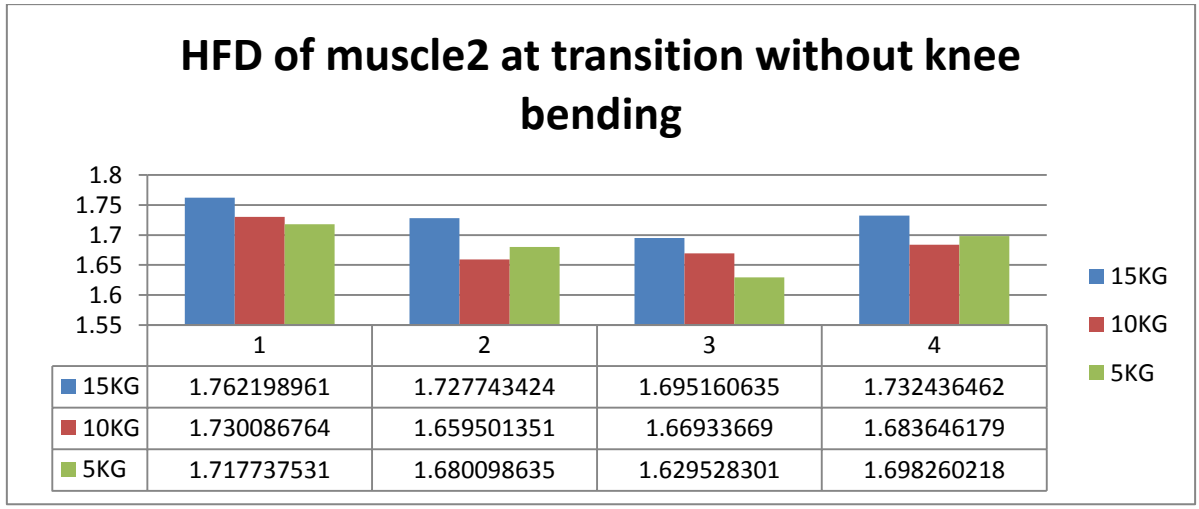

	1	2	3	4
15KG	1.762198961	1.727743424	1.695160635	1.732436462
10KG	1.730086764	1.659501351	1.66933669	1.683646179
5KG	1.717737531	1.680098635	1.629528301	1.698260218

Fig 4.49 HFD of muscle2 at transition without knee bending (transition)

- At transition1 each HFD value for different weight decreases from point 1 to point 2. Which indicate the complexity decreases.
- At transition2 each HFD value for different weight increases from point 1 to point 2. Which indicate the complexity increases.
- From point 2 to point 3 the HFD value for 15kg or 5kg decreases, while for 10kg HFD slightly increases.

VARIATION OF HFD FOR MUSCLE2 AT TRANSITION WITH KNEE BENDING

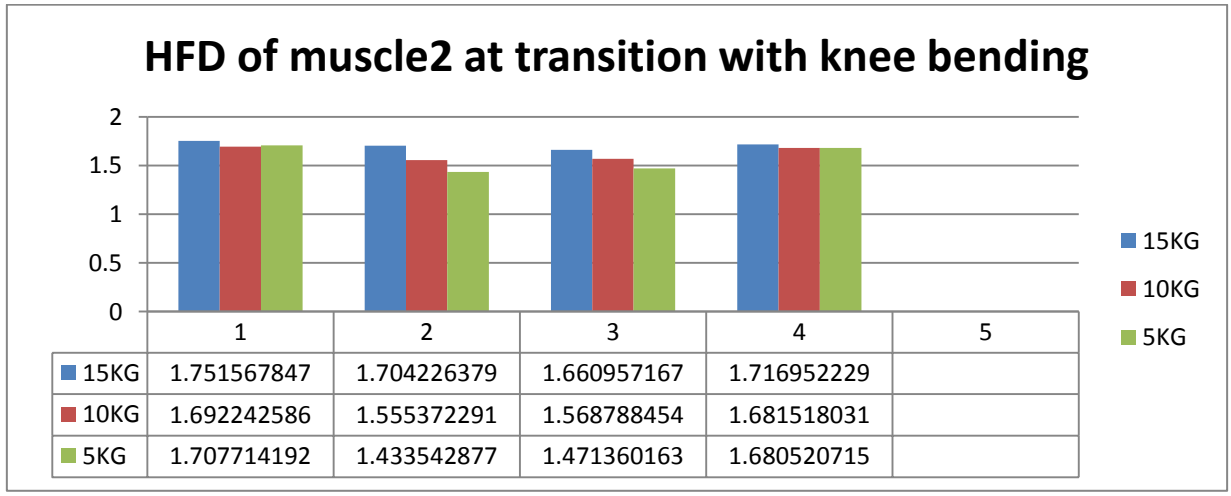

	1	2	3	4	5
15KG	1.751567847	1.704226379	1.660957167	1.716952229	
10KG	1.692242586	1.555372291	1.568788454	1.681518031	
5KG	1.707714192	1.433542877	1.471360163	1.680520715	

Fig 4.50 - HFD of muscle2 at transition with knee bending (transition)

- At transition1 each HFD value for different weight decreases from point 1 to point 2. Which indicate the complexity decreases.
- At transition2 each HFD value for different weight increases from point 1 to point 2. Which indicate the complexity increases.
- From point 2 to point 3 the HFD value for 15kg or 10kg decreases, while for 5kg HFD slightly increases, almost the same.

VARIATION OF RMS FOR MUSCLE1 AT TRANSITION WITHOUT KNEE BENDING

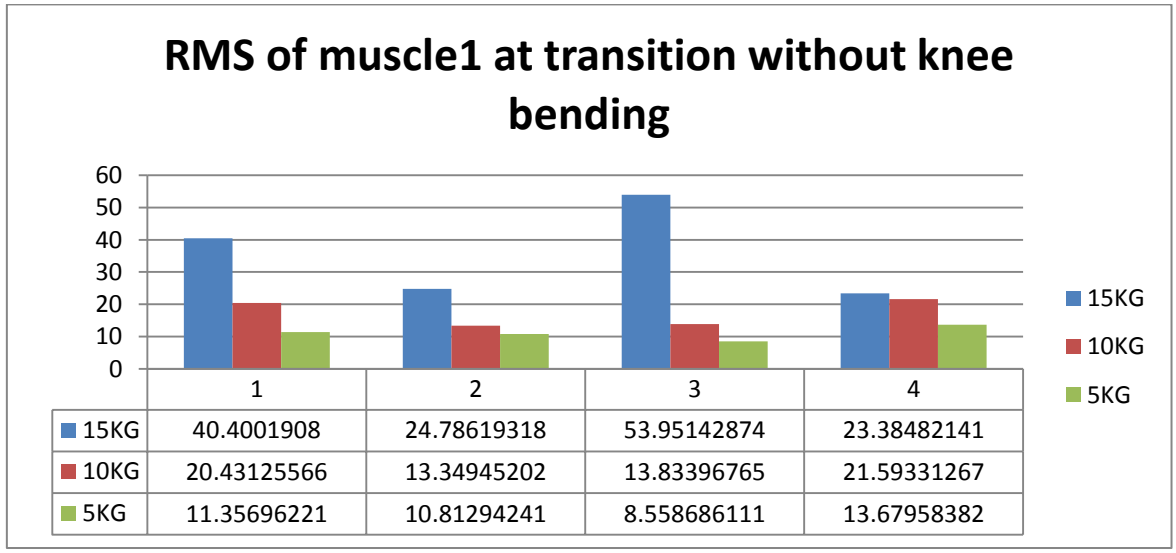

	1	2	3	4
15KG	40.4001908	24.78619318	53.95142874	23.38482141
10KG	20.43125566	13.34945202	13.83396765	21.59331267
5KG	11.35696221	10.81294241	8.558686111	13.67958382

Fig4.51 RMS of muscle1 at transition without knee bending (transition)

- At transition1 each RMS value for different weight decreases from point 1 to point 2. Which indicate the degree of activation or fore produced by muscle decreases.
- At transition2 RMS value for 15kg decreases significantly, while for 10kg or 5kg the RMS value increases marginally.
- From point 2 to point 3 the RMS value for 15kg increases, while for 10kg or 5kg RMS value slightly decreases.

VARIATION OF RMS FOR MUSCLE1 AT TRANSITION WITH KNEE BENDING

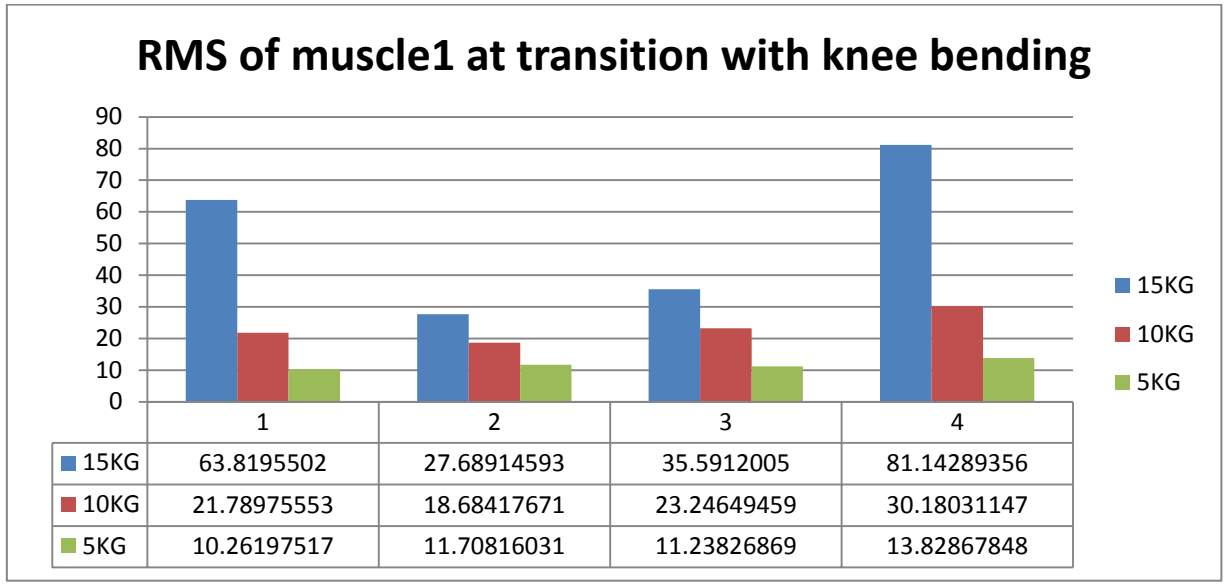

	1	2	3	4
15KG	63.8195502	27.68914593	35.5912005	81.14289356
10KG	21.78975553	18.68417671	23.24649459	30.18031147
5KG	10.26197517	11.70816031	11.23826869	13.82867848

Fig 4.52 RMS of muscle1 at transition with knee bending (transition)

- At transition1 RMS value for 15kg or 10kg decreases significantly, while for 5kg the RMS value increases marginally (almost remain same).
- At transition2 each RMS value for different weight increases from point 1 to point 2. Which indicate the degree of activation or fore produced by muscle increases.
- From point 2 to point 3 the RMS value for 15kg or 10 kg increases, while for 15kg RMS value slightly decreases.

VARIATION OF RMS FOR MUSCLE2 AT TRANSITION WITHOUT KNEE BENDING

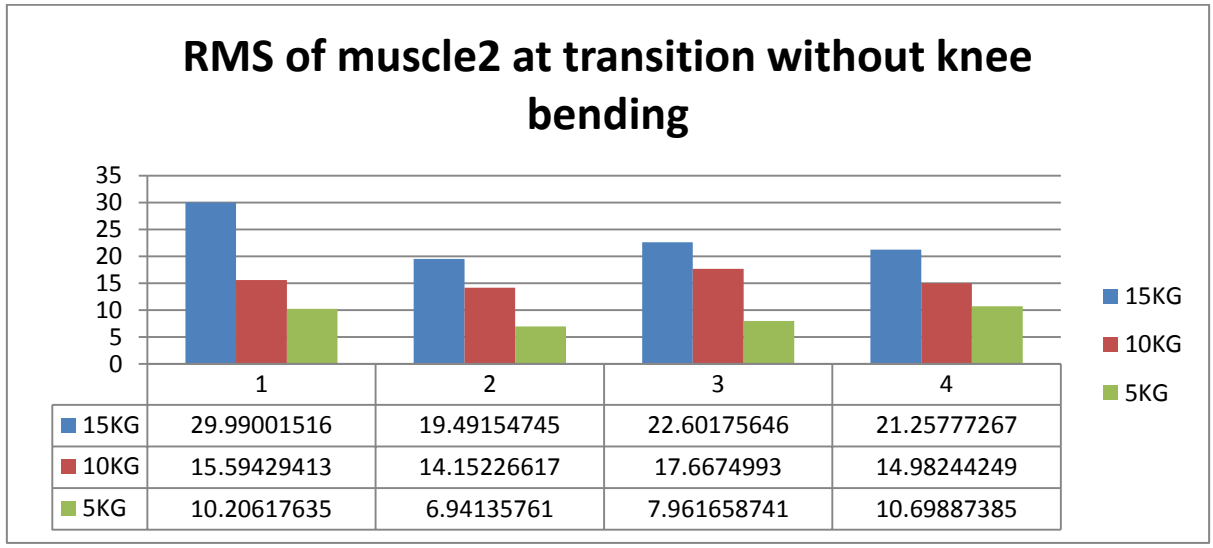

	1	2	3	4
15KG	29.99001516	19.49154745	22.60175646	21.25777267
10KG	15.59429413	14.15226617	17.6674993	14.98244249
5KG	10.20617635	6.94135761	7.961658741	10.69887385

Fig4.53 RMS of muscle2 at transition without knee bending(transition)

- At transition1 each RMS value for different weight decreases from point 1 to point 2. Which indicate the degree of activation or fore produced by muscle decreases.
- At transition2 RMS value for 15kg or 5kg decreases, while for 5kg the RMS value increases.
- From point 2 to point 3 the RMS value for 15kg or 10 kg or 5kg increases

VARIATION OF RMS FOR MUSCLE2 AT TRANSITION WITH KNEE BENDING

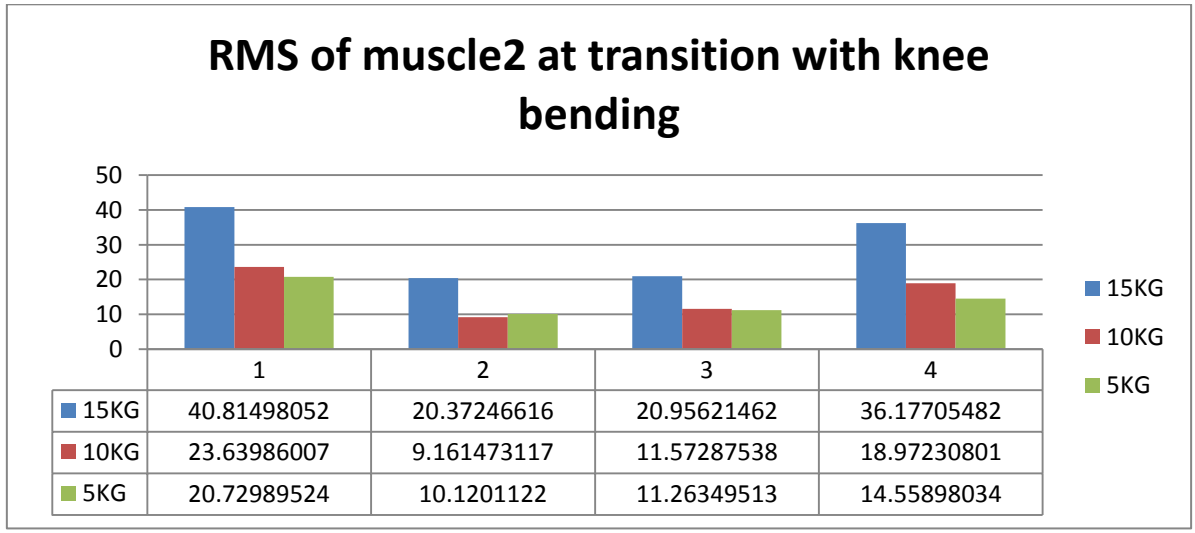

	1	2	3	4
15KG	40.81498052	20.37246616	20.95621462	36.17705482
10KG	23.63986007	9.161473117	11.57287538	18.97230801
5KG	20.72989524	10.1201122	11.26349513	14.55898034

Fig 4.54 RMS of muscle2 at transition with knee bending (transition)

- At transition1 each RMS value for different weight decreases from point 1 to point 2. Which indicate the degree of activation or fore produced by muscle decreases.
- At transition2 each RMS value for different weight increases from point 1 to point 2. Which indicate the degree of activation or fore produced by muscle increases.
- From point 2 to point 3 the RMS value for 15kg or 10 kg or 5kg increases. But the change is so small.

EFFECT OF SURYANAMASKAR ON CARDIOVASCULAR SYSTEM:

METHODOLOGY

DESIGN OF EXPERIMENT:

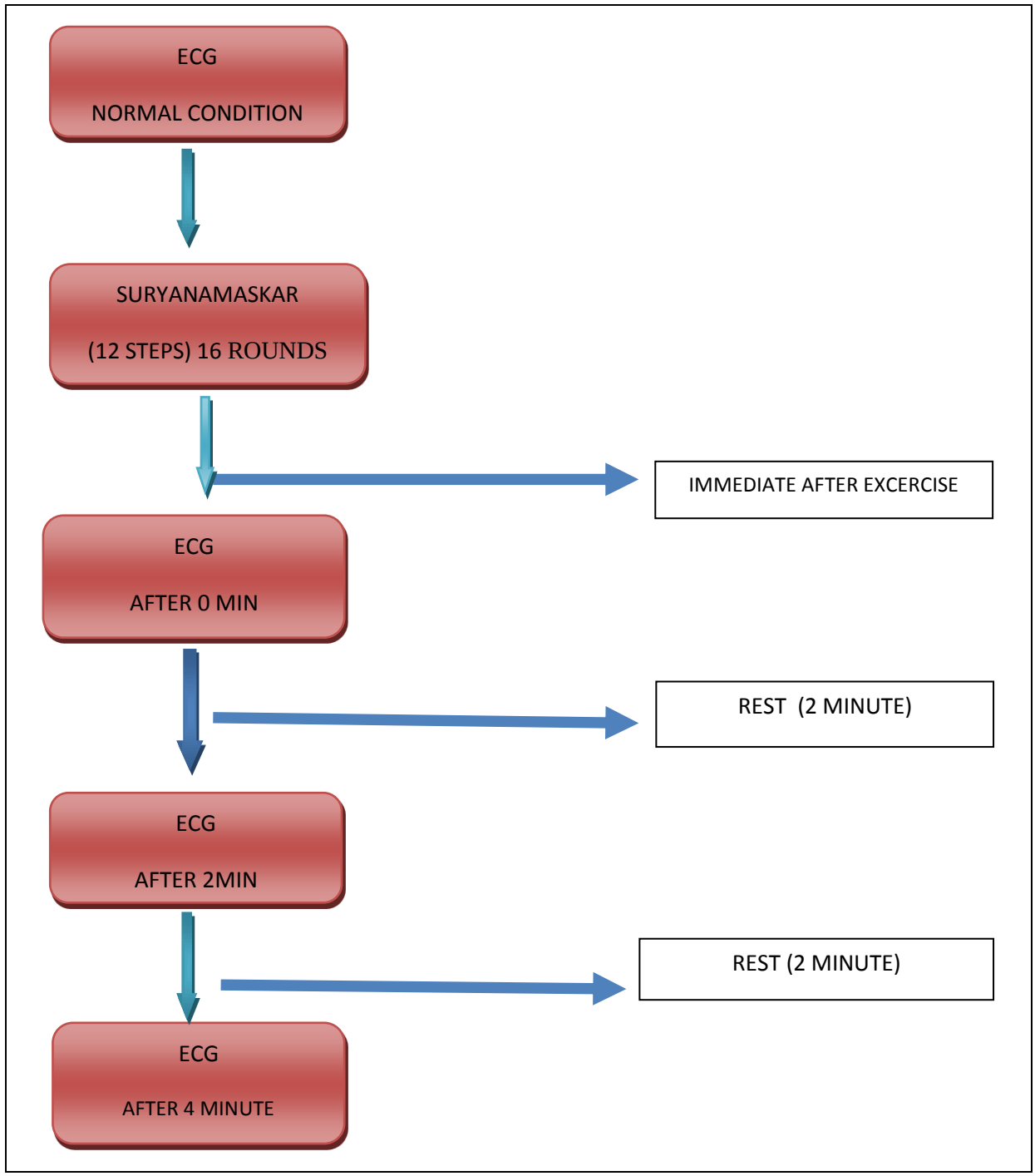

This experiment is based on the effect of Surya Namaskar (Yoga) on the cardiovascular system.

More specifically, effects on heart muscles.

ECG value was taken for one-time duration. All the subjects are asked to take rest for 15 minutes before the normal ECG condition.

The subject had done the 16 rounds Surya Namaskar (one round= 12 steps). Immediate after this yoga exercise (No rest) second ECG data was taken. Then the subject took 2 minutes rest and after that again ECG was taken. Again after 4min final, the ECG data was taken

ANALYSIS: After raw ECG data was taken the signal converted into .csv format. After importing the data in MATLAB we used only lead I for our analysis. The signal analysis was done by the following steps in the next page

FLOWCHART OF ECG ANALYSIS

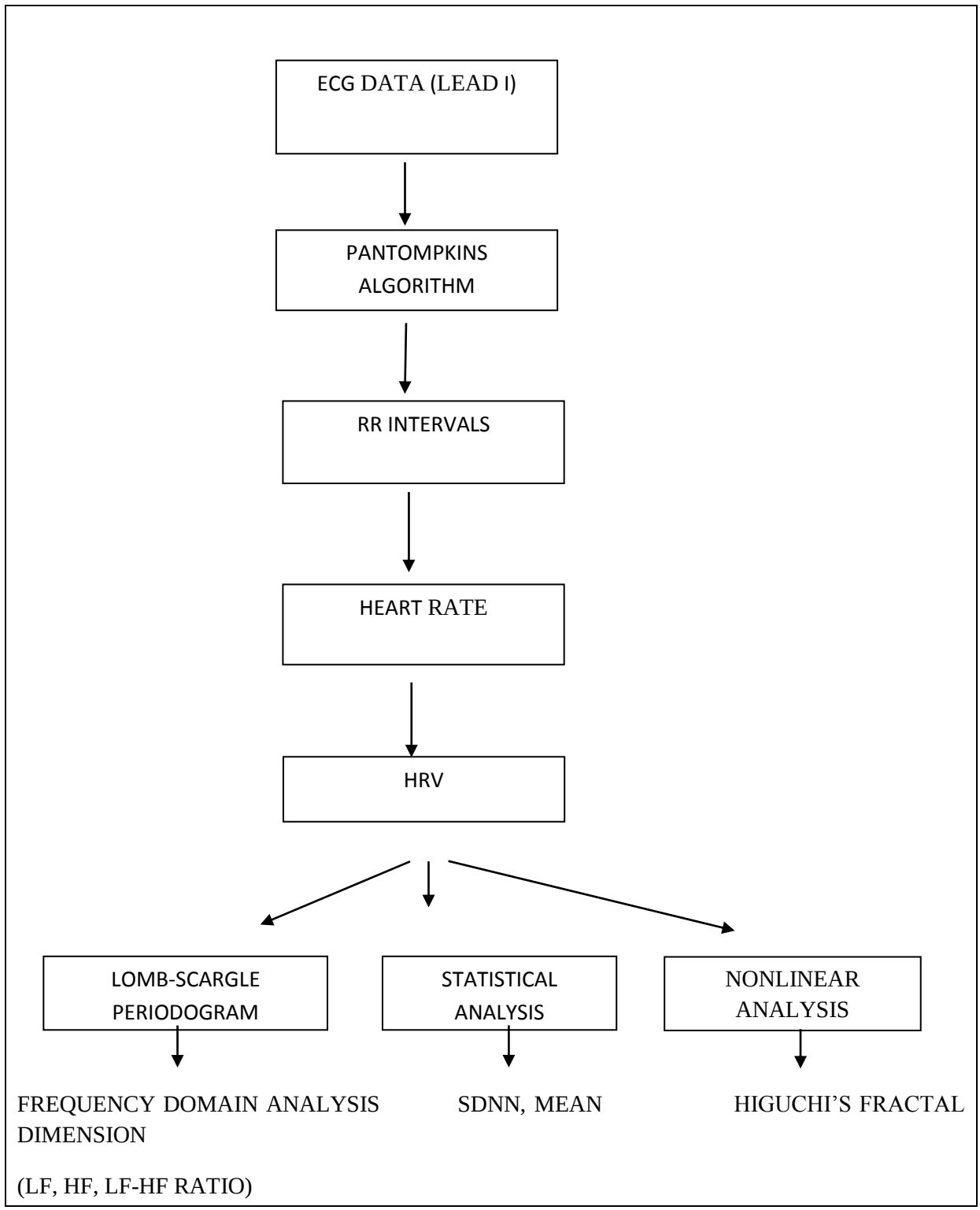

In this experiment, we use only lead I value. The ECG signal was acquired by Einthoven's triangle lead placement rule. The electrodes were placed on the right arm, left arm, left leg and right leg.

- **Lead I** is the voltage between the (positive) left arm electrode and right arm electrode:
- **Lead II** is the voltage between the (positive) left leg electrode and the right arm electrode
- **Lead III** is the voltage between the (positive) left leg electrode and the left arm electrode

RESULTS AND DISCUSSION:

At first, for ECG signal processing we used Pan Tomkins algorithm (QRS Detection). The resulting figure is given below:

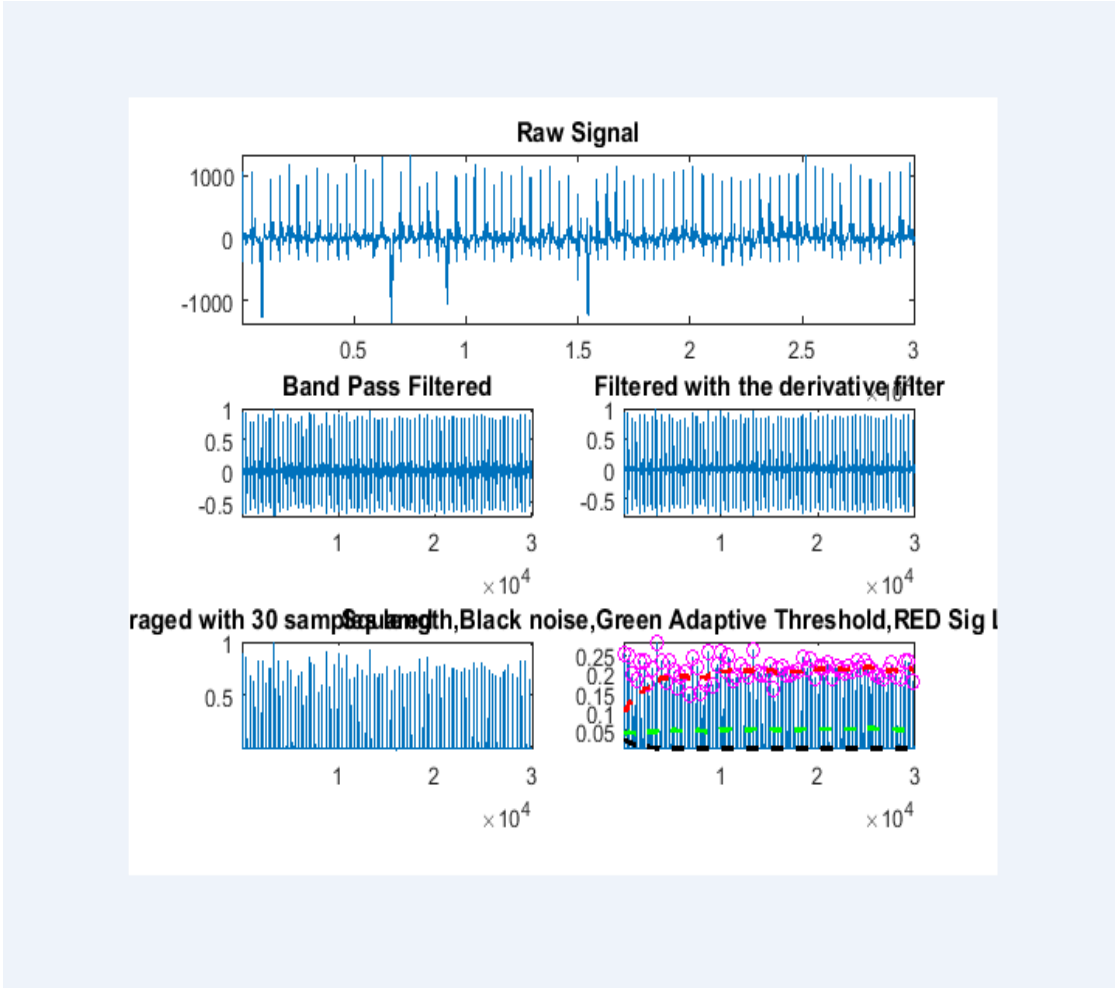

Fig 4.55: filtering the ECG signal.

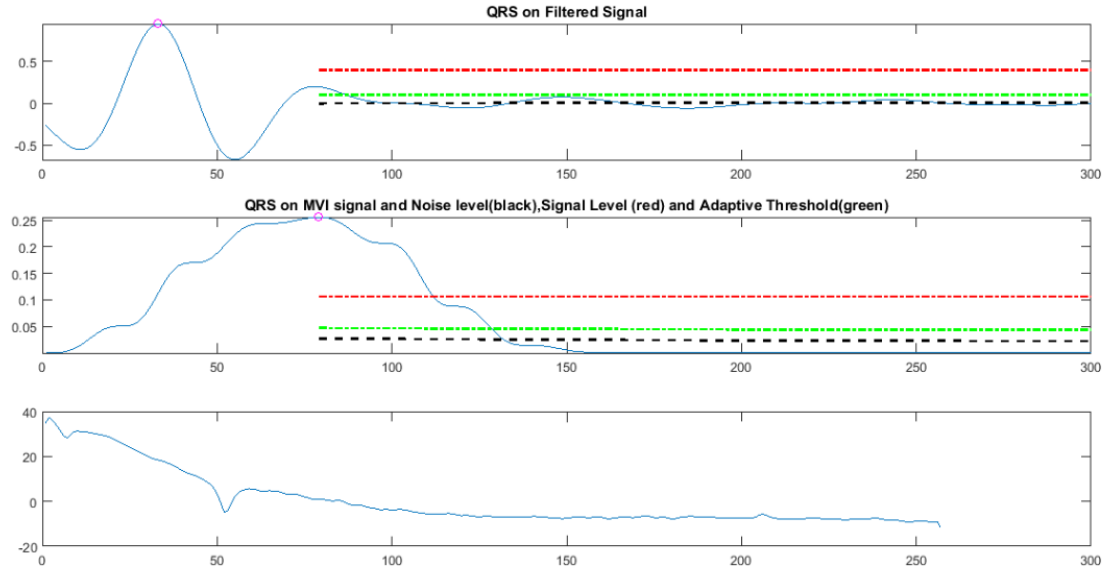

Fig 4.56 QRS on filtered signal thresholding

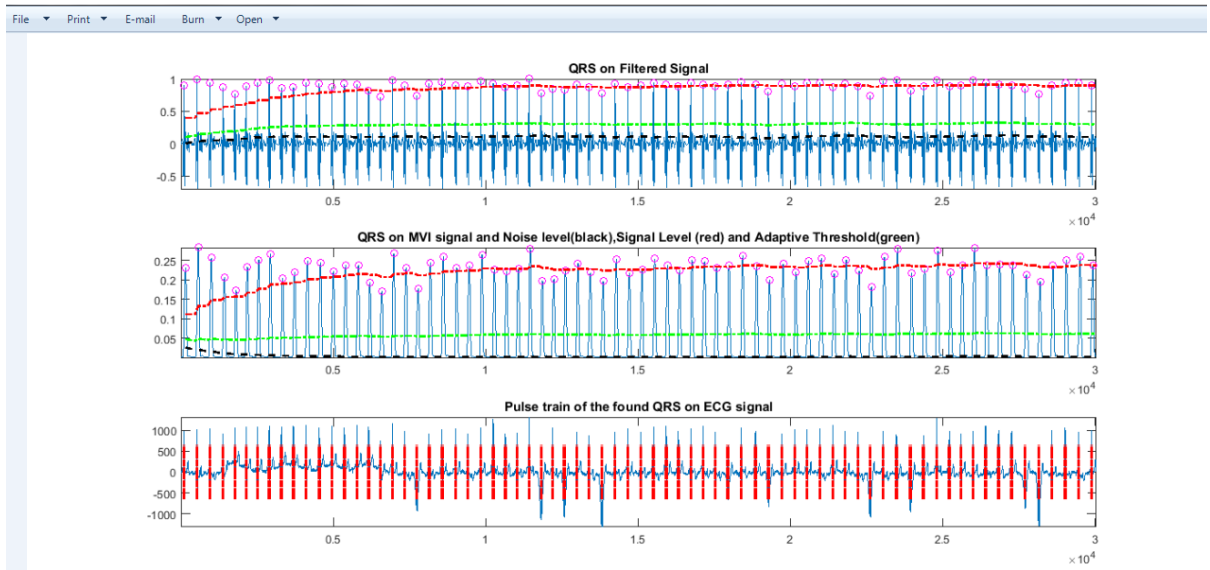

Fig 4.57 QRS peak detection.

VARIATION OF HEART RATE BEFORE AND AFTER SURYA NAMASKAR

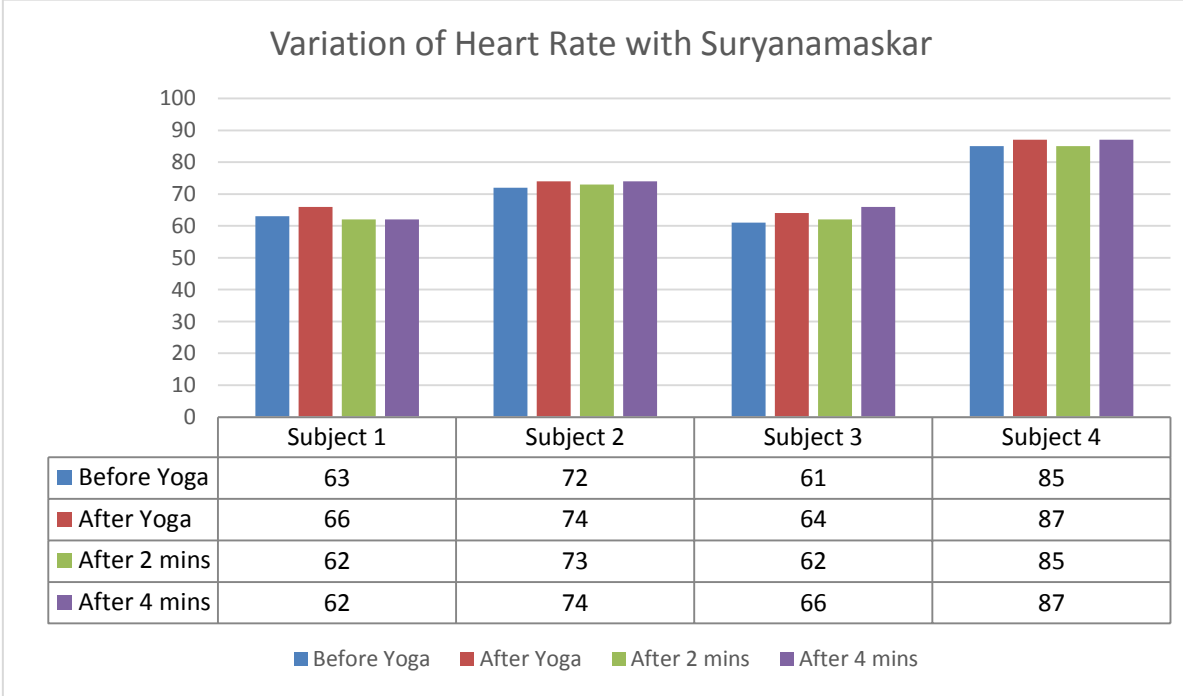

	Subject 1	Subject 2	Subject 3	Subject 4
Before Yoga	63	72	61	85
After Yoga	66	74	64	87
After 2 mins	62	73	62	85
After 4 mins	62	74	66	87

Fig 4.58. Variation of Heart Rate before and after Suryanamaskar.

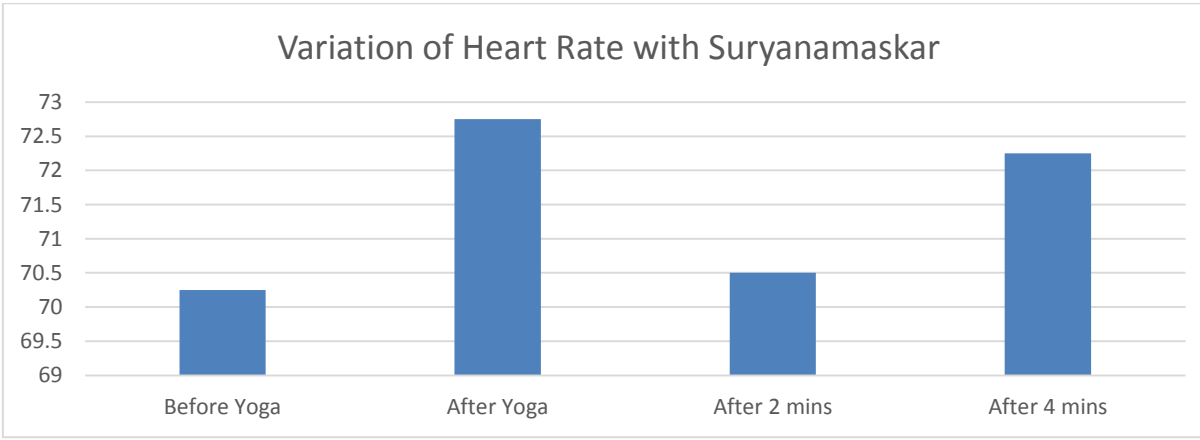

Fig 4.59. Variation of Avg. Heart Rate before and after suryanamaskar

- Here it is observed that for all subjects the immediate after Suryanamaskar Heart Rate increases slightly.
- The Heart rate may be increased or decreased after 2min and 4min of the yoga exercise for different subjects. But the average value of Heart Rate for all subjects again increases after 2min to 4min.

- The heart rate is maximum at immediate after Suryanaskar(Yoga).

VARIATION OF HFD BEFORE AND AFTER SURYANAMASKAR

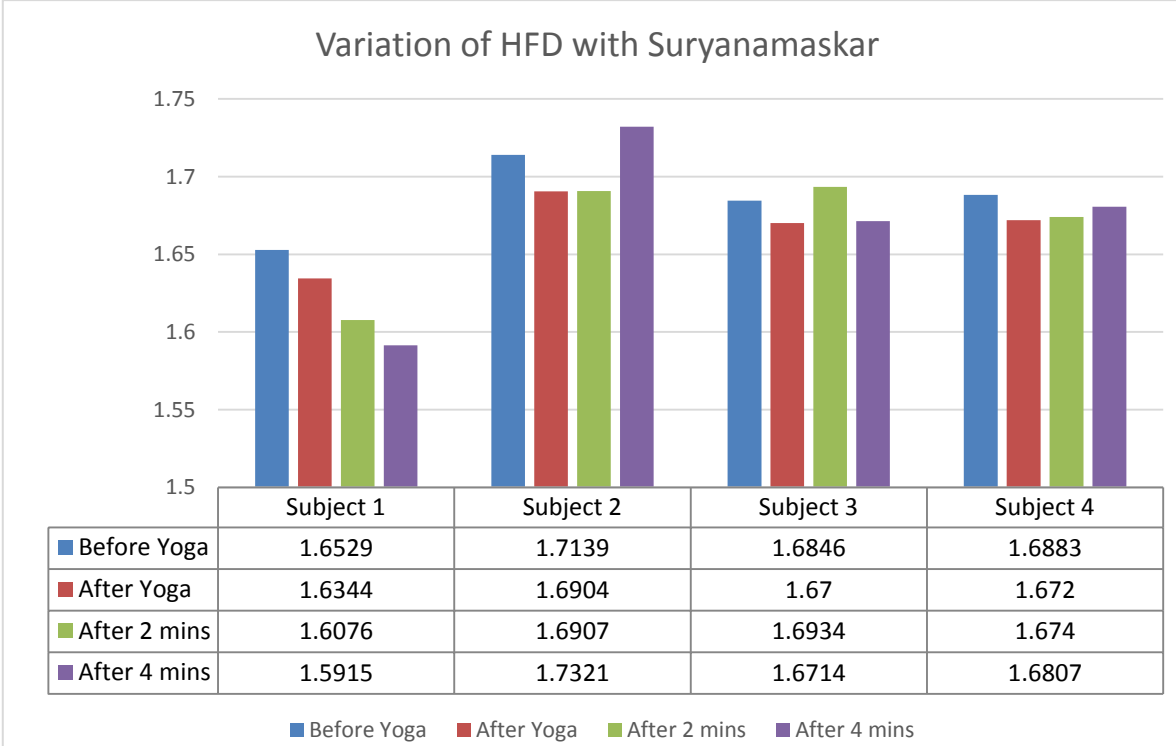

	Subject 1	Subject 2	Subject 3	Subject 4
Before Yoga	1.6529	1.7139	1.6846	1.6883
After Yoga	1.6344	1.6904	1.67	1.672
After 2 mins	1.6076	1.6907	1.6934	1.674
After 4 mins	1.5915	1.7321	1.6714	1.6807

Fig.4.60 Variation of Fractal Dimension before and after Suryanamaskar.

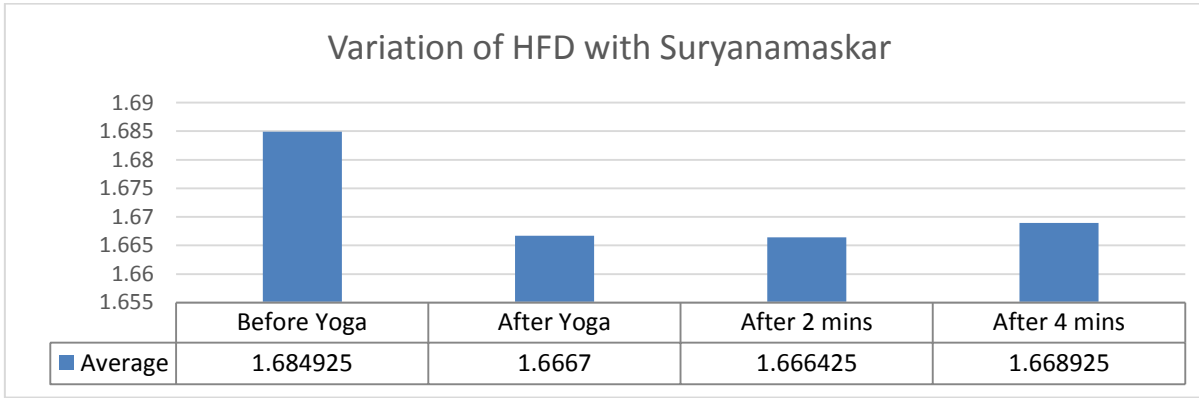

	Before Yoga	After Yoga	After 2 mins	After 4 mins
Average	1.684925	1.6667	1.666425	1.668925

Fig4.61. Variation of average Fractal Dimension before and after Suryanamaskar.

- From the above observations, it is clear that immediate after Suryamaskar The value of Fractal Dimension significantly decreases for all subjects, which indicating reduction in complex nature.

- After 2min of exercise, the Fractal Dimension is gradually increased i.e. the complexity is increasing again with time.
- After 4min of Suryanamaskar, the HFD increases for some subjects compare to the previous stage, while for some subjects this value may increases.
- But if we take the average HFD for all stage then this value increases with time.

VARIATION OF LF-HF RATIO OF HRV BEFORE AND AFTER SURYANAMASKAR

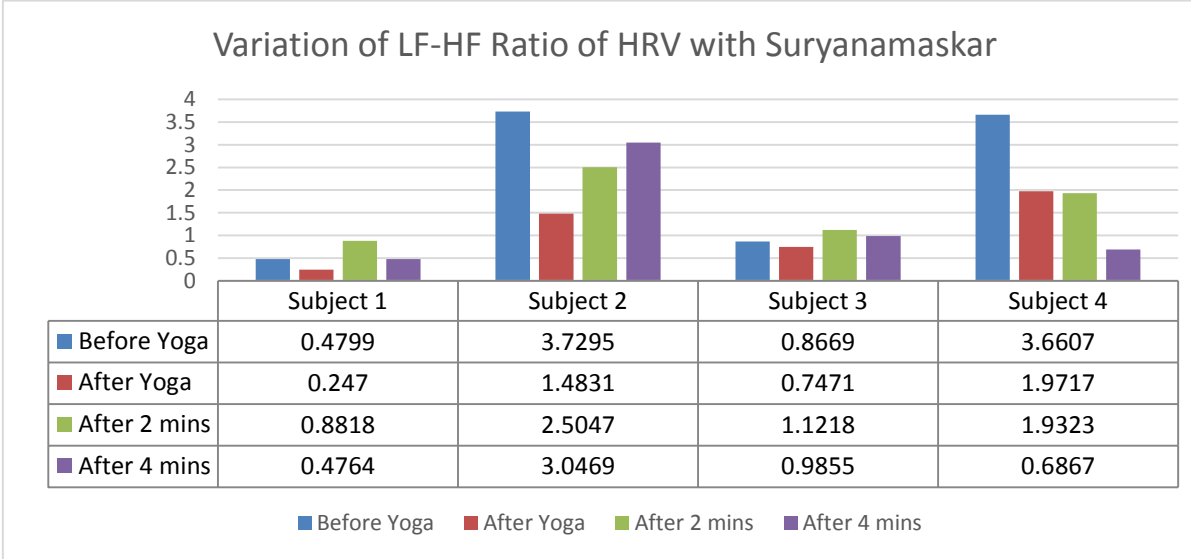

	Subject 1	Subject 2	Subject 3	Subject 4
Before Yoga	0.4799	3.7295	0.8669	3.6607
After Yoga	0.247	1.4831	0.7471	1.9717
After 2 mins	0.8818	2.5047	1.1218	1.9323
After 4 mins	0.4764	3.0469	0.9855	0.6867

Fig.4.62 Variation of LF-HF ratio of HRV before and after suryanamaskar

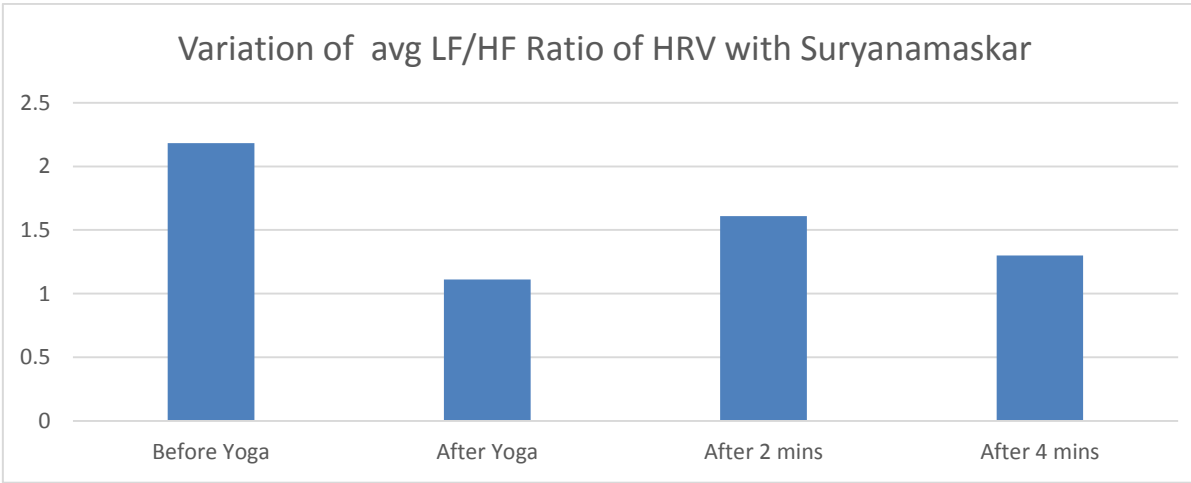

Fig.4.63 Variation of average LF-HF ratio of HRV before and after suryanamaskar

- Immediate after suryanamaskar the value of LF-HF ratio decreases. Thus there is a significant increase in the parasympathetic nervous system activity due to Suryanamaskar exercise.

- After 2min resting the LF-HF ratio increases. But it changes randomly for different subjects. This significantly indicates the stress relaxation condition.

- After 4 min LF-HF ratio may decrease compare to the previous stage. But this value varies with subject to subject.

Discussion: LF/HF ratio is of sympatho/vagal balance, is different for a different subject. This may happen due to the heart condition of the subject, some subjects might have their meal just before yoga, while some subjects might do the yoga in quick time or not take proper rest. May this process should be done in a repeated session.

VARIATION OF HF COMPONENT OF HRV WITH SURYANAMASKAR

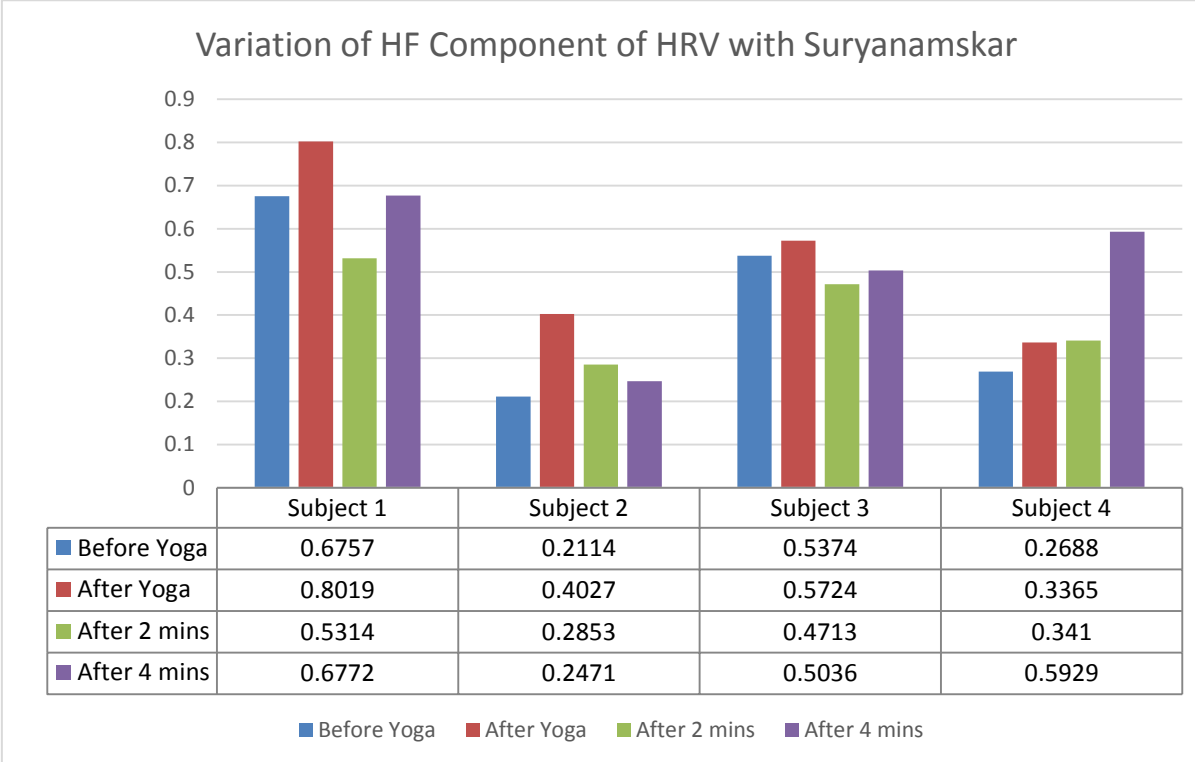

	Subject 1	Subject 2	Subject 3	Subject 4
Before Yoga	0.6757	0.2114	0.5374	0.2688
After Yoga	0.8019	0.4027	0.5724	0.3365
After 2 mins	0.5314	0.2853	0.4713	0.341
After 4 mins	0.6772	0.2471	0.5036	0.5929

Fig 4.64 Variation of HF component of HRV

- Immediate after Suryanamaskar the HF component increases for all subjects. Since the HF component is the marker of the activity of the parasympathetic nervous

system, this is the clearly indicate that yoga gives the subjects a stress relaxation stimulus or Heart works more effectively.

- After 2min of yoga HF component significantly decreases for all subjects
- After 4min of yoga, the HF component increases for some subjects, while for some subjects HF component decreases marginally.

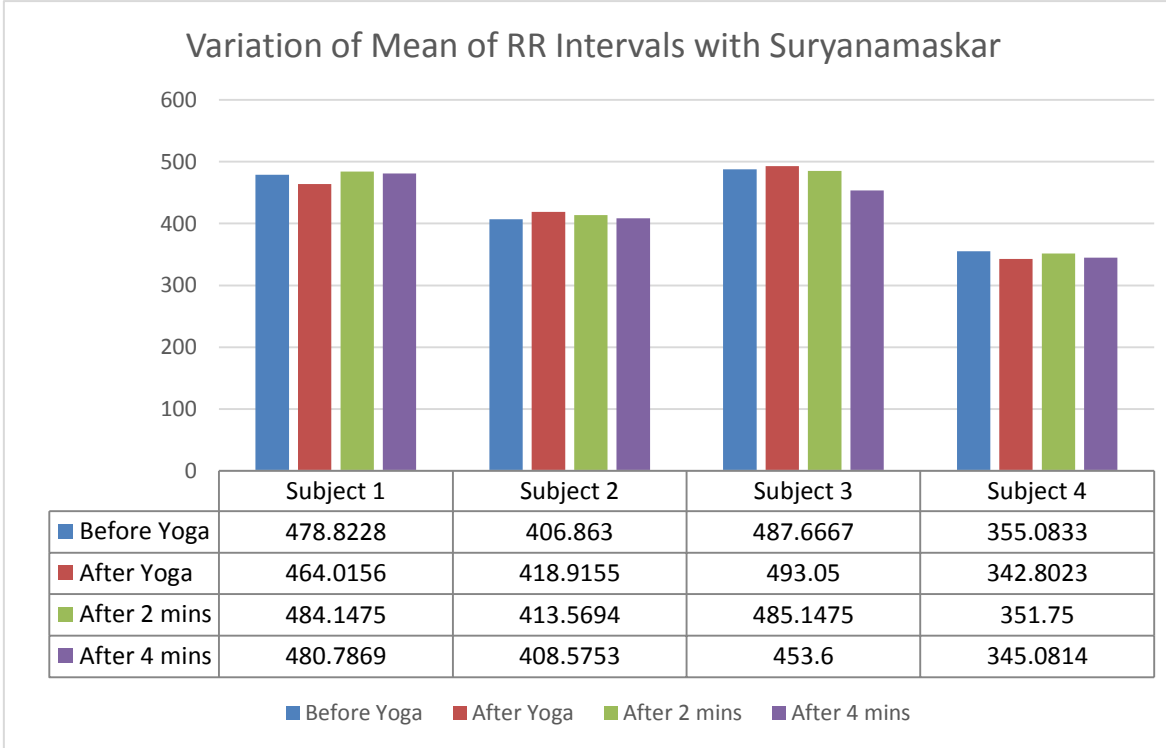

	Subject 1	Subject 2	Subject 3	Subject 4
Before Yoga	478.8228	406.863	487.6667	355.0833
After Yoga	464.0156	418.9155	493.05	342.8023
After 2 mins	484.1475	413.5694	485.1475	351.75
After 4 mins	480.7869	408.5753	453.6	345.0814

Fig: 4.65 Variation of Mean of RR Intervals

- After 2min of yoga, the mean value may decrease or increase depending upon the subject.
- After 4min of yoga, the mean value decreases from its previous state
- After 4min of yoga the min value also gradually decreases.

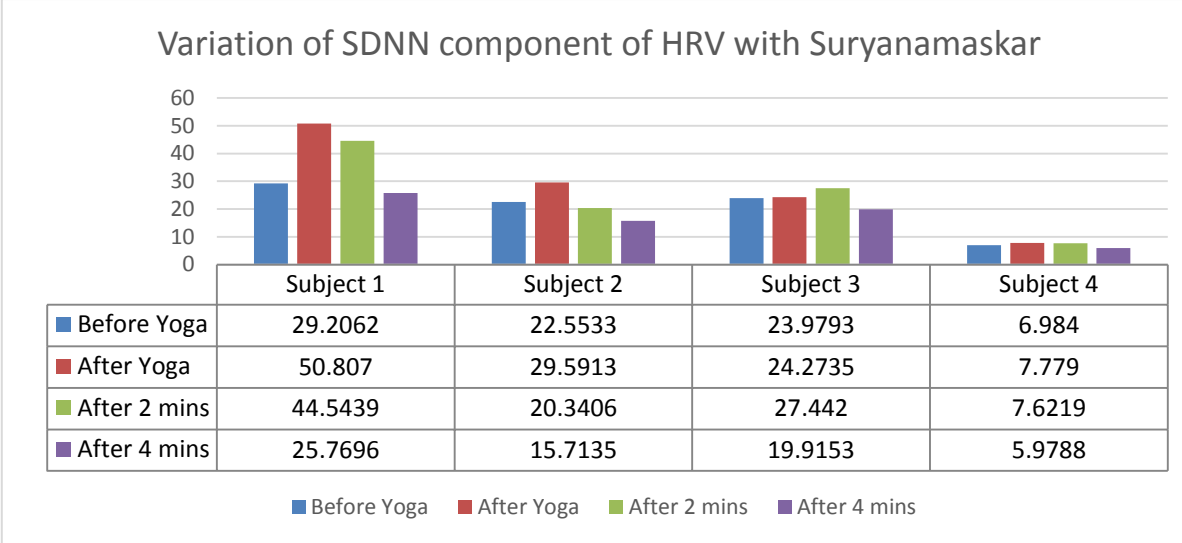

	Subject 1	Subject 2	Subject 3	Subject 4
Before Yoga	29.2062	22.5533	23.9793	6.984
After Yoga	50.807	29.5913	24.2735	7.779
After 2 mins	44.5439	20.3406	27.442	7.6219
After 4 mins	25.7696	15.7135	19.9153	5.9788

Fig: 4.66 Variation of SDNN component of HRV

- Immediate after suryanamaskar the value of SDNN increases significantly.
- After 2 min of yoga, the standard deviation may increase or decreases depending upon the subject.
- After 4min of yoga, the standard deviation value significantly decreases.

CONCLUSION:

Electromyography carries a lot of information about the neuromuscular system in coordinating the musculoskeletal movements of the body. One such application of EMG signal is explored in this work, which is basically obtaining the EMG-Force relationship during voluntary contraction. The proposed EMG-Force relationship using Vrms and Vpp as output parameters in correspondence to hand grip force as the input stimuli has thrown some light into the way of motor unit action potential generation scheme. The trends of Vrms and Vpp provides some insightful findings pertaining to muscular contraction. We have observed that after 60% MVC there is a considerable decrease in values of Vpp indicating saturation condition. Moreover, the trends in Vrms shows that within the range of 40% to 80% MVC the rate of MUAP generation is linear and then falls. We have also seen that involvement of Flexor DigitorumProfundus is much more than Biceps Brachii during application of hand grip force up to 60% MVC, and then the Biceps muscle also come into action to provide the necessary force.

The water bucket lifting EMG based experiment for nonlinear and statistical analysis of various loads with different postures determines a fruitful picture of complexity and degree of activation or estimated force produced by the different muscle groups. The test explains how the trapezius and triceps muscle complexity changes with body movement when the muscle contracts. The muscle complexity decreases with increasing weight of the water bucket. The complexity also significantly different for two muscles when they are involved in the same type of work.

For the higher value of weight, the complexity for trapezius muscle gradually decreases towards lifting to dropping, while for triceps muscle the complexity is minimum at holding.So during lifting and dropping time of water bucket the trapezius muscle involvement is more than triceps, but at holding time the triceps muscle is more effective. The results also clearly give us better ideas that without knee bending , at lifting and dropping time the complexity difference between these two muscles less compare to with knee bending condition. For lighter weight (i.e. 10kg or 5kg) the complexity decreases towards lifting to holding, while gradually increases towards holding to dropping time.

RMS value analysis tells us that force produced by trapezius muscle without knee bending gradually decreases towards lifting to holding or dropping time, while for triceps it first increases at lifting to holding time but then the degree of activation or force decreases again

(but at dropping the value of muscle force is very less than lifting time force). At the time of with knee bending the force value first decreases for lifting to holding then increases at dropping time for trapezius muscle (for 5kg there is no significant change), while for triceps muscle the force value first decreases at lifting to holding and again it increases at drooping.

At the time without knee bending the force for lifting or dropping trapezius muscle produces more force compare to with knee bending condition.

For trapezius muscle, without knee bending at transition the complexity increases at first phase of holding, while at the last phase of holding it decreases due to long holding. Again at transition2, the complexity decreases significantly from its previous state. The complexity with knee bending when 5kg or 10 kg shows some opposite phenomena.

For triceps muscle, the complexity without knee bending at first transition decreases but at second transition it increases again, while with knee bending condition at first transition complexity decreases and at second transition it increases but the changes of complexity are so close to each other. The force produced by muscle also changes simultaneously for two transition period.

So the here we get a relationship of how to force produced by muscle and complexity of muscle changes for various load with different postures.

In the learning process of the effect of Yoga on cardiovascular system revealed a beautiful relationship between heart rate with suryanamaskar (yoga), the heart rate always increases immediate after yoga but after few times it decreases or increases depending upon the subjects.

The nonlinear analysis (HFD) estimated the complexity changes of the cardiovascular system for suryanamaskar with time. It is clear that after yoga the complexity of cardiovascular system decreases, while at resting complexity again raises with time.

The Surya namaskar (yoga) also causes relaxing the system but for a higher resting time the stress relaxing phenomena decreases. This process is completed with a proper order for all subjects.

All parameters change for subjects who are involved in regular exercise is quite periodic, while for normal subjects who are out of exercise habit random changes are found. By repeating the same subjects for several times this might be formed a significant order when the effect of suryanamaskar on the cardiovascular system.

FUTURE SCOPES:

This proposed model needs to be tested and validated on arbitrary EMG signals, which were not used in this mathematical model generation. How effective is Vrms and Vpp in quantifying fatigue point and prediction of the limit of muscular tenacity is also needed to be studied in the near future?

Artificial Intelligence and Neural Network modelling based on these features can also be considered as a possible scope of work in this regard.

The EMG based water bucket lifting model can be applied for the fatigue test of different muscle groups by frequency domain analysis with a long holding time of load. This protocol needs to be tested without any load condition. The muscle groups can be changed to obtain for other joint muscle groups activity with the same or some other postures. This model with deep study may give us proper water bucket lifting technique.

The effect of Suryanamaskar (yoga) on cardiovascular system also needs to be tested on more subjects. The subjects may be normal or habituated with yoga. The repetition with the same subject will give us better knowledge of heart muscle flexibility with yoga. This model can be used for subjects with heart blockage.

PUBLICATION:

A. Biswas, D. parbat, M. Chakraborty, ‘Establishment of EMG-Force relationship obtained during Simultaneous Voluntary Contraction of Biceps and Flexor Digitorum Profundus Muscles ’ 2019 IEEE 5th International Conference for Convergence in Technology (I2CT).

REFERENCES:

1. P. Rameshbabu, “Digital Signal Processing”.

2. Handbook of Biomedical Instrumentation by R. S. Khandpur.

3. G. D. Clifford, F. Azuaje and P. E. Mcsharry “Advanced Methods and Tools for ECG Data Analysis”, London:Egg. In Medicine and Biology, 2006.

4. Elgendi M, Eskofier B, Dokos S, Abbott D. “Revisiting QRS detection methodologies for portable, wearable, battery-operated, and wireless ECG systems.” PLoS One. 2014;

5. International Journal of Innovative Technology and Exploring Engeenering (IJITEE) ISSN:2278-3075, Volume-3, Issue-3, August 2013.

6. NeuroSky, “Brain Wave Signal (EEG) of NeuroSky”, 15 December, 2009.

7. S. Carmel and A. J. Macy, “Physiological signal processing laboratory for biomedical engineering education”, in Engeenering in Medicine and Biology Society, 2005.IEEE-EMBS 2005. 27th Annual International Conference of the, 2006,pp.859-862.

8. P. Kligfield, et al., “Recommendations for the Standardization and Interpretation of the Electrocardiogram”, Journal of the American College of Cardiology, Vol. 49,2007,pp.1109-1127.

9. J. T. Tikkanen, et al., “Long term outcome associated with early repolarization on electrocardiography”, New England Journal of Medicine, Vol. 361,2009,pp.2529-2537.

10. G. Wagner, radiography 10ED : Wolters Kluwer Health, 2001.

11. B. Surawicz and T.Knilans, Chou’s electrocardiography in clinical practice:adult and pediatric:Saunders, 2008.

12. M. Joshi, S. Patel and Dr. L. Hmurcik, “Improvements in Electrocardiography Smoothening and Amplification”, University of Bridgeport, 2008.

13. K. Joshi, “Early Mayocardial Infraction Detection”, Sam Jose State University, 2009.

14. D. Parekh, “Designing Heart Rate, Blood Pressure and Body Temperature Sensor for Mobile On-Call System”, 2010

15. H. C. Burger. Heart and Vector, Physical Basis of Electrocardiography. Philips Technical Libary, 1968.9,90.

16. Y. Weiting, Z. Runjing, “An improved self-adaptive filter based on LMS algorithm for filtering 50 Hz interference in ECG signals”, in: Proceedings of the 8th International Conference on Electronic Measurement and Instruments ICEMI’07, 2007,pp. 3-874–3-878.

17. K. Daqrouq, A.-R. Al-Qawasmi, ECG enhancement using wavelet transform,WSEAS Trans. Biol. Biomed. 7 (2) (2010) 62–72.

18. H.C.Burger and J. B. Van Milaan.Heart-vector and HeartJ, 8:157-161, 1946.8,11,13.

19. Linear Functional in ECG and VCG by Prof. Dr. Martin Burger, M* unstet, February 2013.

20. Physiology 3064,Daniel Sigg, MD, PhD, Siggxool@umn.edu

21. http://www.medic.inenet.com/arrhythmia_irregular_heartbeat/article.htm

22. L. A. Orejarens, H. Jr. Vidiallet, F. Destefano et al. Paroxysmal supraventricular tachycardia in the general population. J Am College Cardiol 1998;31:150-7.

23. Tikkanen I, Metsarinne K, Fyhrquist F. Atrial natriuretic peptide in paroxysmal supraventricular tachycardia. Lancet 1985;2:40-1.

24. Konstantions A. Gatzoulis, Stefanos Archontakis, Polychronis Dilaveris, Dimitrios Tsiachris, Petros Arsenos, Skevos Sideris,, Christodoulos Stefanadis. Ventricular Arrhythmias : From the Electrophysiology Laboratory to Clinical Practice Part I : Malignant Ventricular Arrhythmias: Hellenic J Cardiol 2011;52:525-535.

25. Elizabeth M. Cherry and Flavio H. Fenton, Department of Biomedical Sciences, College of Veterinary Medicine, Cornell University, Ithaca, NY:Heart Structure, Function and Arrhythmias from http://thevirtualheart.org.

26. Koplan BA, Stevenson WG. Ventricular tachycardia and sudden cardiac death. Mayo Clinic Proc. 2009;84:289-297.

27. Calkins H. Kalbfleisch SJ, el – Atassi R, Langberg JJ, Morady F. Relation between efficiency of radio frequency catheter ablation and site of origin of idiopathic ventricular tachycardia. Am J Cardiol. 1993;71:827-833.

28. Bogun F, Bahut M, Knight BP, et al. Comparison of effective and ineffective target sites that demonstrate concealed entrainment in patients with coronary artery disease undergoing radio frequency ablation of ventricular tachycardia. Circulation. 1997;95:183-190.

29. Nogami A, Nai to See, Tada H, et al. Demonstration of diastolic and presystolic Purkinjie potentials as critical potentials in a macroreentry circuit of verapamil – sensitive idiopathic left ventricular tachycardia. J Am Coll Cardiol. 2006;36:811-823.

30. Raghavendra, B. S., Dutt, D. N., 2019.A note on fractal dimensions of biomedical waveforms. Comput. Biol. Med. 39,1006-1012.

31. Mishra, A. K., Raghav, S., 2010.Local fractal dimension based ECG arrhythmia classification. Biomedical. Signal. Process. Control 5,114-123.

32. S.A. Rehman, R.R. Kumar, Performance comparison of adaptive filter algorithmsfor ECG signal enhancement", Int. J. Adv. Res. Comput. Commun. Eng. 1 (2)(2012).

33. Spasic, s., 2007.Spectral and fractal analysis of biosignals and coloured noise. In:Proceedings of the 5th International Symposium on Intelligent Systems and Informatics, pp. 147-149.

34. Raghav, S., Mishra, A., 2008.Fractal feature based ECG Arrhythmia classification. In;Proceedings of the 2008 IEEE Region 10conference (TENCON 2008), pp. 1-5.

35. Kalpan, L. M., 1999.Extended fractal analysis for texture classification and segmentation, IEEE Trans Image Process. 8,1572-1585.

36. Higuchi, T., 1988.Approach to irregular time series on the basis of the fractal theory, Physical D31, 277-283.

37. Sevcik, C., 1988.A procedure to estimate the fractal dimension of waveforms, complex. Int 5.

38. Katz., M., 1988.Fractals and the analysis of waveforms. Comput. Biol. Med. 18,145-156.

39. Castiglioni, P., 2010.What is wrong in Kat'z method? Comments on "a note on fractal dimensions of biomedical waveforms".Comput.Biol.Med 40.950-952.

40. Goge, A., Chan, A., 2004.Investigating classification parameters for continuous myoelectrically controlled prosthese. In:Proceedings of the 28th Conference of the Canadian Medical and Biological Engineering Society, pp. 141-144.

41. Wittn, I. H., Frank, E., 2005.Date Mining:Practical Machine Learning Tools and Techniques, 2nd edition Elsevier, Amsterdam, The Netherlands.

42. Alpaydin, E., 2010.Introduction to Machine Learning 2nd edition MIT Press, Cambridge, MA, USA.

43. Thomton, C. J., 2002.Truth from Trash:How Learning Make Sense. MIT Press, Cambridge, MA, USA.

44. Greene, J., 2001.Feature subset selection using Thomton's separability index and it's applicability to a number of sparse proximity bassed classification. In:Proceedings of the 12th Annual Symposium of the Pattern Recognition Association of South Africa.

45. Jolliffe, I. T., 2002.Principal Component Analysis, 2nd edition Springer, Berlin, Germany.

46. Gitter, J. A., Czemiecki, M. J, 1995.Fractal analysis of the electromyographic interference pattern. J. Neurosci. Methods 58,103-108.

47. Peçanha T, Silva -Júnior ND, ForjazCL. Heart rate recovery:autonomic determinants, methods of assessment and association with mortality and cardiovascular diseases. Clin Physiol Function Imaging 2014;34(5) :327-39.DOI: 10.1111/cpf.12102.

48. Watanbe J, Thamilarasan M, Blackstone EH, Thomas JD, Lauer MS, Heart rate recovery immediately after treadmill exercise and left ventricular systolic dysfunction as predictors of morality:the case of stress echocardiography. Circulation. 2001;104(16) :1911-6.

49. Vanderlei LCM, Pastre CM, Hoshi RA, Carvalho TD, Godoy MF. Basic notions of heart rate variability and it's clinical applicability. Rev: Bras Cir Cardiovascular. 2009;24(2) ;205-17.DOI:10.1590/S0102-76382009000200018.

50. Valenti VE. The recent use of heart rate variability for research. J Hum Growth Dev. 2015;25(2) :137-40.

51. Sassi R, Cerutti S, Lombardi F,Malik M, Hulkuri HV, Peng CK, et al. Advanced in heart rate variability signal analysis: joint position statement by the e-Cardiology and the ESC Working Group and the European Heart Rhythm Association co-endorsed by the Asia Pacific Heart Rhythm Society. Europe. 2015;17(9) :1314-53.DOI:10.1093/europace/euv015.

52. Higuchi T. Approach to an irregular time series on the basis of the fractal theory. Physical D. 1988;31(2) :277-83.DOI:10.1016/0167-2789(88) 90081-4.

53. Wajnsztejn R, Carvalho TD, Garner DM, Vanderlei LCM, Godoy MF, Raimundo RD, et al. Heart rate variability analysis by chaotic global techniques in children with attention deficit hyperactivity disorder. Complexity. 2015.21:412-9.DOI:10.1002/cplx.21700.

54. Harriss DJ, Atkinson G. Ethical Standards in Sport and Exercise Science Research. 2014 Update. Int J Sports Media. 2013;34(12) :1025-8.DOI:10.1055/s-0033-1358756.

55. Camm AJ. Malik M, Bigger JT, Breithardt G, Cerutti S, Cohen RJ. Heart rate variability: standards of measurement, physiological interpretation and clinical use. Task Force of the European Society of Pacing and Electrophysiology. Circulation. 1996;93(5) :1043-65.

56. Gupta, V., Suryanarayanam, S., Reddy, N. P., 1997.Fractal analysis of surface EMG signals from the biceps. Inter. J. Med. Inf. 45,185-192.

57. Hu, X., Wang, Z. Z., Ren, X. M., 2005b.Classification of surface EMG signal with fractal dimension. J. Zhejiang Univ. Sci. B6, 844-848.

58. Tricot, C., 1995.Curves and Fractal Dimension.Springer, Berlin, Germany.

59. Castiglioni, P., 2010.What is wrong in katz's method? Comments on " a note on fractal dimensions of biomedical waveforms". Comput. Biology. Med. 40,950-952.

60. Naik, G. R., Arjunan, S., Kumar, D., 2011. Applications of ICA and fractal dimension in SEMG signal processing for subtle movement analysis:a review. Australas. Physical. Eng. Sci. Med. 34,179-193.

61. Phinyomark, A., Quaine, F., Charbonnier, S., Service, C., Tarpin-Bernard, F., Laurillau, Y., 2013b.A feasibility study on the use of anthropocentric variables to make muscle -computer interface more practical. Eng. Apple. Artif. Intell. 26,1681-1688.

62. A. L. V. Coelho, C. A. M. Lima, Assessing fractal dimension methods as feature extractors for EMG signal classification, Engineering Applications of Artificial Intelligence 36(2014) 81-98, Elsevier.

63. Yamakawa T, Matsumoto G, Aoki T. "A low-cost long-life R-R interval telemeter with automatic gain control for various ECG amplitudes," Journal of Advanced Research in Physics, 2012 [cited 2017 Jul 24]; 3(1):011205

65.S. Hargittai, "Savitzky-Golay least-squares polynomial filters in ECG signal processing", in: Proceedings of the Computers in Cardiology, Lyon, 2005, pp.763–766.

66. G.M.S. Sajjad, H. Rahman, A.K. Dey, A.M. Biswas, Z. Islam, A.K.M.J. Hoque, "Performance comparison of modified LMS and RLS algorithms in denoising of ECG signals", Int. J. Eng. Technol. 2 (3) (2012) 466–468.

67. Eckberg DL. "Sympathovagal balance", Circulation 1997; 96:3224-3232. [72]Goldberger AL. "Non-linear dynamics for clinicians: chaos theory, fractals, and complexity at the bedside", Lancet 1996; 347:1312-1314.

68. Kaufmann T, Sütterlin S, Schulz SM, Vögele C. ARTiiFACT: A tool for heart rate artifact processing and heart rate variability analysis. Behav Res 2011; 43:1161-70.

69. Berntson GG, Bigger JT, Eckberg DL, Grossman P, Kaufmann PG, Malik M, Nagaraja HN, Porges SW, Saul JP, Stone PH, Vander Molen MW. Heart rate variability: origins, methods, and interpretive caveats. Psychophysiology 1997; 34:623-648.

70. Pan,J.,& Tomkins, W.J.(1985). A real time QRS detection algorithm. IEEE transaction on Biomedical engineering.,(3),230-236.

71. Tompkins , W.J.(1993).Biomedical digital signal processing . Editorial PrenticeHall.

72. Scargle, J.D.(1982). Studies in astronomical time series analysis. II statistical aspect of unevenly space data. The Astrophysical Jourrnal , 263,835-853.

73. De Luca CJ. The use of surface electromyography in biomechanics. J Appl Biomech;13(2):135-163,(1997)

74. Keen, D. A., Chou, L.-W., Nordstrom, M. A., &Fuglevand, A. J. (2012). Short-term synchrony in diverse motor nuclei presumed to receive different extents of direct cortical input. *Journal of Neurophysiology*, *108*, 3264–3275. doi:10.1152/jn.01154.2011 PMID:23019009

75. Mochizuki, G., Ivanova, T. D., & Garland, S. J. (2005). Synchronization of motor units in human soleus muscle during standing postural tasks. *Journal of Neurophysiology*, *94*, 62–69. doi:10.1152/jn.01322.2004 PMID:15744004

76. Andrés Felipe Ruiz-Olaya**,** Modeling the Human Elbow Joint Dynamics from Surface Electromyography, DOI: 10.4018/978-1-4666-6090-8.ch005, IGI Global.

77. Lawrence JH, De Luca CJ. Myoelectric signal versus force relationship in different humanmuscles. J App Physiol;54(6):1653–1659;(1983)

78. Lenhardt SA., McIntosh KC, and Gabriel DA. The surface EMG-force relationship duringisometric dorsiflexion in males and females. Electromyogr. Clin. Neurophysiol;48:000-000.(2008)

79. Gerdle, B, Karlsson S, Crenshaw AG, Elert J, Fridén J. The influences of muscle fiberproportions and areas upon EMG during maximal dynamic knee Extensions. Eur J ApplPhysiol;81(1-2):2–10, (2000)

80. Woods JJ, and Bigland-Ritchie B. Linear and non-linear surface EMG/force relationshipsin human muscles. An anatomical/functional argument for the existence of both. Am JPhys Med Rehabil ;62(6)287–99;(1983)